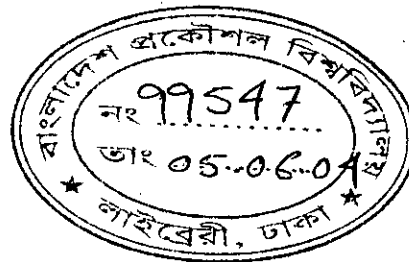


# **NONLINEAR FINITE ELEMENT ANALYSIS OF REINFORCED CONCRETE PLATES IN PUNCHING SHEAR**

by

**DEWAN SHAIKH MD. SHAHEEDUL ISLAM**



A thesis submitted to the Department of Civil Engineering,  
**Bangladesh University of Engineering and Technology, Dhaka**  
in partial fulfillment of the requirement for the degree of

**MASTER OF SCIENCE IN CIVIL ENGINEERING (STRUCTURAL)**

**MARCH, 2004**



The thesis titled '**Nonlinear Finite Element Analysis of Reinforced Concrete Plates in Punching Shear**' submitted by Dewan Shaikh Md. Shaheedul Islam, Roll No. 040204311(F), Session April 2002 has been accepted as satisfactory in partial fulfillment of the requirement for the degree of Master of Science in Civil Engineering (Structural) on 31 March, 2004.

**BOARD OF EXAMINERS**



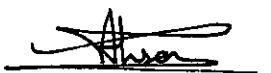
**Dr. Ahsanul Kabir**  
Professor  
Department of Civil Engineering  
BUET, Dhaka-1000.

Chairman  
(Supervisor)



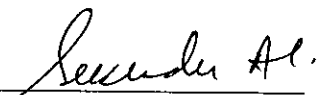
**Dr. M. Shamim Z. Bosunia**  
Professor  
Department of Civil Engineering  
BUET, Dhaka-1000.

Member




**Dr. Raquib Ahsan**  
Assistant Professor  
Department of Civil Engineering  
BUET, Dhaka-1000.

Member



**Dr. Sk. Sekender Ali**  
Professor and Head  
Department of Civil Engineering  
BUET, Dhaka-1000.

Member  
(Ex-Officio)

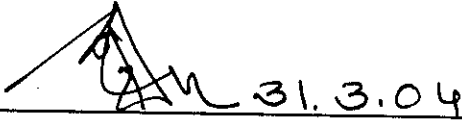


**Dr. Md. Abdur Rashid**  
Associate Professor  
Department of Civil Engineering  
DUET, Gazipur.

Member  
(External)

## **CANDIDATE'S DECLARATION**

It is hereby declared that this thesis or any part of it has not been submitted elsewhere for the award of any degree or diploma (except for publication).

  
\_\_\_\_\_

**Dewan Shaikh Md. Shaheedul Islam**

**To**

**My**

**Mother**

**(Whom I lost during the progress of the research work)**

# TABLE OF CONTENTS

<b>Declaration</b>	iv
<b>Acknowledgement</b>	xviii
<b>Abstract</b>	xix
<b>List of Symbols</b>	xvi
<b>Chapter 1 INTRODUCTION</b>	
1.1 General	1
1.2 Objective of the Study	2
1.3 Methodology	3
1.4 Outline of the Thesis	6
<b>Chapter 2 LITERATURE REVIEW</b>	
2.1 Introduction	7
2.2 Punching Shear Mechanism	7
2.3 Experimental Investigations	9
2.3.1 Effect of Concrete Strength	9
2.3.2 Size Effect	9
2.3.3 Effect of Shear Reinforcement	10
2.3.4 Edge Condition Effect	11
2.3.5 Plate-Column Connection Behaviour	12
2.3.6 Shear Strengthening Techniques	13
2.3.7 Miscellaneous Studies	14
2.4. Analytical Investigation	14
2.4.1 Beam -Strip Approach	15
2.4.2 Truss Model Approach	15
2.4.3 Fracture Mechanics	16
2.4.4 Plasticity Model	16

2.4.5 Equivalent Frame Method	17
2.4.6 Miscellaneous Studies	18
2.5 Finite Element Method	19
2.6 Punching Shear Prediction Equations	22
2.6.1 Regan's Equation	22
2.6.2 Bazant and Cao's Equation	23
2.6.3 Gardener's Equation	24
2.6.4 Code Provision Equations	25
2.6.4.1 ACI Code Provisions	25
2.6.4.2 BS Code Provisions	26
2.6.4.3 Canadian Code Provisions	27
2.6.4.4 European Code Provisions	28
2.6.4.5 BNBC Code Provisions	29
2.6.5 Concluding Remarks	29
<b>Chapter 3 FINITE ELEMENT MODELING</b>	
3.1 Introduction	31
3.2 The finite Element Packages	31
3.3 An overview of ANSYS	32
3.4 Modeling of Reinforced Concrete Plate	33
3.4.1 Element Types Adopted	34
3.4.2 Element Performance	36
3.4.3 Material Properties	40
3.4.3.1 Concrete	40
3.4.3.2 Steel Reinforcement	45
3.4.4 Failure Criteria for Concrete	46
3.4.5 Loading and Boundary Conditions	48
3.4.6 Finite Element Discretisation (Mesh Sensitivity)	52
3.5 Remarks	53

<b>Chapter 4</b>	<b>NONLINEAR FINITE ELEMENT ANALYSIS AND MODEL PERFORMANCE</b>	
4.1	Introduction	54
4.2	Nonlinear Solution Strategies	54
4.2.1	Incremental Loading and Equilibrium Iterations	55
4.2.2	Convergence Criteria and Tolerance	56
4.2.3	Load Stepping and Failure Definition for Nonlinear FE Analysis	57
4.2.4	Shear Transfer Coefficient	58
4.3	Mesh Sensitivity (Nonlinear)	58
4.4	Comparison of Numerical Results with Experimental data	60
4.5	Discussions	65
<b>Chapter 5</b>	<b>INFLUENCE OF MATERIAL AND GEOMETRIC PARAMETERS ON PUNCHING SHEAR STRENGTH</b>	
5.1	Introduction	67
5.2	Material Parameters	67
5.2.1	Concrete Strength	68
5.2.2	Flexural Reinforcement	72
5.2.2.1	Reinforcement Ratio	72
5.2.2.2	Yield Strength	73
5.3	Geometric Parameters	74
5.3.1	Plate Thickness (Span-Depth Ratio)	75
5.3.2	Column Size	77
5.3.3	Support Condition	79
5.4	Remarks	80

**Chapter 6 INFLUENCE OF SHEAR REINFORCEMENT ON  
PUNCHING SHEAR STRENGTH**

6.1 Introduction	82
6.2 Shear Reinforcement	82
6.2.1 Types of Shear Reinforcement	84
6.2.1.1 Vertical Shear Reinforcement	84
6.2.1.2 Inclined Shear Reinforcement	85
6.2.1.3 Nonconventional Shear Reinforcement	87
6.3 Limitations and Assumptions in FE Modeling of various forms of Shear Reinforcement	88
6.4 Effects of Bent bar Shear Reinforcement	88
6.5 Effects of Closed hoop Shear Reinforcement	91
6.6 Effects of Open Link Shear Reinforcement	93
6.7 Effects of Hat type Shear Reinforcement	95
6.8 Discussion on Effective Shear Reinforcement	97
6.9 Final Remarks	99

**Chapter 7 A RATIONALE FOR PUNCHING SHEAR  
PREDICTION EQUATION**

7.1 General	100
7.2 ACI 318-02 Code provision	101
7.3 Comparison of Analytical and Experimental results with ACI 318-02 Code Provision	102
7.4 Scope of Modification	104
7.5 Suggested Modification to the ACI Method	104
7.6 Provision for Shear Reinforcement	112
7.7 Concluding Remarks	112



<b>Chapter 8</b>	<b>CONCLUSIONS AND RECOMMENDATIONS</b>	
8.1	General	114
8.2	Summary and Conclusions	114
8.3.	Recommendations for Future Studies	117
	<b>References</b>	119
	<b>Appendix A</b>	
	Typical ANSYS Script File	126

## List of Figures

### Chapter 2

- 2.1 A square column tends to shear out a pyramid from a footing or flat plate 8

### Chapter 3

- 3.4.1 Eight-node Solid 65 Element 35
- 3.4.2 Two-node Link 8 Element 36
- 3.4.3 Comparison of Deflection of Various FE Elements with Theoretical Prediction 38
- 3.4.4 Variation of Deflection with number of Elements for Different Element Types 38
- 3.4.5 Variation of Deflection of Solid 65 Element 39
- 3.4.6 Typical Uniaxial Compressive and Tensile Stress-Strain Curve for Concrete [Bangash (1989)] 41
- 3.4.7 Concrete Stress-Strain Curve 45
- 3.4.8 Idealised Stress-Strain Curve for Steel Reinforcement 46
- 3.4.9 Failure Surface of Concrete in 3-D 48
- 3.4.10 A Test Slab Section of Elstner and Hognestad (1956) 49
- 3.4.11 Typical Finite Element Model of the Plate 49
- 3.4.12 Plates With Different Boundary Conditions and Loading 50
- 3.4.13 Typical Tension Reinforcement Mat 51
- 3.4.14 Typical Compression Reinforcement Mat 51
- 3.4.15 Typical Tension, Compression and Column Stub Reinforcement 51
- 3.4.16 Mesh Optimisation 52

### Chapter 4

- 4.2.1 Newton-Raphson Iterative Solution (ANSYS) 56

4.3.1	Mesh Sensitivity (Nonlinear) Load-deflection Curve for Mesh Sensitivity	60
4.4.1	Comparative Load-Deflection Response for A-1a	62
4.4.2	Comparative Load-Deflection Response for A-7b	62
4.4.3	Comparative Load-Deflection Response for A-7	63
4.4.4	Comparative Load-Deflection Response for B-14	63
4.4.5	Comparative Load-Deflection Response for B-16	64
 <b>Chapter 5</b>		
5.2.1	Variation of Ultimate Load Capacity of the Test and FE Analysis with Varying Compressive Strength of Concrete	69
5.2.2	Load-deflection response of FE Analysis for Slabs A-1a through A-1e	69
5.2.3	Variation of Ultimate load with Varying Compressive Strength of Concrete for Different Reinforcement Ratio	71
5.2.4	Load-deflection Response with Varying Concrete Compressive Strength for Reinforcement Ratio of 2.5%	71
5.2.5	Influence of Flexural Reinforcement on Load- deflection Response	72
5.2.6	Influence of Reinforcement Ratio on Punching Shear for varying Concrete Compressive Strength	73
5.2.7	Variation of Ultimate Strength due to change in Yield Strength of Reinforcement	74
5.3.1	Variation of Punching Shear Strength with Plate Thickness	76
5.3.2	Influence of Span-Depth Ratio on Ultimate Load	77
5.3.3	Comparative Load-deflection Response for different Column size	78

5.3.4	Variation of Punching Shear Strength with Column Size	79
5.3.5	Comparative Load-deflection Response for Different Edge Condition of the Plate	80
<b>Chapter 6</b>		
6.2.1	Typical Vertical and Inclined Shear Reinforcement	83
6.2.2	Various Types of Vertical Shear Reinforcement	85
6.2.3	Bent-bar Shear Reinforcement	86
6.2.4	Shearband Reinforcement	87
6.4.1	Bent-bar Shear Reinforcement	89
6.4.2	Influence of Bent-bar Shear Reinforcement on Load-deflection Response of Flat Plates	90
6.4.3	Comparative Load-deflection Response of Bent-bar Shear Reinforcement	91
6.5.1	Closed hoop Shear Reinforcement (Vertical)	92
6.5.2	Closed hoop Shear Reinforcement (Inclined)	92
6.5.3	Effect of Closed hoop Shear Reinforcement	93
6.6.1	Open link Shear Reinforcement (Vertical)	94
6.6.2	Open link Shear Reinforcement (Inclined)	94
6.6.3	Effect of Open link Shear Reinforcement	95
6.7.1	Hat type Shear Reinforcement (Vertical)	96
6.7.2	Hat type Shear Reinforcement (Inclined)	96
6.7.3	Effect of Hat type Shear Reinforcement	97
6.8.1	Relative Performance of Various types of Shear Reinforcement	98
6.8.2	Effect of Inclination of Shear Reinforcement for three Different types	99

## Chapter 7

7.5.1	Variation of $\lambda$ with Steel Ratio	106
7.5.2	Variation of $\gamma$ with Concrete strength $f'_c$ for $\rho \geq 2.50$ %.	106
7.5.3	Comparison of Results of Test, FE, ACI and Modified Formula (6 Test Slabs)	107
7.5.4	Comparison of Test Results with ACI and Modified ACI Formula (Further 4 Test Slabs)	108
7.5.5	Comparison of Test Results with ACI and Modified ACI Formula (Moe's Test Slabs)	109
7.5.6	Comparison of Test Results with Gardener's Equation, British, Canadian and ACI Code Provisions	111

## List of Tables

### Chapter 3

3.4.1	Concrete Material Properties Used	43
3.4.2	Details of Slabs Tested by Elstner and Hognestad (1956)	43

### Chapter 4

4.4.1	Comparison of Numerical with Experimental Results	61
-------	--	----

### Chapter 7

7.1	Comparison of Results	103
7.2	Comparison of Test Results with FE, ACI and Modified ACI Formula (6 Test Slabs)	107
7.3	Comparison of Results of Test, ACI and Modified Formula (Further 4 Test Slabs)	108
7.4	Comparison of Results of Test, ACI and Modified Formula (Moe's Test Slabs)	109
7.5	Comparison of Results with Gardener's Equation, British Code and Canadian Code provisions	110

## List of Symbols and Abbreviations

The following notation and abbreviation is used in the thesis:

$a$	Span length of plate
$b$	Diameter of punch
$b_0$	Perimeter of critical section of slab or footing at a distance of $d/2$ away from the column face
$c$	Width of column or side length of loaded area
$d$	Effective depth of section
$d_a$	Maximum aggregate size
$E_c$	Modulus of elasticity of concrete
$E_s$	Modulus of elasticity of steel
$f$	Stress at any strain $\epsilon$
$f'_c$	Concrete cylinder compressive strength
$f_{cu}$	Uniaxial cube (compressive strength of concrete
$f_r$	Modulus of rupture of concrete
$f_t$	Direct tensile strength of concrete
$f_y$	Yield strength of reinforcing steel
$h$	Thickness of slab
$q$	Applied pressure
$U$	Total deflection
$V_{cm}$	Ultimate shear force by proposed equation
$V_p$	Punching shear strength in Newton (N)
$V_u$	Ultimate shear force
$v_u$	Nominal shear stress at failure
$\beta_c$	Ratio of long side to short side of concentrated load or reaction area
$\beta_t$	Shear transfer coefficient
$\lambda$	Factor defined in section 7.5

$\gamma$	Factor defined in section 7.5
$\phi$	Strength reduction factor
$\varepsilon$	Strain at stress $f$
$\varepsilon_c$	Strain at the ultimate compressive strength $f'_c$
$\varepsilon_{cu}$	Ultimate strain
$\nu$	Poisson's ratio
$\rho$	Reinforcement ratio
$\sigma_{cu}$	Peak compressive stress
$\sigma_m$	Maximum tensile strength of concrete
CFRP	Carbon Fiber Reinforced Polymers
FE	Finite Element
FEA	Finite Element Analysis
FEM	Finite Element Method/Finite Element Model
GUI	Graphical User Interface



## ACKNOWLEDGEMENT

The author wishes to convey his profound gratitude to Almighty Allah for allowing him to bring this effort to fruition. The author would like to express his sincere appreciation and gratitude to his supervisor, Dr. Ahsanul Kabir, Professor, Department of Civil Engineering, Bangladesh University of Engineering and Technology (BUET), for his constant guidance, generous help, invaluable suggestions, continued encouragement and remarkable patience throughout the progress of this research work.

The author is grateful to Dr. K. M. Amanat, Associate Professor, Department of Civil Engineering, BUET, for his suggestions and help regarding finite element modeling in ANSYS.

The author is indebted to the Head of the Department of Civil Engineering, BUET for providing all the facilities of the department in materializing this work. The author gratefully acknowledges the cooperation of all concerned persons of the department, Civil Engineering Library, BUET Central Library and Computer Center for their assistance that were enjoyed by the author.

Last but far from least the author wishes to express his gratitude to his beloved wife for her continuous encouragement and homage during this study.

## ABSTRACT

Punching shear is one of the most critical phenomena for flat plate building systems due to the brittle nature of this failure mode. The region of a slab in the vicinity of a column could fail in shear by developing a failure surface in the form of a truncated cone or pyramid. This type of failure, called a punching shear failure, is usually the source of collapse of flat plate and flat slab buildings. It is one of the topics of intensive research in recent years by various researchers in the field of concrete structure. Numerous tests have been carried out to evaluate the punching shear strength of slabs. Several theories have been put forward to predict the strength observed in these tests.

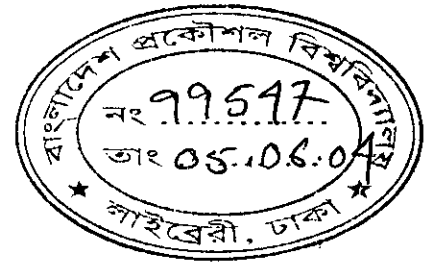
An attempt has been made in this research to study the punching shear of reinforced concrete flat plates. Before carrying out the systematic computational investigation, existing literature on the relevant field based on experimental investigation, analytical methods, numerical models and various Codes of Practice is thoroughly reviewed. A 3-dimensional reinforced concrete flat plate model was generated. The formulation has been checked against experimental results of tests on slabs subjected to punching shear. From a comparison of the numerical and the experimental results, it is concluded that the adopted model of the Finite Element Analysis package (ANSYS) is suitable for analyzing reinforced concrete plates. The good agreement obtained between the numerical and the experimental results establish the validity and accuracy of the computational model.

A systematic study is carried out to determine the punching shear capacity due to variations of different structural parameters like span-depth ratio, reinforcement ratio, support condition, shear reinforcement etc. The parametric study indicated that the analysis is able to predict the influence of several of the most commonly considered parameters on the punching shear behaviour of slabs. From the graphical presentation of the various parameters a designer can visualize and choose the most suitable one to enhance the punching shear strength. The results of the analysis confirm the general understanding of the behaviour of slabs in punching shear. It was seen that the addition of shear reinforcement has a significant effect on the punching shear strength of the slab/plates. The models with shear reinforcement showed a more ductile behavior than those without shear reinforcement. The results indicate that the inclined stirrups are technically superior. These are also very easy to install, and would thus seem to be a promising form of shear reinforcement for flat plates.

This study shows that both span-depth ratio effects and the type of support condition have significant influence on the punching shear strength in concrete slabs. Size effect and reinforcement ratio effects are not considered in ACI 318-02 Code (also BNBC 1993) provision; as such there is scope for review of these codes taking all the parameters into consideration. Hence, a modification to the ACI 318-02 Code equation is proposed and the performance of the proposed modification is verified. Finally, based on the findings of the study, conclusion and recommendations are put forward.

## Chapter 1

### INTRODUCTION



#### 1.1 General

From an architectural and construction viewpoint, the flat plate system is a very common and competitive structural system for cast-in-place slabs in buildings since no beams, column capitals, or drop panels are involved, which means that formwork becomes extremely simple. That lead to architecturally pleasing buildings and bridges as well as simplifying and accelerating site operations. They allow easy and flexible partitioning of space and reduce the overall height of tall buildings. Flat plates, being thin members, are uneconomical of steel, but they are economical of formwork. Because formwork represents over half the cost of reinforced concrete, economy of formwork often means overall economy. Reduced story height resulting from the thin floor, the smooth ceiling, and the possibility of slightly shifting column location to fit the room arrangements are factors contributing in the overall economy. However, the structural concept is at great disadvantage, because of the risk of brittle punching failure at columns.

In the design of reinforced concrete flat plates, the regions around the column always pose a critical analysis problem. Column tends to punch through the flat plates, flat slabs and footings because of the shear stresses, which act in them around the perimeter of the columns. Punching shear failure is referred to as a local shear failure that could occur around concentrated load or column supports. Shear failure, both beam and punching type, may be considered more dangerous than flexure failure. This may be so because of greater uncertainty in predicting shear failure, which is likely to occur suddenly with no advance warning of distress. Large research efforts have been made in the past and are still being continued to develop methods for a reliable

prediction of the punching shear capacity. Numerous tests have been carried out to evaluate the punching shear strength of slabs. Several theories have been put forward to estimate the strength observed in these tests.

From the literature, it is observed that three approaches are available at present to assess the punching shear capacity of flat plates. The first is by testing of models or the prototypes. The second is the use of empirical relations of different Codes of Practices based on experimental and analytical results. The third is various numerical analyses using computer software. When all the methods have their own merits and demerits, for design and evaluation purposes, the last two methods are more suitable. Of these the last one is accepted as more reliable too. Yet, the core of a reliable numerical analysis lies on an adequate constitutive model that can represent the material behaviour. The element discretisation of the plate with suitable finite element type is also vital. Further investigations is necessary in this regard and this is an effort to understand the punching behaviour of reinforced concrete flat plates using Solid 65 Element of the package software ANSYS.

## **1.2 Objectives of the Study**

Based on the background summarized in the foregoing sections, the present research aims at covering the following objectives:

- a. To model numerically the punching shear behaviour of reinforced concrete flat plates using finite element package 'ANSYS' and compare various test results with finite element analysis.
- b. To determine complete load-deflection response of reinforced concrete flat plates and estimate the ultimate load carrying capacity of such structures.

- c. To examine the effect of strength and ratio of flexural reinforcement on the ultimate load carrying capacity of flat plates.
- d. To study the effect of plate thickness (span-depth ratio) on the punching shear strength of flat plates.
- e. To study the effect of different types of shear reinforcement on the punching shear strength of flat plates.
- f. To investigate the effectiveness of the ACI 318-02 Building Code equations in predicting punching shear strength of flat plates. Compare the predictions with numerical solution and test results. Hence, suggest direction for possible improvement.

### **1.3 Methodology**

Before carrying out the systematic computational investigation, existing literature on the relevant field based on experimental investigation, analytical methods, numerical models and various Codes of Practice is thoroughly reviewed.

The main obstacle to finite element analysis of reinforced concrete structures is the difficulty in characterizing the composite material properties. Much effort has been spent in search of a realistic model to predict the behaviour of reinforced concrete structures. Due mainly to the complexity of the composite nature of the material, proper modeling of such structures is not straightforward and still an active area of research.

The implementation of nonlinear material laws in finite element analysis codes is generally tackled by the software development industry in one of the two ways. In the first instance, the material behaviour is programmed independent of the elements to which it may be specified. Using this approach the choice of element for a particular physical system is not limited and best practice modeling techniques can be used in identifying an appropriate element type to which any, of a range, of nonlinear material properties are assigned. This is the most versatile approach and does not limit the analyst to specific element types in configuring the problem of interest. Notwithstanding this, however, certain software developers provide specific specialised nonlinear material capabilities only with dedicated element types.

Concrete is a quasi-brittle material and has different behaviour in compression and tension. The steel for the finite element model is assumed as an elastic-perfectly plastic material and identical in tension and compression. A nonlinear finite element programme (ANSYS) is used for this analysis to predict elastic behaviour up to cracking. ANSYS is the most widely used general purpose software of FE analysis. It has versatile applications in the field of static, dynamic, heat transfer, etc. ANSYS also offers linear and non-linear (material, geometric, and boundary conditions) analysis. It provides a dedicated isoparametric three-dimensional eight noded solid element, Solid 65, to model the nonlinear response of brittle materials based on a constitutive model for the triaxial behaviour of concrete. The element is capable of plastic deformation, cracking in three orthogonal directions, and crushing. The internal reinforcement is modeled using three dimensional spar elements Link 8 with plasticity. To develop a realistic model link elements are used as discrete reinforcement connecting solid element nodes rather than smeared reinforcement.

In this study, perfect bond between concrete and reinforcement is assumed. To provide the perfect bond, the link element for the steel reinforcing is connected between nodes of each adjacent concrete solid element, so that the two materials share the same nodes. The nonlinear effects due to the cracking and crushing of concrete upto ultimate load and the yielding of steel reinforcement is included. The model is a smeared crack model, in the sense that it will not track individual macro cracks. An incremental finite element technique is used which simulates the nonlinear load-deflection behaviour of reinforced concrete structure.

To obtain more accurate results from finite element analysis it is important to fix the optimum number of element. It has been observed that for a particular problem the results often vary upto a certain number of elements and after that result becomes constant. Optimum meshing is checked by elastic analysis for constant load from the plot of deflection vs. number of mesh. The load deflection property of the element is also verified with the Theory of Plates results (Timoshenko, 1959) within elastic limit.

To carry out finite element analysis in order to predict the behaviour of any structure, it is essential to verify the developed model against some experimental results and/or other theoretical results to ensure that the developed model is tracing the actual response closely. Results of the nonlinear finite element analysis are compared with the test results obtained from Elstner and Hognestad (1956) to ensure the acceptability of the numerical model used.

The effects of some numerical parameters are studied in order to establish the stability of the overall solution process and as a basic guide for subsequent analytical problems. The numerical parameters selected for sensitivity analysis of the solution procedure are; load increment size, element mesh size, shear transfer coefficient, and convergence criteria.

A systematic parametric study is carried out to determine the punching shear capacity due to variations of different structural parameters like span-depth ratio, reinforcement ratio, support condition, shear reinforcement etc. Afterwards, based on the findings of the study, conclusion and recommendations are put forward.

#### **1.4 Outline of the Thesis**

The thesis consists of 8 chapters. The current chapter is Chapter 1, which introduces the general background of the research work and summary of aims and objectives and methodology. Literature review and review of codes and theories for determining the punching shear capacity of flat plates are described in Chapter 2. Chapter 3 describes the finite element modeling of reinforced concrete flat plates. Chapter 4 gives details of nonlinear FE analysis for determination of punching shear by ANSYS. Performance of the model is verified against different experimental results in this chapter too. Chapter 5 is dedicated to a thorough parametric study to identify the effects of concrete material and geometric parameters on the punching shear capacity of flat plates. Investigation and findings of this chapter leads to recommendations on the choice of structural parameters to enhance the punching shear strength. Chapter 6 discusses the influence of different shear reinforcement on the punching shear behaviour of flat plates. Chapter 7 presents a rationale for the punching shear prediction equation. The conclusions made from the study are presented in Chapter 8. This chapter also recommends future work for possible extension of the current study.



## Chapter 2

### LITERATURE REVIEW

#### 2.1 Introduction

Punching shear is one of the most critical phenomena for flat plate building systems due to the brittle nature of this failure mode. The region of a slab in the vicinity of a column could fail in shear by developing a failure surface in the form of a truncated cone or pyramid. This type of failure, called a punching shear failure, is usually the source of collapse of flat plate and flat slab buildings. It is one of topics of intensive research in recent years by various concrete structure researchers. Numerous tests have been carried out to evaluate the punching shear strength of slabs. Several theories have been put forward to predict the strength observed in these tests. This chapter summarizes the experimental investigations and analytical approach adopted by different researchers along with provisions of various building codes.

#### 2.2 Punching Shear Mechanism

When a two-way slab is heavily loaded with a concentrated load or where a column rests on a two-way footing, diagonal tension cracks form that encircle the load or column. These cracks are not visible, except as flexural cracks. Such cracks extend into compression area of the slab and encounter resistance near the load similar to the shear-compression condition. The slab or footing continue to take load and finally fails around and against the load or column, punching out a pyramid of concrete as indicated in Figure 2.1. Diagonal cracks do not form further out from the load or column because of rapid increase in the failure

perimeter. The initial diagonal cracks thus proceed to failure in punching shear type of failure directly around the load.

In compromising between initial cracking and the final shear condition at failure for different ratios between column (or load) dimension and footing (or slab) thickness, different Codes recommend a single punching shear strength calculated at a pseudo-critical distance from the column face or edge of the load.

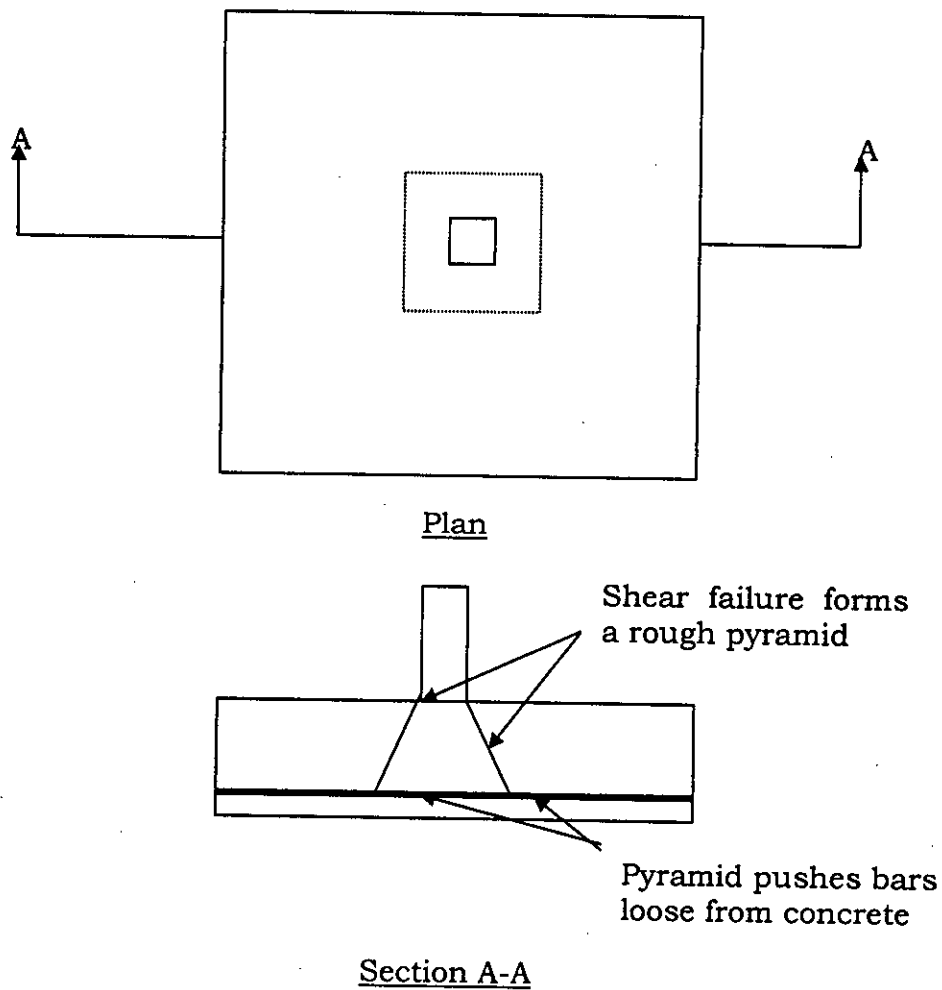


**Figure 2.1** A square column tends to shear out a pyramid from a footing or flat plate

### **2.3 Experimental Investigations**

Several experimental investigations have been carried out to evaluate the punching shear strength of flat plates and slabs. These investigation covers both concrete material and geometric parameters like concrete strength, influence of reinforcement type and ratio, column size, plate thickness, edge conditions etc. Some of these are briefly summarized in the following subsections.

#### **2.3.1 Effect of Concrete Strength**

Gardner (1990) presents the result of an investigation relating punching shear to concrete strength and steel ratio. It is concluded that the shear capacity is proportional to the cube root of concrete strength and steel ratio. It is also opined that the shear perimeter should be increased by using large columns and column capitals, if the punching shear capacity is in doubt. Elstner and Hognestad (1956) presented a research report on the methods and results of experimental work on the shearing strength of reinforced concrete slabs subjected to a centrally located concentrated load. The test findings show that the shearing strength of slabs is a function of concrete strength as well as several other variables like percentage of tension reinforcement, size of column, conditions of support and loading, distribution of tension reinforcement, and amount and position of shear reinforcement.

#### **2.3.2 Size Effect**

Punching shear tests of geometrically similar reinforced concrete slabs of different sizes have been carried out by Bazant and Cao (1987). The test prediction summarized that the punching shear failure of slab without stirrup is not plastic but brittle. Results of an experimental investigation on the punching shear strength of reinforced concrete slabs with varying

span to depth ratio have been summarized by Lovrovich and McLean (1990). It is reported that the ACI Code does not recognize span to depth ratio effects or the effects of restraining action at the support when treating punching shear in reinforced concrete slabs. It is also observed that punching shear strengths are much greater than the values permitted by the ACI Code.

Broms (1990a) presented a design method to predict the punching strength and deflection of flat plates at interior columns. Failure is assumed to occur when the compression zone of the slab in the vicinity of the column is distressed by either high radial compression stress or by a high tangential compression strain. Size effects and the effect of increasing concrete brittleness with increasing strength are both considered. The method showed excellent agreement with results from punching tests reported in the literature, with conditions ranging from ductile flexural failures to brittle punching failures, from small test specimens to a full-sized structure, and from symmetrical to unsymmetrical loadings.

### **2.3.3 Effect of Shear Reinforcement**

Yamada, et al. (1990) performed a research programme for the determination of the effect of shear reinforcement type and ratio on the punching shear strength of monolithic slab column connections. The first type of shear reinforcement consisted of hat-shaped units, very advantageous from the points of view of prefabrication and field installation. The second type consisted of double-hooked shear bars, more difficult to install but with very efficient anchorage. Experimental results showed that the hat-shaped shear reinforcement was not effective because of lack of proper anchorage. Double-hooked reinforcement showed high effectiveness, which resulted in a considerable increment of the punching shear resistance of the

connection. Olivera, et al. (2000) introduced a novel form of inclined stirrups and reported the results of test slabs with such reinforcement. Companion tests of slabs without shear reinforcement and slabs with vertical stirrups were also reported. The inclined stirrups were shown to function well and produced punching resistances superior to those obtained with vertical stirrups.

Four reinforced concrete slab-column sub-assemblies were subjected to a high intensity shear and moment transfer at the column-slab connections by Pillai et al. (1982). The effectiveness of shear reinforcement in increasing the shear strength and preventing punching failure and in improving the ductility of the connections were assessed. It was found that shear reinforcement in the slab at the connections prevented punching failure and generally doubled their ductility. Ghoneim and MacGregor (1994a) presented the results of 19 tests of reinforced concrete plates simply supported on four edges. The plates were subjected to combined inplane compressive and lateral loads. The variables in the experimental investigation included the loading type, plate slenderness, inplane load level, aspect ratio, reinforcement ratio in the two orthogonal directions, and loading sequence. The test programme was successful in providing data relating to the behaviour of reinforced concrete plates under combined inplane compressive and lateral loads.

#### **2.3.4 Edge Condition Effect**

Alam (1997) presented punching tests conducted on reinforced concrete slabs with their edges restrained as well as unrestrained. The significant positive effect of edge restraint on the punching failure, resulting in enhancing the ultimate punching strength, has been noticed. Aghayere and MacGregor (1990b) presented the results of tests on nine reinforced concrete plates simply supported along four edges and subjected to

combined uniaxial compression and uniform transverse loads. The results of the investigation led to the conclusion that the presence of an axial in-plane load can lead to a reduction in the transverse load capacity of a concrete plate. This reduction depends on the in-plane load level, the width to thickness ratio, the concrete strength, the amount of reinforcement, and the aspect ratio of the plate.

Kuang and Morley (1992) tested 12 restrained reinforced concrete slabs with varying span to depth ratio, percentage of reinforcement, and degree of edge restraint. It is reported that the punching shear strengths are much higher than those predicted by ACI 318 and BS 8110 codes. The study suggested that there is a definite enhancement in punching shear strength as the degree of edge restraint increases. The enhanced punching shear capacity was a result of compressive membrane action caused by restraining action at the slab boundaries.

### **2.3.5 Plate-Column Connection Behaviour**

Hammill and Ghali (1994) reported test results of five full-scale reinforced concrete flat plate connections with corner columns subjected to shear-moment transfer. The tests showed that the equations of the codes (ACI 318-89 and Canadian Standard CAN-A23.3-M84) are conservative and can be improved by addition of an appropriate equation for the fraction of the unbalanced moment resisted by eccentric shear stress. It is shown that the codes, or their commentaries, need to provide the equations necessary to determine the extent of the shear-reinforced zone for a corner column connection. Mortin and Ghali (1991) reported test results of six full-scale reinforced concrete flat plate connections with edge columns subjected to shear-moment transfer with and without shear reinforcement, to verify the effectiveness of the stud shear reinforcement. The results confirmed the effectiveness of this type of shear reinforcement in improving shear strength and ductility.

### 2.3.6 Shear Strengthening Techniques

El-Salakawy et al. (2003) presented new shear strengthening technique for concrete slab-column connections. The aim of the programme was to test a new method for strengthening existing reinforced concrete slabs for punching shear. The new strengthening technique consists of shear bolts externally installed in holes drilled through the slab thickness. It is found that the presence of shear bolts substantially increased the punching capacity and the ductility of the connections. Elgabry and Ghali (1990) presented rules to design and detail stud-shear reinforcement in accordance with the 1989 ACI Building Code (ACI 318-89). Because of the effectiveness of anchorage, design rules that reduce the amount of shear reinforcement are suggested and applied. Shaaban and Gesund (1994) carried out experimental study to determine whether addition of steel fibers to the concrete mix could significantly increase the punching shear strength of reinforced concrete flat plates. Thirteen slab specimens and their companion cylinder specimens were tested. Test results of this study indicated that the addition of steel fibers to the concrete mix did significantly enhance the punching shear strength of slabs.

Binici and Bayrak (2003) presented a strengthening technique for increasing punching shear resistance in reinforced concrete flat plates using carbon fiber reinforced polymers (CFRPs). This strengthening method employed CFRP strips in the vertical direction as shear reinforcement around the concentrated load area in a specified pattern. The results showed that, by using a sufficient amount of CFRP strips in an efficient configuration, the failure surface can be shifted away from the column. The load carrying capacities of the strengthened reinforced concrete slabs were increased with increasing amount of vertical CFRP reinforcement used in a wider area.

### **2.3.7 Miscellaneous Studies**

Broms (2000) presented a design concept that examines the punching failure mode of flat plates, verified by test, and design recommendations are given. The system provided excellent safety against progressive collapse of flat plate buildings, a basic requirement that seems to be overlooked in many current concrete codes. Loo and Chiang (1993) carried out a comparative study on the methods of punching shear strength analysis of reinforced concrete flat plates. It is found that the ACI and the British methods are applicable only to flat plates with torsion strips; the codes also tend to give unsafe predictions for the punching shear strength.

Mitchell and Cook (1984) investigated the slab structures after initial failure in order to determine a means of preventing progressive collapse. Analytical models for predicting the post-failure response of slabs are presented and the predictions are compared with experimental results. These analytical models along with experimental investigation enabled the development of simple design and detailing guidelines for bottom slab reinforcement, which is capable of hanging the slab from the columns after initial failures due to punching shear and flexure. Rangan (1990) presented the background theory and the punching shear design provisions contained in the Australian Standard for Concrete Structures, AS 3600-1988. The correlation of the design equations with test data is also presented. It is believed that the Australian method could serve as a useful alternative to the ACI Building Code provisions.

### **2.4 Analytical Investigation**

Several investigations have been carried out using various analytical models and theories to evaluate the punching shear strength of flat plates and slabs. These investigation covers beam-strip approach, truss



model approach, fracture mechanics, plasticity model, equivalent frame method, and assumed deflection method. Some of these are briefly summarized in the following subsections.

#### **2.4.1 Beam-Strip Approach**

Siao (1994) adopted a beam-strip approach to predict the punching shear strength of flat slabs with and without shear reinforcements. Predicted results were compared with existing experimental data previously reported by other researchers. Good agreement was observed. Elstner and Hognestad (1956) utilized the beam-strip approach in their investigation of flat slab punching shear strength. Several beam-strip specimens were tested but reached no useful conclusion, as the specimens failed in flexure.

#### **2.4.2 Truss Model Approach**

A truss-model-based design procedure is developed for transversely reinforced slabs by Marti (1990). The truss model approach for shear design of beam is extended to transversely reinforced slabs, and the application of the newly developed design procedures is illustrated for the case of a thick transfer plate in a highrise building. Alexander and Simmonds (1992) proposed that punching shear failure could be represented by a truss model and that failure is due to the concrete cover failing to contain the out-of-plane component of force between the reinforcement and the concrete compression struts. It is assumed that concrete tensile capacity is related to the square root of the concrete strength. The truss model does not include components of the shear failure mechanism such as aggregate interlock and friction, dowel action of the longitudinal steel, and shear carried across uncracked concrete. The study led to the conclusion that concrete cover of the top mat

reinforcement in slabs of usual span and loading may be as significant to punching shear strength as is the flexural depth of the slab.

### **2.4.3 Fracture Mechanics**

Bazant and Cao (1987) used fracture mechanics, a theory which is based on energy and stability criteria instead of strength criteria to investigate the size effect on punching shear strength. The salient aspect of fracture mechanics is the size effect. The nominal stress at failure of geometrically similar structures decreases as the structure size increases for fracture mechanics. The model used was essentially a modified shear perimeter approach and it was assumed that the shear strength was directly proportional to the concrete strength. It is reported that the larger the slab thickness, the steeper the post-peak decline of the load deflection diagram; thus, the punching shear behaviour of thin slabs is closer to plasticity, and that of thick slabs is closer to linear elastic fracture mechanics. This independently confirms the applicability of the size-effect law, since this law predicts exactly such kind of behaviour.

### **2.4.4 Plasticity Model**

Salim and Sebastian (2002) presented plasticity model for predicting punching shear strengths of reinforced concrete slabs. The upper-bound theory of plasticity is employed to predict the punching shear failure loads of reinforced concrete slabs without shear reinforcement and without in-plane restraint. A parabolic Mohr failure criterion is adopted for the concrete to ensure that the important variation in angle of friction of the concrete with stress state is represented, with the material assumed to be rigid-perfectly plastic. The problem is treated as three-dimensional axisymmetric. It is found that the predictions correlate well with a range of experimental data for low, normal, and high strength

concretes, and for both small-scale and large-scale slabs. A theoretical solution for the punching shear strength of concrete slabs is presented by Bortolotti (1990). By applying the theory of plasticity, the form of the failure surface generatrix visualizes processes of strain softening by tension and compression in concrete. A comparison with the experimental results in literature shows that the theoretical equations are valid as long as the slabs are rigid enough to prevent displacements of the border of the slab. If border displacements and rotations are allowed, the theoretical values disagree with the experiment.

#### **2.4.5 Equivalent Frame Method**

Equivalent frame method was derived with the assumption that the analysis would be done using the moment distribution method. In the equivalent frame method the structure is divided for analysis, into continuous frames centered on the column lines and extending both longitudinally and transversely. Murray et al. (2003) proposes a modification to the ACI 318-02 equivalent frame method of analysis of reinforced concrete flat plate for exterior panels. Two existing code methods were examined viz, ACI 318-02 and BS 8110. The derivation of the torsional stiffness of the edge strip as proposed by ACI 318-02 is reviewed and a more accurate estimate of this value is proposed, based on both theoretical analysis and experimental results. The proposed method leads to a more accurate prediction of the moments in the plate at the column front face, at the panel midspan, and in the edge column. Robertson (1997) applied the effective width and equivalent frame analysis methods to a flat plate test specimen. The theoretical moment distribution and lateral drift show poor agreement with the test specimen results. A modified two-beam analytical model is proposed. The modified model is able to reproduce both the slab moment distribution and lateral drift observed in the test specimen.

#### 2.4.6 Miscellaneous Studies

Aghayere and MacGregor (1990a) developed a method of analysis for determining the load-deflection response of concrete plates simply supported on four edges and subjected to combined action of axial or eccentric in plane loads and transverse loads based on the assumed deflection method. In the assumed deflection method, a deflection function is assumed for the beam-column throughout the entire load range. A method of analysis is developed based on the assumed deflection method. In this way calculation of the strength of a plate is reduced to a one-degree of freedom problem. Material nonlinearities are taken into account using moment curvature relationships, which include tension-stiffening effects. The results from the analysis are compared to test results from an experimental program carried out by the authors. Good agreement was obtained for square simply supported plates and rectangular plates with an aspect ratio of 1.5.

Loo and Falamaki (1992) presented an analytical procedure for evaluating the punching shear strength of the corner and edge connections of reinforced concrete flat plates with spandrel beams. A comparative study is carried out based on the authors' own model test data and those published by others. The results indicate that the proposed analytical procedure is accurate and reliable. Regan and Jorabi (1988) have shown that analysis using current code provision and making separate calculations of full width shear strength and punching shear are inappropriate. It is proposed that design checks should be based on nominal shear stresses obtained as the sum of stresses arising from two components of load bearing action. The first is a symmetrical spreading of concentrated load and the second is the spanning of the slab carrying the spread load between supports.

## 2.5 Finite Element Method

In this method, the slab is divided into a number of subregions or finite elements, which are generally triangular, rectangular or quadrilateral in shape. They are considered interconnected only at discrete points, called nodes, at the corners of the individual elements.

The main problem in the application of the finite element method to linear elastic slab systems is to obtain a suitable force-displacement relationship between the nodal forces and the corresponding displacements at the nodal degrees of freedom. A further complication, in applying the method to reinforced concrete, is the derivation of a suitable set of constitutive relations to model the slab behavior under various loading conditions.

Modeling transverse shear by finite elements is one way of predicting behavior. In order to model transverse shear, proper finite element formulations must be used. For plate and shell structures this usually means using either three-dimensional elements or two-dimensional elements to model parts which can be approximated by such models. Three-dimensional elements are powerful and are an excellent choice for modeling details of the structure, but are inefficient for global analysis.

Gonzalez-Vidoso et al. (1988) used existing experimental data for reinforced concrete slabs failing in punching to validate a nonlinear finite element programme for concrete. The programme combines a general-purpose linear finite element analysis system called FINEL with a nonlinear iterative procedure based on the modified Newton-Raphson method and the residual-force concept. The iterative procedure incorporates constitutive laws describing the strength and deformational properties of concrete and steel, as well as criteria for the onset and propagation of the cracking process, which is treated following the

smear-crack approach. The constitutive model is implemented by following a standard stiffness approach. Reinforcing is implemented in the finite element model by smearing it in isotropic layers. The concrete-steel interaction is governed by the assumption of perfect bond. Isoparametric elements are used to model both concrete and steel. Theoretical predictions showed good agreement with actual ultimate loads, regimes of behavior, crack patterns, and experimentally available load-deflection curves.

Loo and Guan (1997) presented a nonlinear-layered finite element method capable of analyzing cracking and punching shear failure of reinforced concrete flat plates with spandrel beams or torsion strips. Incorporating a layered approach with transverse shear capabilities, the procedure takes into account the full interaction between cracking and failure analysis. The study is focused on the implementation of a non linear finite element procedure for determining both the deflection and the punching shear strength, at corner and edge-column connections of reinforced concrete flat plates with or without spandrel beams. Cracked concrete is treated as an orthotropic material using a smeared crack approach. Tension stiffening is included to represent the behaviour of cracked concrete in tension. A strain hardening plasticity approach is employed to model the compressive behaviour of concrete. An eight-node degenerated shell element with biquadratic serendipity shape functions is adopted in conjunction with the layered approach. The model makes use of the transverse shear deformations associated with the Mindlin hypothesis. A postprocessor has been developed to present in graphical form, the crack patterns, finite element mesh and configurations, as well as the deformed shape of the slab. This significantly enhances the presentation of the cracking and failure processes of reinforced concrete flat plates. A comparative study is carried out in an effort to verify the accuracy and reliability of the

proposed analytical procedure. Good correlation with the experimental results is observed.

Harmon and Zhangyuan (1989) analyzed transverse shear failures of reinforced concrete plates and shells using layered shell element that has been modified to model shear behavior more accurately. Three-dimensional failure criteria are used to predict transverse shear failure. The analytical results are compared with experimental results for beams, plates and shells subjected to concentrated forces. Good agreement between analysis and experiment is obtained for plates with and without shear reinforcement and for shells without reinforcement.

Polak (1998) examined the applicability of the finite element, layered, shell formation in the global analysis of reinforced concrete slabs when subjected to high concentrated transverse loads. A detailed finite element formulations based on the layered, degenerate shell elements is adapted, which can be used for the global analysis of plate-type structures and which accounts for the transverse shear effects. The layered approach, through the rigorous treatment of the states of strain and stress can model complex behavior of both thin and thick plates. The nonlinear solution algorithm is based on an iterative, full-load, secant stiffness formulation. The convergence criteria used are based on changes in deformations where displacements and rotations are examined separately. The formulation accounts for nonlinearities due to constitutive behavior and changing structural geometry. The results of finite element effective stiffness analyses are compared to both experimental results and the results in the layered analyses. Polak commends that the layered approach is a detailed, versatile and comprehensive approach to model nonlinear behavior of members subjected to bending. And the effective stiffness approach is simpler and less time consuming. For typical slab systems, the effective stiffness formulations can provide results with accuracy comparable to

the accuracy of the layered approach. Polak also checked the sensitivity of the proposed formulation when applied to the analysis of slabs with different reinforcement ratios, boundary conditions, and reinforcement orientations.

A model for predicting punching shear failures at interior slab-column connections was developed by Hueste and Wight (1999) based on experimental results obtained at various universities. This model has been incorporated into a new RC slab element for the nonlinear analysis program, DRAIN-2DM, along with the desired unloading behaviour when a punch occurs. The RC slab element was tested by modeling a four story RC frame building that experienced punching shear damage during the Northridge Earthquake. The observed punching shear failures were successfully post calculated using the RC slab element.

## **2.6 Punching Shear Prediction Equations**

All design codes give provisions for checking punching shear capacity. These are empirical relations based on experimental and analytical results. In general, the punching shear clauses are extensions of the beam shear provisions of codes. Besides, several researchers have put forward their prediction equations based on respective experimental and/or analytical results. Some of these equations and code provisions are summarized in the following subsections.

### **2.6.1 Regan's Equation**

Regan (1981) developed an equation to calculate punching shear capacity. Regan's shear perimeter for rectangular columns was a rounded rectangle located  $1.25d$  out from the column; for circular



columns, it was the circular perimeter located  $1.25d$  out from the column:

$$V_u = K_o K_{sc} K_s (p \times f'_c)^{1/3} \times d (\sum_c + 7.85d) \quad (2.6.1)$$

Where,

$V_u$  = ultimate shear force

$K_o = 0.13$  for normal density concrete

$K_{sc} = 1.15 \times [4\pi \times \text{column area} / (\text{column perimeter})^2]^{1/2}$

$K_s$  = size effect term  $(300/d)^{1/4}$  (SI units)

$p$  = steel ratio

$f'_c$  = concrete strength

$d$  = effective depth of slab, mm

$\sum_c$  = perimeter of the column

### 2.6.2 Bazant and Cao's Equation

Bazant and Cao (1987) were primarily concerned with size effects, but they did propose a formula for punching shear

$$v_u = C \left(1 + \frac{d}{\lambda_0 d_a}\right)^{-1/2} \quad (2.6.2)$$

in which

$$\text{constant } C = k_1 f'_c \left(1 + k_2 \frac{d}{b}\right) \quad (2.6.3)$$

Where,

$v_u$  = nominal shear stress at failure;

$f_t'$  = direct tensile strength of concrete;

$d_a$  = maximum aggregate size;

$\lambda_0$  = empirical parameter, 28.5;

$k_1, k_2$  = empirical constants, ( $k_1 = 0.155, k_2 = 0.35$ )

$b$  = diameter of punch; and

$d$  = slab thickness.

### 2.6.3 Gardner's Equation

Gardner recommended that the cube root relationship and shear perimeter approach of BS Code be adopted. Hence, it is recommended that a punching shear expression of the following form be adopted

$$v_c = 27.32[(p \times f_c')^{1/3} \times [(15.75/d)]^{1/4}] \quad (\text{U.S. units}) \quad (2.6.4)$$

Where,

$v_c$  = shear strength in psi;

$d$  = effective slab depth in inch;

$p$  = steel ratio; and

$f_c'$  = cylinder strength in psi

$$v_c = 0.99[(p \times f_c')^{1/3} \times [(400/d)]^{1/4}] \quad (\text{S.I. units}) \quad (2.6.5)$$

Where,

$v_c$  = shear strength in MPa;

$d$  = effective slab depth in mm;

$p$  = steel ratio; and

$f_c'$  = cylinder strength in MPa

The shear perimeter should be rectangular at a distance 1.5 times the effective slab depth outside the column.

### 2.6.4 Code Provision Equations

For the design of flat plates, flat slabs and column footings punching shear strength of concrete in the vicinity of columns, concentrated loads or reaction is one of the design criterion which governs the design. Thus, the critical shear section for this type of shear should be located so as the perimeter of critical section is a minimum, but need not approach closer than a certain distance from edge or corners of columns, concentrated load or reaction areas. Different Code provisions provide the location of this critical section differently. But for all the Codes, when this is done, the shear strength is taken almost independent of the column size, slab depth and span-to-depth ratio.

#### 2.6.4.1 ACI 318, 2002 Code Provisions

According to ACI 318-02 code, the critical section for shear in slabs subjected to bending in two directions follow the perimeter ( $b_o$ ) located at a distance  $d/2$  from the periphery of the concentrated load. It further assumes that the shear capacity of the concrete is proportional to the square root of the concrete strength. According to this Code, for non-prestressed slabs and footing, nominal punching shear strength provided by concrete ( $V_c$  in pound or Newton) shall be smallest of the following three equations;

In F.P.S. Unit:

$$V_c = (2 + 4/\beta_c) \sqrt{f'_c} b_o d \quad (2.6.6)$$

$$V_c = (2 + \alpha_s d/b_0) \sqrt{f'_c} b_0 d \quad (2.6.7)$$

$$V_c = 4 \sqrt{f'_c} b_0 d \quad (2.6.8)$$

In S.I. Unit:

$$V_c = (1 + 2/\beta_c) \sqrt{f'_c} b_0 d / 6 \quad (2.6.9)$$

$$V_c = (1 + 0.5\alpha_s d/b_0) \sqrt{f'_c} b_0 d / 6 \quad (2.6.10)$$

$$V_c = 0.33 \sqrt{f'_c} b_0 d \quad (2.6.11)$$

Here,

$\beta_c$  = ratio of long side to short side of concentrated load or reaction area.

$f'_c$  = uniaxial cylinder strength of concrete in psi or MPa.

$b_0$  = perimeter of critical section of slab or footing at a distance of  $d/2$  away from the column faces in inch or mm.

$d$  = Effective depth ( distance from extreme compression fiber to centroid of longitudinal tension reinforcement) in inch or mm.

$\alpha_s$  = 40 for interior column, 30 for edge column, 20 for corner column.

#### 2.6.4.2 British ( BS 8110, 1985) Code Provisions

The punching shear requirements of the current British Standard BS 8110: (1985) are very similar to those proposed by Regan. According to BS 8110: (1985) Code the critical shear perimeter is taken as a rectangle

located at a distance of  $1.5d$  from the edge of column regardless of whether the columns are rectangular or circular in section and punching shear strength of concrete is given by the following equation;

$$V_p = 0.79 \sqrt[3]{100\rho} \sqrt[3]{f_{cu}/25} \sqrt[3]{400/d} \{4(c+3d)\}d \quad (2.6.12)$$

Where,

$\rho \leq 3.0$  percent,  $400/d \geq 1.0$  and  $f_{cu} \leq 40$  MPa

$V_p$  = punching shear strength in Newton ( N)

$\rho$  = reinforcement ratio in percentage.

$f_{cu}$  = uniaxial, cube ( compressive) strength of concrete in MPa.

$c$  = width of column or side length of loaded area in mm.

$d$  = effective depth in mm.

#### 2.6.4.3 Canadian (CAN3-A23.3-M84,1984) Code Provisions

According to CAN3-A23.3-M84 (1984) Code, the punching shear strength is evaluated at the critical section which is assumed to be located at a distance  $d/2$  from the periphery of the concentrated load. The punching shear strength provided by the concrete is given by the following equation,

$$V_p = 0.4 \sqrt{f'_c} b_o d \quad (\text{S.I. unit}) \quad (2.6.13)$$

Where,

$V_p$  = Punching shear strength provided by concrete in Newton(N)

$f'_c$  = Ultimate cylinder strength of concrete in MPa

$b_o$  = Perimeter of critical section of slab or footing in mm

$d$  = Effective depth in mm.

#### 2.6.4.4 European( CEB-FIP,1978) Code Provisions

According to CEB-FIP (1978) Code, the critical section for punching shear follows the perimeter ( $b_0$ ) located at a distance  $d/2$  from the periphery of the concentrated load. The punching shear strength provided by the concrete is given by the following equation,

$$V_p = v_c b_0 d \quad (2.6.14)$$

Where,

$V_p$  = Punching shear strength provided by concrete in Newton(N)

$b_0$  = Perimeter of critical section of slab or footing in mm

$d$  = Effective depth in mm.

$v_c$  = concrete shear strength in MPa given by :

$$v_c = 1.6\tau_{rd}k(1 + \rho/2)$$

Here,

$$\tau_{rd} = 0.075(f'_c)^{2/3}$$

$f'_c$  = Ultimate cylinder strength of concrete in MPa

$$k = (1.6 - d/1000) \geq 1.0$$

$$\rho \leq 0.8 \text{ percent}$$

### 2.6.4.5 Bangladesh (BNBC, 1993) Code Provisions

According to this Code, for non-prestressed slabs and footing, the critical section for shear in slabs subjected to bending in two directions follow the perimeter ( $b_0$ ) located at a distance  $d/2$  from the periphery of the concentrated load. According to this Code, for non-prestressed slabs and footing, nominal punching shear strength provided by concrete ( $V_c$  in Newton) shall be smallest of the following three equations;

$$V_c = 0.17(1 + 2/\beta_c)\sqrt{f'_c}b_0d \quad (2.6.15)$$

$$V_c = 0.17(1 + \alpha_s d/b_0)\sqrt{f'_c}b_0d \quad (2.6.16)$$

$$V_c = 0.33\sqrt{f'_c}b_0d \quad (2.6.17)$$

Here,

$\beta_c$  = Ratio of long side to short side of concentrated load or reaction area.

$f'_c$  = Uniaxial cylinder strength of concrete in MPa.

$b_0$  = Perimeter of critical section of slab or footing  $d/2$  out from the column in mm.

$d$  = Effective depth in mm.

$\alpha_s$  = 20 for interior column, 15 for edge column, 10 for corner column.

### 2.6.5 Concluding Remarks

Provisions of punching shear strength of British Standard BS 8110: 1985 and those proposed by Regan are very similar. According to BS 8110 (1985) Code, the critical shear perimeter is taken as a rectangle

located at a distance of  $1.5d$  from the edge of column regardless of whether the columns are rectangular or circular in section and Regan's shear perimeter for rectangular columns was a rounded rectangle located  $1.25d$  out from the column; for circular columns, it was the circular perimeter located  $1.25d$  out from the column. For all other codes, the punching shear strength is evaluated at the critical section, which is assumed to be located at a distance  $d/2$  from the periphery of the concentrated load. It is to be further noted that BNBC (1993) adopted ACI Code with minor modification.



## Chapter 3

### FINITE ELEMENT MODELING

#### 3.1 Introduction

With the advent of sophisticated numerical tools for analysis like the finite element method (FEM), it has become possible to model the complex behaviour of reinforced concrete plates. The actual work regarding the finite element modeling of reinforced concrete plate has been described in this chapter. Representation of various physical model with the finite elements, properties assignment to them, representation of various physical phenomenon etc. have been discussed in relation to the package software used in this study.

#### 3.2 The Finite Element Packages

A number of good finite element analysis computer packages are available in the field of civil engineering. They vary in degree of complexity, usability and versatility. Some of such packages are:

- ABAQUAS      ● ADINA              ● ANSYS              ● DIANA              ● FEMSKI
- MARC              ● Micro Feap              ● SAP 90              ● STAAD              ● STRAND

A few of these programs are intended for a special type of structure. For example Micro Feap P1 is developed for the analysis of plane frames and truss while Micro Feap P2 is for the analysis of slab and grid system. Of these, the package ANSYS has been used in this study for its relative ease of use, detailed documentation, flexibility and vastness of its capabilities. The version of ANSYS has been used was the special Student's Edition.

### 3.3 An Overview of ANSYS

The ANSYS programme was introduced in 1970, by Swanson Analysis System (1995). Since then ANSYS Support Distributors have grown as part of a commitment to provide latest finite element analysis and design technology to engineers, worldwide. ANSYS capabilities can be utilized in computers that range from PCs to super main frames. ANSYS is a general-purpose programme constantly updated with new features, enhancements of existing features, and error corrections. The version of the programme followed in this research work, is Revision 5.4.

ANSYS is one of the most powerful and versatile packages available for finite element structural analysis. The term structural implies not only civil engineering structures such as bridges and buildings, but also naval, aeronautical and mechanical structures such as ship hulls, aircraft bodies, and machine housings as well as mechanical components such as pistons, machine parts and tools. The primary unknowns (nodal degrees of freedom) calculated in a structural analysis are displacements. Other quantities such as strains, stresses, and reaction forces, are then derived from the nodal displacements. Especially, its graphical representations are very distinct.

A typical ANSYS analysis has three distinct steps:

Build the model.

Apply loads and obtain the solution.

Review the results.

Building a finite element model requires more of an ANSYS user's time than any other parts of the analysis. At first a job name and a 'title of the analysis' needs to be specified. Then the element types, element real

constants, material properties and model geometry with boundary conditions are defined. Depending on the application, material properties may be linear or nonlinear, isotropic, anisotropic, orthotropic, constant temperature or temperature dependent. Once material properties have been defined, the next step in an analysis is generating a FE mesh with nodes and elements that adequately describe the model geometry. Applied loads are prescribed at appropriate location on element and nodes and then solved for nodal unknowns. After obtaining the solution the result of the ANSYS analysis can be reviewed with postprocessors.

ANSYS programme is user friendly. It has a comprehensive graphical user interface (GUI) that gives user easy, interactive access to program functions, commands, documentations and reference material. An intuitive menu system helps user to navigate through the ANSYS programme. User can input data using a mouse, a keyboard or a combination of both.

### **3.4 Modeling of Reinforced Concrete Plate**

Reinforced concrete plate, speaking in a very common sense, is a mass of hardened concrete with steel reinforcement embedded within it. This arrangement when in use acts as a single material with the steel providing adequate tensile capacity to concrete, which has high compression capacity. However, the interaction between the concrete mass and the steel reinforcement is not very simple, when subjected to various loading conditions. Complicated physical phenomenon such as bond slip, anchorage failure etc comes into play at different condition. Hence the whole of reinforced concrete may not be treated as a single material during FEM analysis and may not be modeled as a unique composite material.

In nonlinear modelling of reinforced concrete an appropriate material model is usually the most critical factor for successful and accurate analysis. Many constitutive models based on plasticity and nonlinear elasticity have been proposed. The modelling of reinforced concrete, as outlined in this thesis, used separate materials and elements for the concrete and steel reinforcement. Concrete is defined by 3-D solid elements and steel is embedded in concrete with the help of link elements. Although 3-D solid element with provisions for reinforcement could have been used, it was not used in the modelling. The separate treatment in the element level ensures better approximation of the actual condition. This option was favoured over the alternative smeared stiffness capability as it allowed the reinforcement to be precisely located whilst maintaining a relatively coarse mesh for the surrounding concrete medium. The inherent assumption is that there is full displacement compatibility between the reinforcement and the concrete and that no bond slippage occurs.

To develop a realistic model link elements are used as discrete reinforcement connecting solid element nodes rather than smeared reinforcement. In this study, perfect bond between materials is assumed. To provide the perfect bond, the link elements for the steel reinforcing are connected between nodes of each adjacent concrete solid element, so that the two materials share the same nodes. The nonlinear effects due to the cracking and crushing of concrete and the yielding of steel reinforcement has been included. The concrete cracking is modeled as a smeared crack, in the sense that it would not track individual macro cracks. An incremental finite element technique is used which simulates the nonlinear load-deflection behaviour of reinforced concrete structure.

#### **3.4.1. Element Types Adopted**

For representing the concrete, an eight-node solid element Solid 65, was used. The solid element has eight nodes with three degrees of freedom

at each node viz translations in the nodal  $x$ ,  $y$ , and  $z$  directions. The element is capable of plastic deformation, cracking in three orthogonal directions, and crushing. The most important aspect of this element is the treatment of nonlinear material properties. The geometry, node locations, and the coordinate system for this element are shown in Figure 3.4.1. The element is defined by eight nodes and the isotropic material properties.

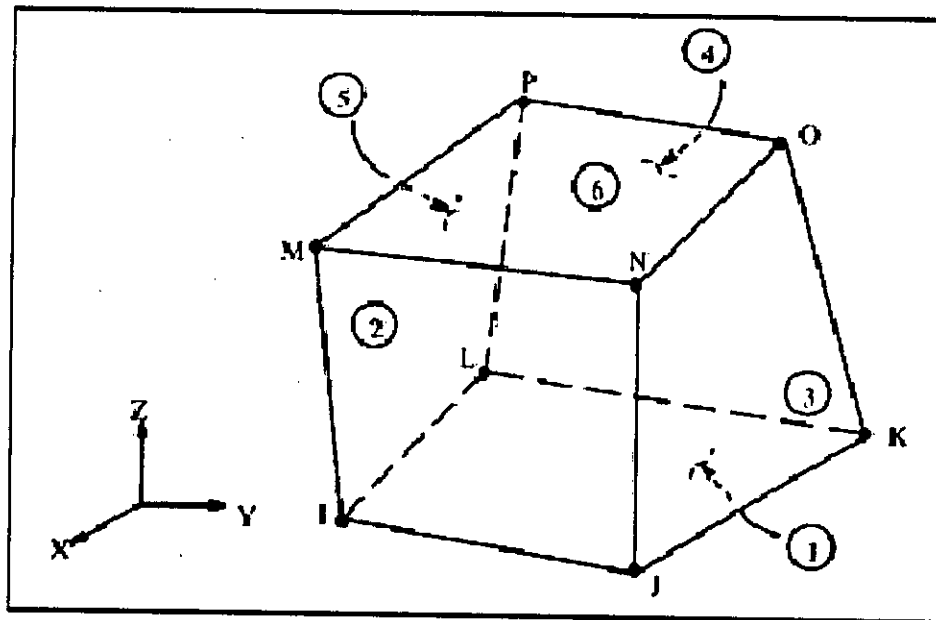


**Figure 3.4.1** Eight-node Solid 65 Element

The steel for the finite element models is assumed as an elastic-perfectly plastic material and identical in tension and compression. The internal reinforcement is modeled using three dimensional spar elements Link 8 with plasticity. Two nodes are required for this element. Each node has three degrees of freedom, translation in the nodal  $x$ ,  $y$ , and  $z$  directions. The element is also capable of plastic deformation. The geometry and node locations for this element type are shown in Figure 3.4.2.

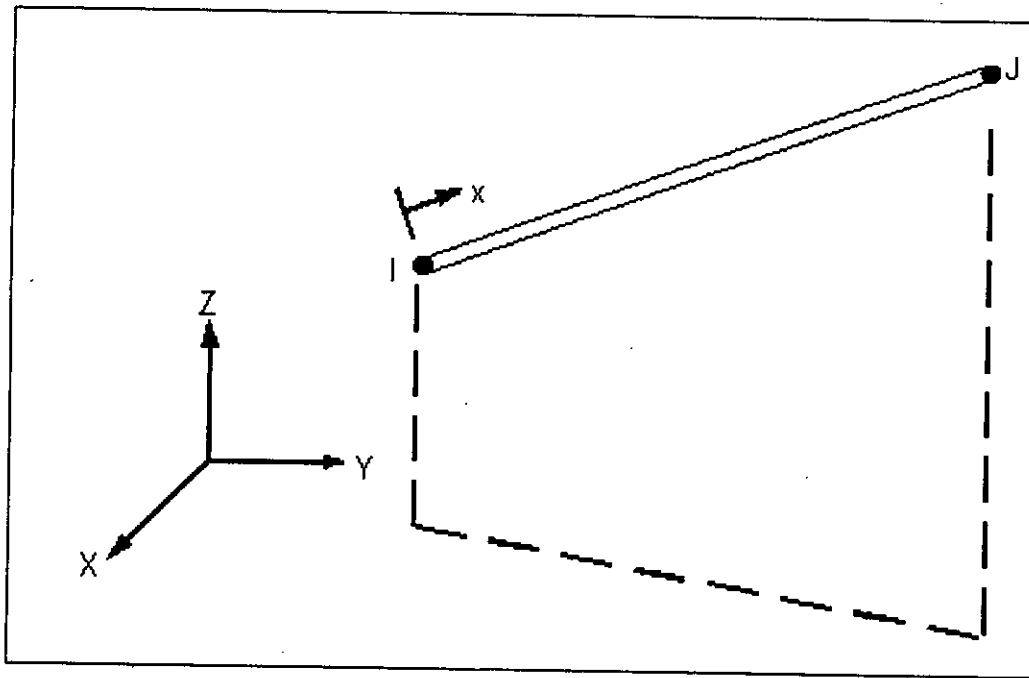


**Figure 3.4.2** Two-node Link 8 Element

### 3.4.2 Element Performance

Before adopting the aforementioned elements in the Reinforced Concrete Plate model, their performance in tracing load-deflection response is checked with other alternative ANSYS elements and Timoshenko Theory of Plate solution within elastic limit. For this purpose a square plate has been modelled with different types and varying number of elements. Four-node shell element (Shell 63), eight-node shell (Shell 93), eight-node brick (Solid 65) and twenty-node brick (Solid 95) elements with mesh 8x8, 10x10, 12x12, 16x16, 20x20, 24x24 and 32x32 were used.

The other parameters used are as follows:

- Plate dimension is 120 in × 120 in × 6 in

- $E_c = 3 \times 10^6$  psi
- Poisson's ratio,  $\nu = 0.15$
- The applied load on the plate is 10 psi

The deflection of square plates with all edges built in (Timoshenko Theory of Plates) is calculated by the formula:

$$U = \frac{0.00126qa^4}{D} \quad (3.4.1)$$

where,

$U$  = total deflection of plate

$q$  = applied pressure

$a$  = span length of the plate

$$D = \frac{Eh^3}{12(1-\nu^2)}$$

$h$  = thickness of the slab.

The vertical deflections from the FE analysis have been compared with the one calculated using Equation. 3.4.1 for various element types. The result is presented in Figure 3.4.3 It has been observed that the variations of theoretically computed deflection with the corresponding values predicted by FE analysis is about 3 percent only and may be considered acceptable for all practical purposes.

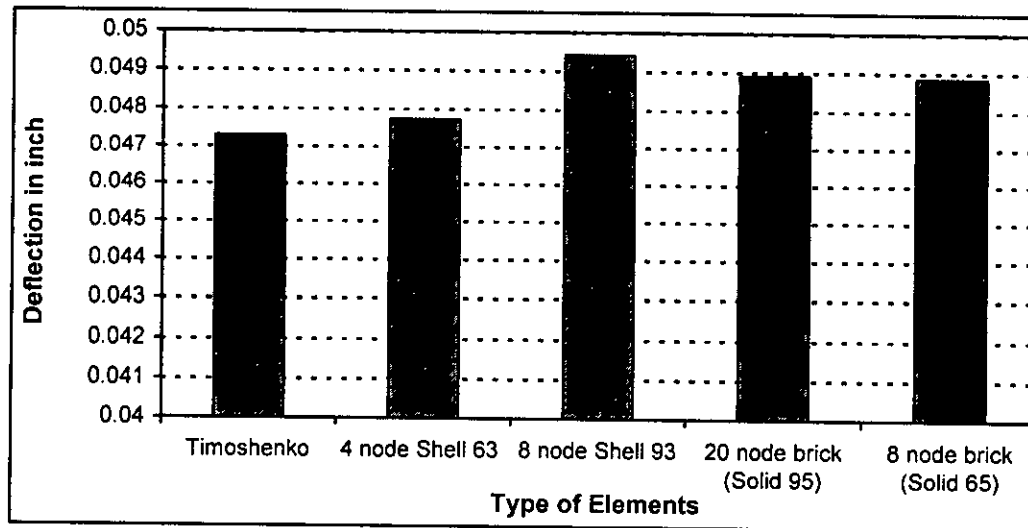


**Figure 3.4.3** Comparison of Deflection of Various FE Elements with Theoretical Prediction

The variations of deflection with number of elements used in the analysis for different element types have been presented in the Figure 3.4.4.

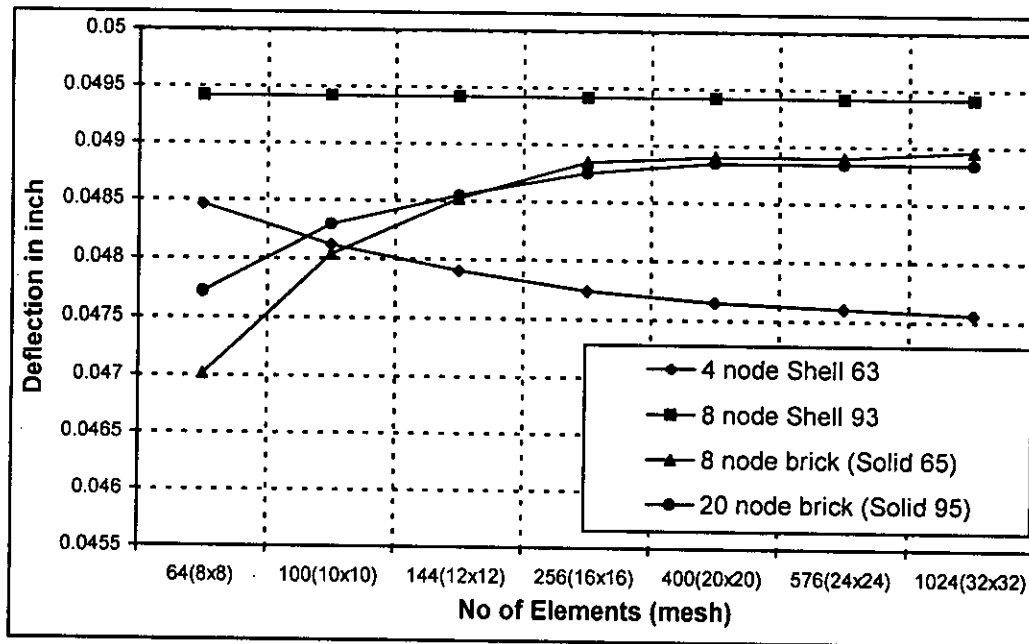


**Figure 3.4.4** Variation of Deflection with number of Elements for Different Element Types



It can be observed that the change in deflection as element mesh increase beyond 20x20 size is small and consistent for all element types. Considering the usefulness of 3-D element for reinforced concrete, 8-node brick (Solid 65) element is chosen.

Next, the performance of Solid 65 element is checked with respect to number of layers across the thickness. Then a 1/4 th of the layered model has been discretised and checked for performance. Figure 3.4.5 shows that the variation is within acceptable limit. Finally, the effect of reinforcement in plate was included using link element available with ANSYS. The difference of maximum deflection with and without link is only 0.001 inch in the elastic range of study. As such 8-node brick (Solid 65) element and Link 8 elements are adopted here for modeling reinforced concrete plate behaviour.

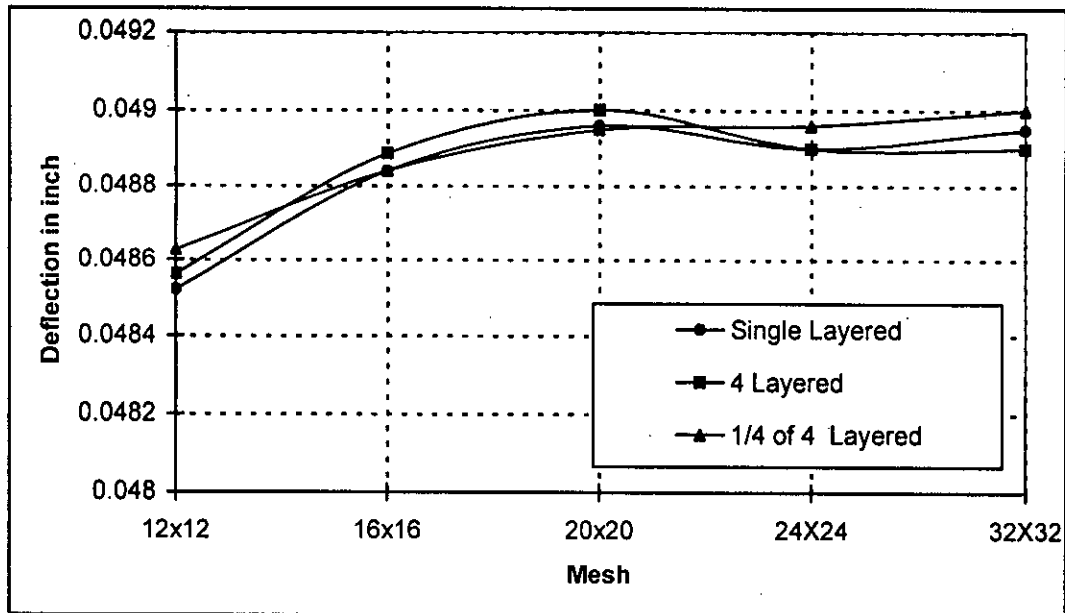


**Figure 3.4.5** Variation of Deflection of Solid 65 Element

### 3.4.3 Material Properties

An understanding of the materials characteristics and behaviour under load is fundamental to understanding the performance of structural concrete. Performance of a structure under load depends to a large degree on the stress-strain relationship of the material from which it is made, under the type of stress to which the material is subjected in the structure. In ANSYS, depending on the application, material properties may be:

- Linear or nonlinear
- Isotropic, orthotropic, or anisotropic
- Constant temperature or temperature-dependent.

Material properties for the constituent model are described in the following subsection.

#### 3.4.3.1 Concrete

Development of a material model for the behaviour of concrete is not a straightforward task. Concrete is a quasi-brittle material and has different behaviour in compression and tension. The tensile strength of concrete is typically 8 to 15 % of the compressive strength [Shah, et al. (1995)]. Figure 3.4.6 shows a typical stress-strain curve for normal weight concrete [Bangash (1989)].

In compression, the stress-strain curve for concrete is linearly elastic up to about 30 percent of the maximum compressive strength. Above this point, the stress increases nonlinearly up to the maximum compressive strength. Beyond the maximum compressive strength  $\sigma_{cu}$ , the curve descends into a softening region, and eventually crushing failure occurs

at an ultimate strain of  $\epsilon_{cu}$ . In tension, the stress-strain curve for concrete is approximately linearly elastic up to the maximum tensile strength. After this point, the concrete cracks and the strength decreases gradually to zero [Bangash (1989)].

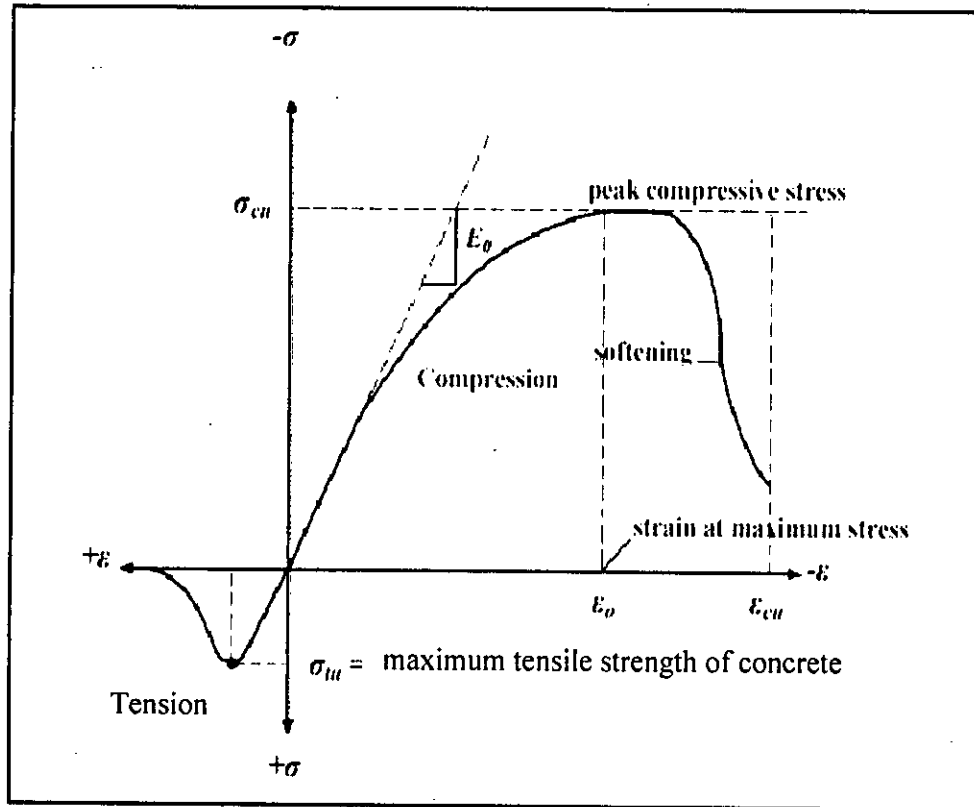


**Figure 3.4.6** Typical Uniaxial Compressive and Tensile Stress-Strain Curve for Concrete [Bangash (1989)]

For concrete, ANSYS require input data for material properties as follows:

Elastic modulus ( $E_c$ ).

Ultimate uniaxial compressive strength ( $f'_c$ ).

Ultimate tensile strength (modulus of rupture,  $f_t$ ).

Poisson's ratio ( $\nu$ ).

Shear transfer coefficient ( $\beta_t$ ).

Compressive uniaxial stress-strain relationship for concrete.

The modulus of elasticity ( $E_c$  in psi units), i.e., the slope of the initial straight portion of the stress-strain curve, is seen to be larger the higher the strength of the concrete [Nilson (1997)]. For normal sand and stone concretes,  $E_c$  is computed with reasonable accuracy from the empirical equation found in the ACI Code:

$$E_c = 57500\sqrt{f'_c} \quad (3.4.2)$$

For compressive strengths in the range from 6000 to 12000 psi, the ACI Code equation overestimates  $E_c$  for both normal weight and lightweight material by as much as 20 percent [Nilson (1997)]. Numerical expression, Equation 3.4.3 [Nilson (1997)] is used for normal density concretes with  $f'_c$  in the range of 3000 to 12000 psi:

$$E_c = (40,000\sqrt{f'_c} + 1,000,000) \left( \frac{w_c}{145} \right)^{1.5} \quad (3.4.3)$$

where  $w_c$  is the unit weight of the hardened concrete in pcf.

Value of ultimate uniaxial compressive strength ( $f'_c$ ) is obtained from the test data of Elstner and Hognestad (1956).

Modulus of rupture ( $f_r$ ) is calculated by Equation 3.4.4 (ACI 318-99):

$$f_r = 7.5\sqrt{f'_c} \quad (3.4.4)$$

At stresses lower than about  $0.7 f'_c$ , Poisson's ratio for concrete fall within the limits of 0.15 to 0.20 [Nilson (1997)]. In this study Poisson's ratio for concrete is assumed to be 0.17.

The shear transfer coefficient,  $\beta_t$ , represents conditions of crack face transmitting shear due to aggregate interlock. Based on a number of trials,  $\beta_t$  was set equal to 0.35. Shear transfer coefficient is discussed in detail in Chapter 4, Article 4.2.4.

A summary of the concrete properties used in this finite element modeling study is shown in Table 3.4.1. For this purpose five slabs from Elstner and Hognestad (1956) were taken as reference. Other parameters of the test slabs are shown in Table 3.4.2. It is to be noted that the ratio of the longitudinal reinforcement is applicable for the entire slab.

**Table 3.4.1** Concrete Material Properties Used

Plate No.	$E_c$ (ksi)	$f'_c$ (psi)	$f_r$ (psi)	$v$	$\beta_t$
A-1a	2597	2040	339	0.17	0.35
A-7	3659	4050	477	0.17	0.35
A-7b	3659	4050	477	0.17	0.35
B-14	4922	7330	642	0.17	0.35
B-16	4922	7330	642	0.17	0.35

**Table 3.4.2** Details of Slabs Tested by Elstner and Hognestad (1956)

Slab No.	$h$ inch	$d$ inch	$d_{punch}$ inch x inch	$f_y$ ksi	Longitudinal Reinforcement	
					Tension Mat $\rho$ percent	Compression Mat $\rho$ percent
A-1a	6.00	4.63	10 x 10	48.20	1.15	0.56
A-7	6.00	4.50	10 x 10	46.60	2.47	1.15
A-7b	6.00	4.50	10 x 10	46.60	2.47	1.15
B-14	6.00	4.50	10 x 10	47.20	3.00	----
B-16	6.00	4.50	10 x 10	47.20	3.00	----

To construct the uniaxial compressive stress-strain curve for concrete in this study, numerical expressions [Desayi and Krishnan (1964)], Equation 3.4.5 and 3.4.6, were used along with Equation 3.4.7 [Gere and Timoshenko (1997)].

$$f = \frac{E_c \varepsilon}{1 + (\varepsilon / \varepsilon_0)^2} \quad (3.4.5)$$

$$\varepsilon_0 = \frac{2f'_c}{E_c} \quad (3.4.6)$$

$$E_c = \frac{f}{\varepsilon} \quad (3.4.7)$$

Where:

$f$  = stress at any strain  $\varepsilon$ , psi

$\varepsilon$  = strain at stress  $f$

$\varepsilon_0$  = strain at the ultimate compressive strength  $f'_c$

Figure 3.4.7 shows the typical compressive uniaxial stress-strain relationship that was used in this study. The curve starts at zero stress and strain. Point no. 1, at  $0.30 f'_c$ , is calculated for the stress-strain relationship of the concrete in the linear range (Equation 3.4.4). The last point is at  $\varepsilon_0$  and  $f'_c$ . The remaining points are obtained from Equation 3.4.2, in which  $\varepsilon_0$  is calculated from Equation 3.4.3. A perfectly plastic behaviour is assumed after the last point.

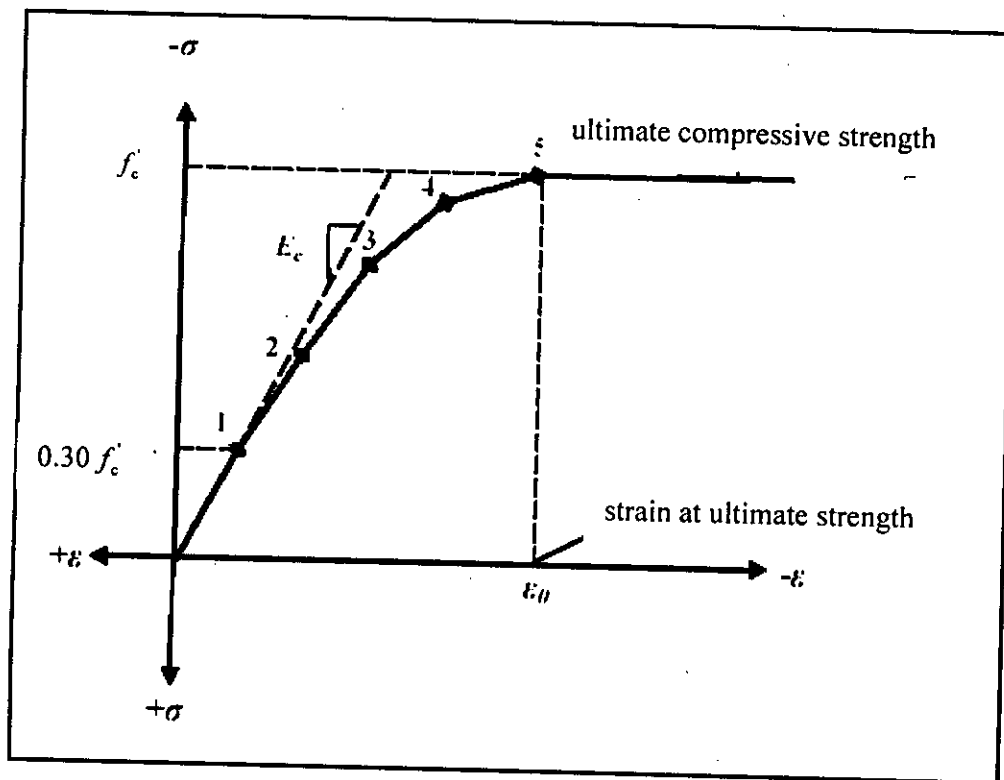


**Figure 3.4.7** Concrete Stress-Strain Curve

### 3.4.3.2 Steel Reinforcement

The steel for the finite element model is assumed as an elastic-perfectly plastic material and identical in tension and compression. The properties, i.e., elastic modulus and yield stress, for the steel reinforcement used in this study follow the design material properties used for the experimental investigation as shown in Table 3.4.2 [Eltner and Hognestad (1956)]. Poisson's ratio of 0.3 was assumed for steel reinforcement. Figure 3.4.8 shows typical stress-strain relationship for steel reinforcement.

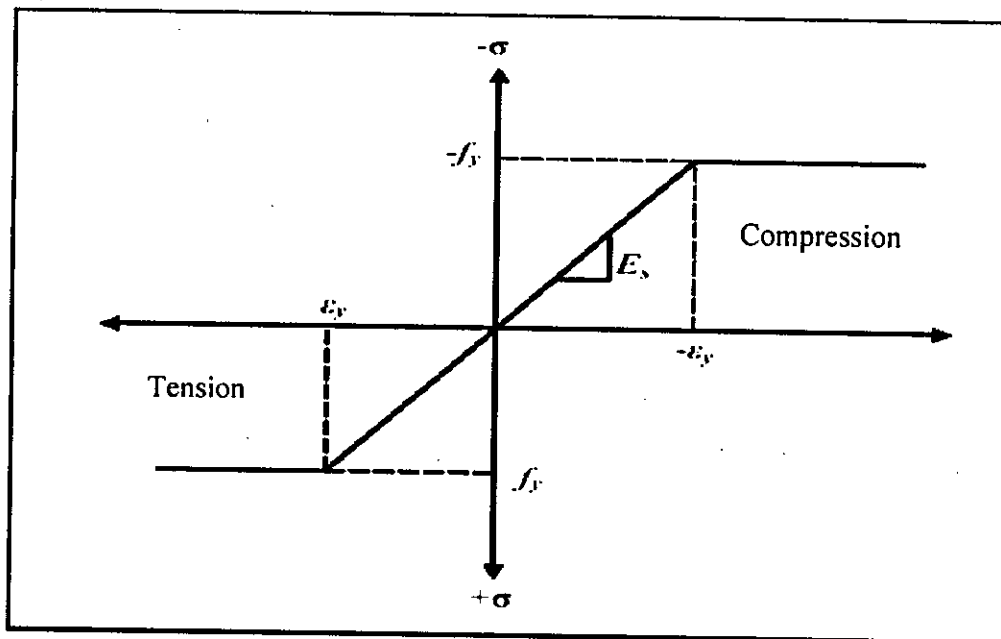


**Figure 3.4.8** Idealised Stress-Strain Curve for Steel Reinforcement

#### 3.4.4 Failure Criteria for Concrete

The element includes a smeared crack analogy for cracking in tension zones and a plasticity algorithm to account for the possibility of concrete crushing in compression zones. Each element has nine sampling points (The Gaussian integration points) at which cracking and crushing checks are performed. The element behaves in a linear elastic manner until either of the specified tensile or compressive strengths are exceeded. Cracking or crushing of an element is initiated once one of the element principal stresses, at an element integration point, exceeds the tensile or compressive strength of the concrete. Cracked or crushed regions, as opposed to discrete cracks, are then formed perpendicular to the relevant principal stress direction with stresses being redistributed locally. The element is thus nonlinear and requires an iterative solver. In the numerical routines the formation of a crack is achieved by the modification of the stress-strain relationships of the element to introduce



a plane of weakness in the requisite principal stress direction. The amount of shear transfer across a crack can be varied between full shear transfer and no shear transfer at a cracked section. The crushing algorithm is akin to a plasticity law in that, once a section has crushed any further application of load in that direction develops increasing strains at constant stress. Subsequent to the formation of an initial crack, stresses tangential to the crack face may cause a second, or third, crack to develop at an integration point.

The model is capable of predicting failure for concrete materials. Both cracking and crushing failure modes are accounted for. The two input strength parameters i.e., ultimate uniaxial tensile and compressive strengths are required to define a failure surface for concrete. Consequently, a criterion for failure of concrete due to a multiaxial stress state can be calculated [William and Warnke (1975)].

A three-dimensional failure surface for concrete adopted in this study is shown in Figure 3.4.9. The most significant nonzero principal stresses are in the x and y directions, represented by  $\sigma_{xp}$  and  $\sigma_{yp}$ , respectively. Three failure surfaces are shown as projections on the  $\sigma_{xp} - \sigma_{yp}$  plane. The mode of failure is a function of the sign of  $\sigma_{zp}$  (principal stress in the z direction). For example, if  $\sigma_{xp}$  and  $\sigma_{yp}$  are both negative (compressive) and  $\sigma_{zp}$  is slightly positive (tensile), cracking would be predicted in a direction perpendicular to  $\sigma_{zp}$ . However, if  $\sigma_{zp}$  is zero or slightly negative, the material is assumed to crush (ANSYS 1997). In a concrete element, cracking occurs when the principal tensile stress in any direction lies outside the failure surface. After cracking, the elastic modulus of the concrete element is set to zero in the direction parallel to the principal tensile stress direction. Crushing occurs when all principal stresses are compressive and lie outside the failure surface.

Subsequently, the elastic modulus is set to zero in all directions (ANSYS 1997), and the element effectively disappears.

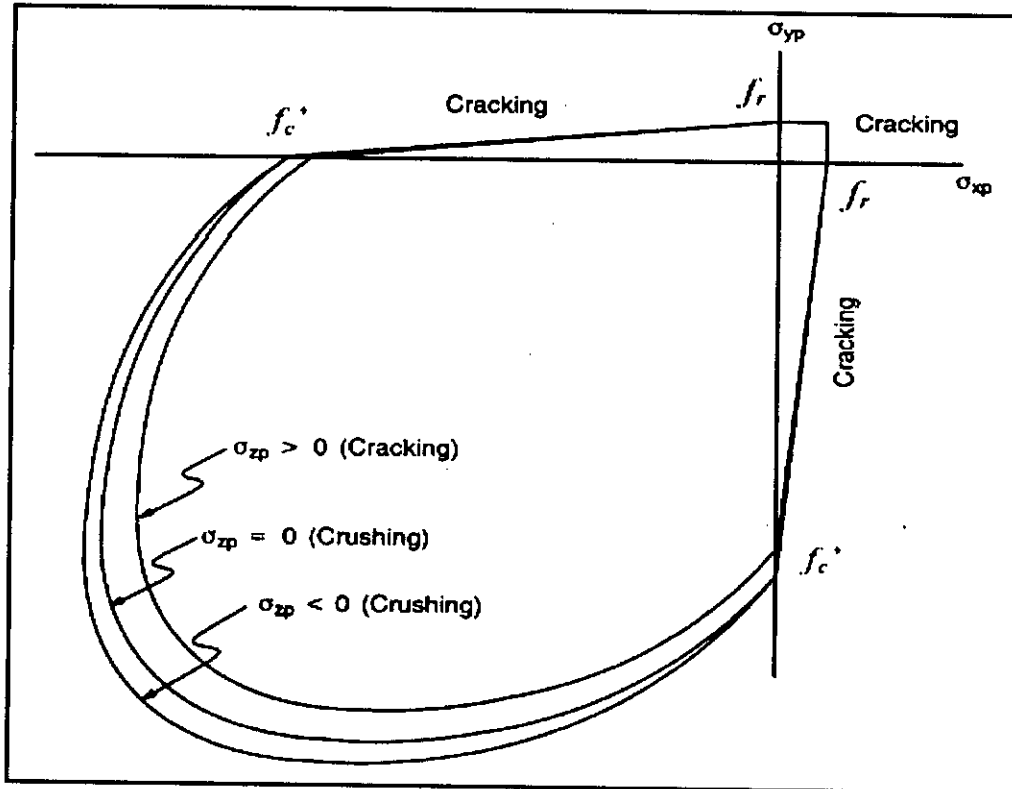


**Figure 3.4.9** Failure Surface of Concrete in 3-D

### 3.4.5 Loading and Boundary Conditions

The finite element models are loaded at the same locations as the test slab of Elstner and Hognestad (1956). A typical section of the test slab is shown in Figure 3.4.10. In the experiment, the column stub dimension used for loading was 10" x 10" and the slabs were restrained in the vertical direction over supports. To study the effect of varying support condition a full-size plate with dimensions of 70" x 70" x 6" is used for finite element model as shown in Figure 3.4.11. Different support condition along with the applied loading is shown in Figure 3.4.12. The plates are supported at the edges and loaded through a centrally located

column stub of 10" x 10" as indicated in the figure. In the FE model, the boundary condition of  $U_y=0$  along the supports is used to simulate the test condition. Typical reinforcement for tension and compression mat are shown in Figure 3.4.13 and 3.4.14 respectively. Figure 3.4.15 includes tension, compression and column stub reinforcement, all in one figure.

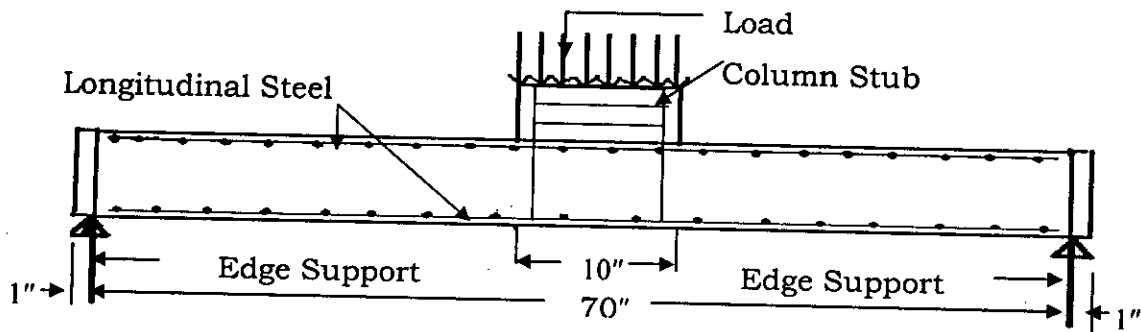


**Figure 3.4.10** A Test Slab Section of Elstner and Hognestad (1956)

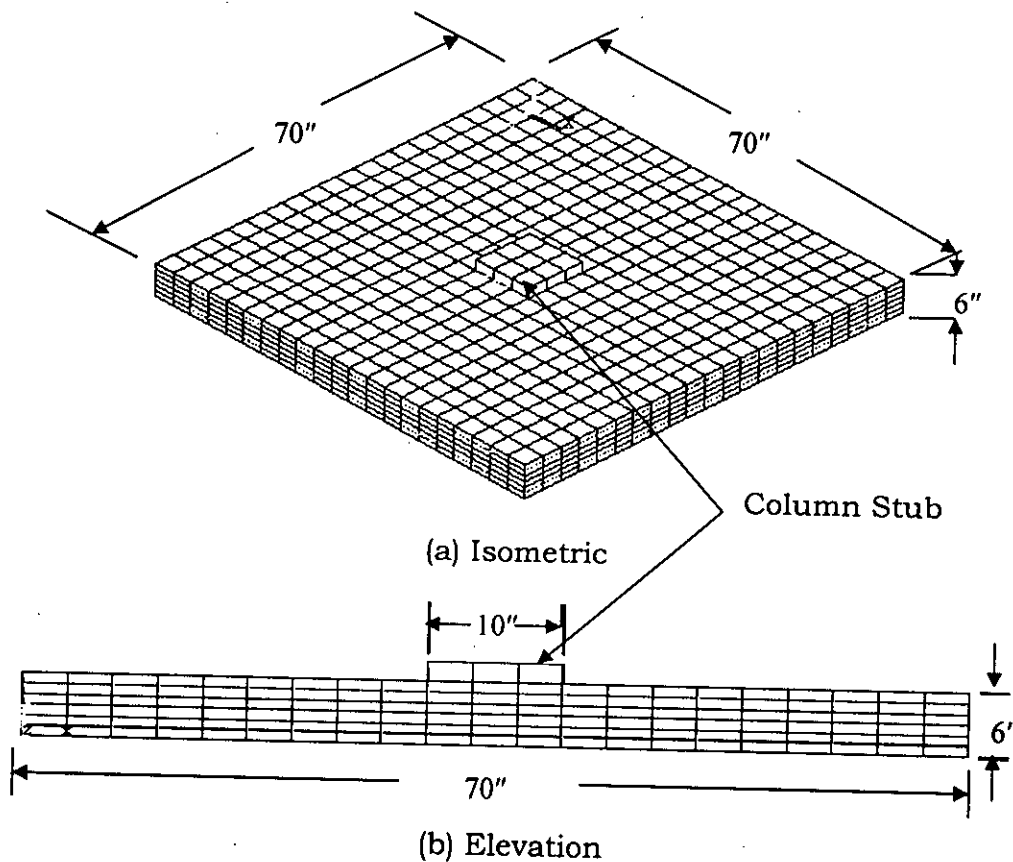
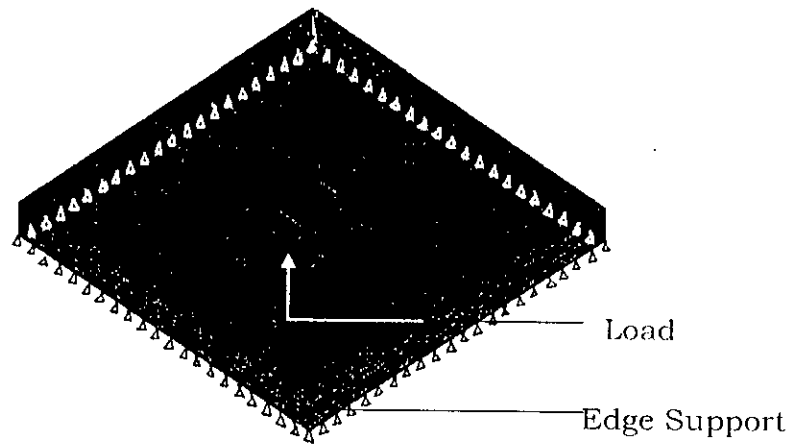
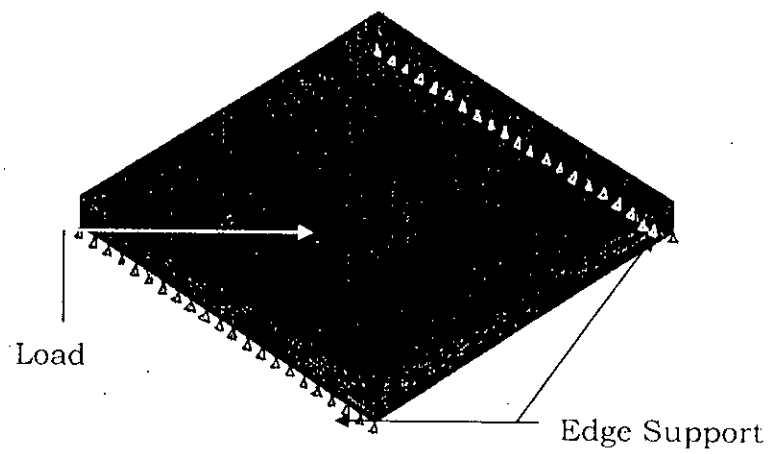


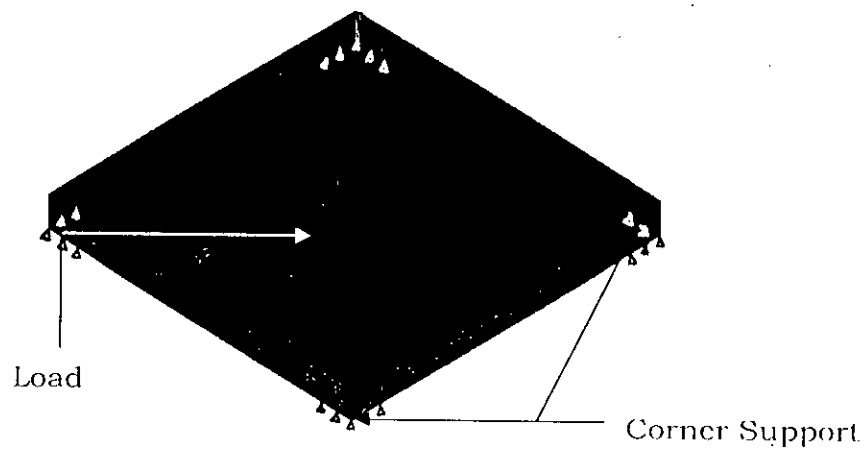
**Figure 3.4.11** Typical Finite Element Model of the Plate



(a) Symmetrical Support on Four Edges



(b) Symmetrical Support on Two Opposite Edges



(c) Symmetrical Support on Four Corners

**Figure 3.4.12** Plates With Different Boundary Conditions and Loading

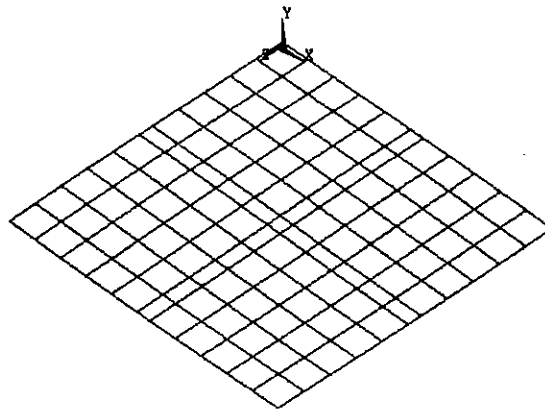


**Figure 3.4.13** Typical Tension Reinforcement Mat

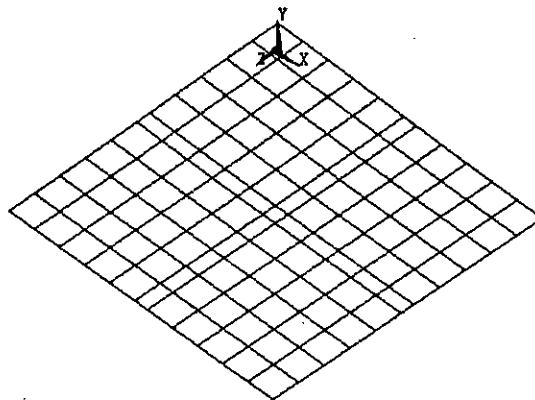


**Figure 3.4.14** Typical Compression Reinforcement Mat

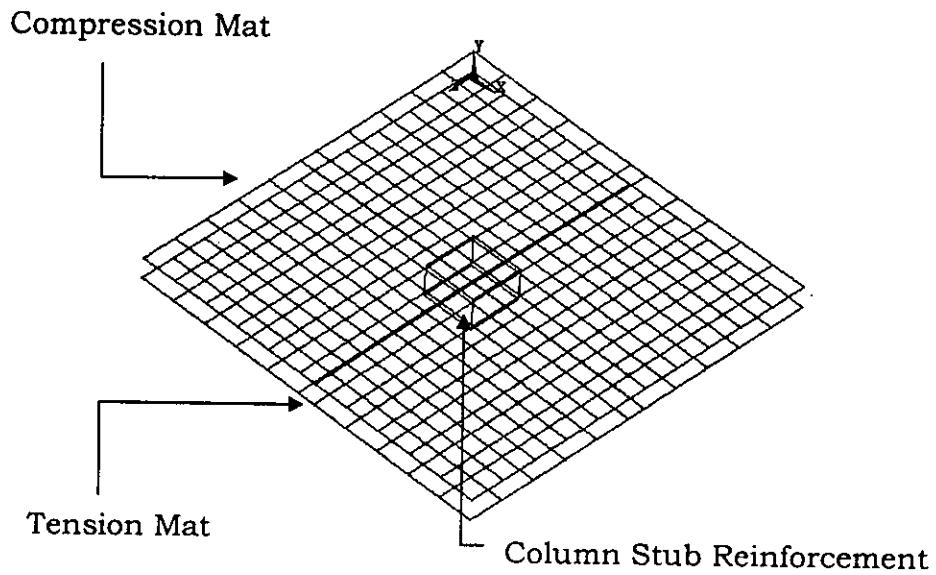


**Figure 3.4.15** Typical Tension, Compression and Column Stub Reinforcement

Handwritten mark or signature.

### 3.4.6 Finite Element Discretisation (Mesh Sensitivity)

As an initial step, a finite element analysis requires mapping of the actual structure using finite elements forming element mesh. In other words, the model is divided into a number of small elements, and after loading, stress and strain are calculated at integration points of these small elements. An important step in finite element modeling is the selection of the mesh density. A convergence of results is obtained when an adequate number of elements are used in a model. This is practically achieved when further increase in the mesh density has negligible effect on the results. It has been observed that for a particular problem the results often vary up to a certain number of elements and after that result becomes more or less constant. From the element performance a preliminary idea can be formed for required meshing. Optimum meshing was checked for elastic analysis subject to constant load from the plot of centre deflection versus number of mesh as shown in Figure 3.4.16. The figure shows that the difference in deflection was negligible when mesh density increased from 21x21 to 28x28. Therefore, the 21x21 mesh model with 6 layers across the thickness has been selected resulting in a total 2646 brick elements to discretise the plate.

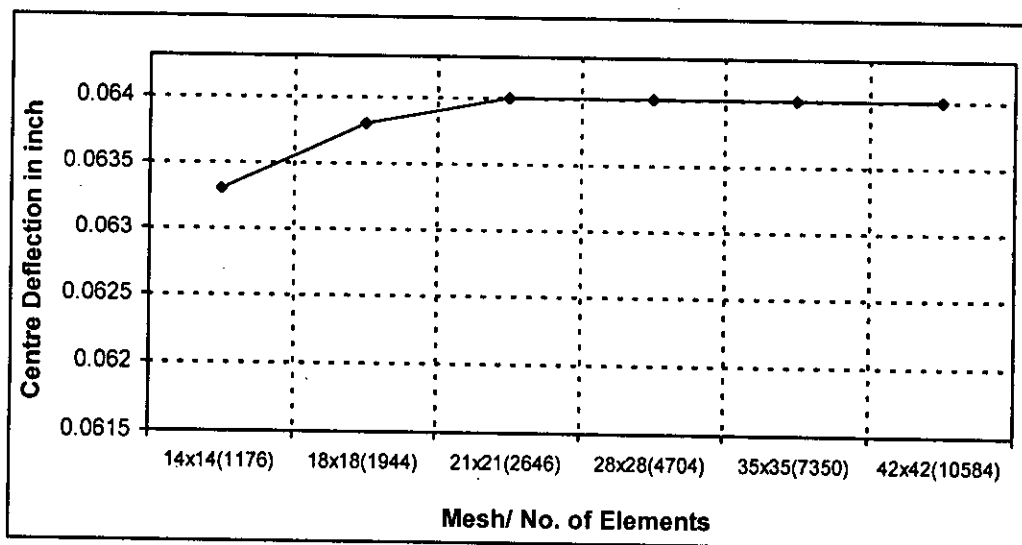


**Figure 3.4.16** Mesh Optimisation

### 3.5 Remarks

After considering all the factors discussed above a complete model of reinforced concrete plate is put under test for nonlinear analysis to predict the punching shear strength. Different parametric studies were systematically carried out to assess the sensitivity of the adopted model in predicting punching behaviour of reinforced concrete plates. And wherever possible, the numerical results obtained are compared with available test data to validate the finite element model used for the analysis of reinforced concrete plates subjected to punching loads. Finally, for completeness, a typical ANSYS script file to generate FE model of reinforced concrete plate is given in Appendix A. This may be very useful for a new user to this programme.

## Chapter 4

# NONLINEAR FINITE ELEMENT ANALYSIS AND MODEL PERFORMANCE

### 4.1 Introduction

The actual work regarding the finite element modeling of reinforced concrete plate has been described in chapter 3. In this chapter various parameters of nonlinear solution is described. A suitable solution strategy is adopted to obtain the solution of the model. The results of nonlinear finite element analysis have been compared with the experimental results to observe the performance of the finite element model. The findings are discussed to highlight the important observations.

### 4.2 Nonlinear Solution Strategies

For reinforced concrete structures, cracking and crushing in concrete through the depth as well as yielding of reinforcing steel are the major sources of material nonlinearity. Cracking results in the permanent loss of both tensile stiffness and the tensile strength in a direction normal to the crack, but the stiffness and strength characteristics in other direction may remain unaltered. In case of crushing, the concrete is simply assumed to lose its entire rigidity and strength in all directions. Nonlinear finite element models for reinforced concrete plates can be classified into two different categories based on stiffness evaluation schemes. They are: (i) the modified stiffness approach and (ii) layered approach. In this study layered approach is used where concrete is assumed to be homogeneous and initially isotropic. The stiffness of the



element starts to decrease at the onset of cracking. The effects of some numerical parameters are studied in order to establish the stability of the overall solution process and as a basic guide for subsequent analytical problems. The numerical parameters selected for sensitivity analysis of the solution procedure are; load increment size, element mesh size, shear transfer coefficient, and convergence criteria.

#### **4.2.1 Incremental Loading and Equilibrium Iterations**

Nonlinear solution technique and overall nonlinear solution strategy to be adopted are very important for non-linear pre- and post-yielding analyses of concrete members. In nonlinear solution, the total load applied to a FEM is divided into a series of load increments called load steps. At the completion of each incremental solution, the stiffness matrix of the model is adjusted to reflect nonlinear changes in structural stiffness before proceeding to the next increment. The ANSYS programme uses Newton-Raphson equilibrium iterations for updating the model stiffness.

Newton-Raphson equilibrium iterations provide convergence at the end of each load increment within prescribed tolerance limit. Prior to each solution, the Newton-Raphson approach assesses the out-of-balance load vector, which is the difference between the restoring forces (the loads corresponding to the element stresses) and the applied loads. Subsequently, the program carries out a linear solution, using the out-of-balance loads, and checks for convergence. If convergence criteria are not satisfied, the out-of-balance load vector is re-evaluated, the stiffness matrix is updated, and a new solution is attained. This iterative procedure continues until the problem converges (ANSYS 5.4). In this study Full Newton-Raphson option with Sparse Direct Solver was used for speed and robustness of the solution. Newton-Raphson iterative solution technique is shown in Figure 4.2.1.

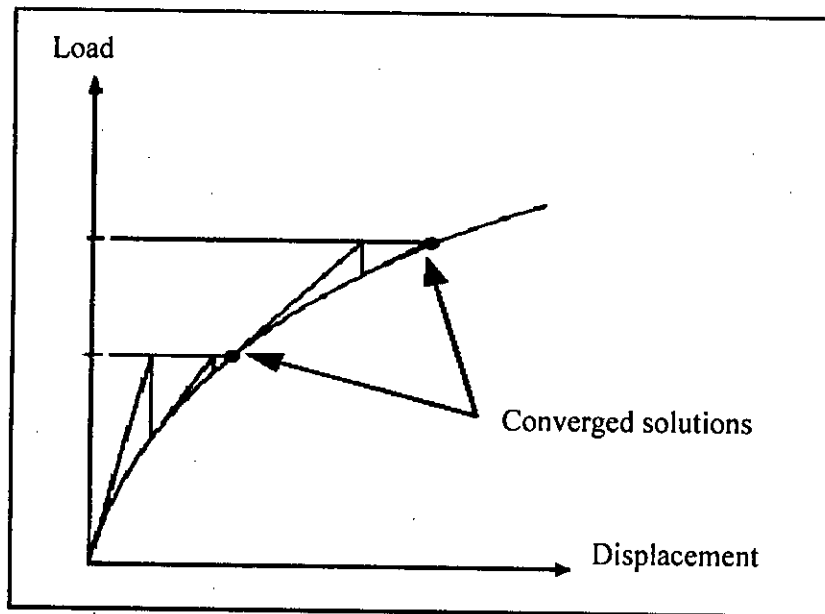


**Figure 4.2.1** Newton-Raphson Iterative Solution (ANSYS)

#### 4.2.2 Convergence Criteria and Tolerance

To finish the iterative process in incremental-iterative methods, convergence criteria must be defined. It is important in the incremental-iterative solution strategy that the solution obtained at the end of each iteration be checked to see whether it has converged to a tolerable convergence limit. The decision about the convergence criterion to be used in the non-linear iterative solution strategy is important. Choice of convergence criterion depends on the type of structure, degree of accuracy required, efficiency in solution process required etc. ANSYS offers various options of convergence criterion. In this study, the convergence behavior of the models depended on behavior of the reinforced concrete. For the reinforced concrete solid elements, convergence criteria were based on force and displacement, and convergence tolerance limits were initially selected by the ANSYS. It was observed that convergence of the solutions was difficult to achieve and

took long computation time. Using only displacement checking with convergence tolerance limit increased to maximum of 5 times the default tolerance limits (1 %), computation time reduced to almost 1/3 rd with nearly similar results. Therefore, convergence criteria were based on displacement with tolerance limit 0.05 in order to save CPU time.

#### **4.2.3 Load Stepping and Failure Definition for Nonlinear FE Analysis**

The load step sizes are varied and adjusted, depending upon the reinforced concrete behavior occurring in the model. For the nonlinear analysis, automatic time stepping in the ANSYS programme predicts and controls load step sizes. Based on the previous solution history and the physics of the models, if the convergence behavior is smooth, automatic time stepping will increase the load increment up to a selected maximum load step size. If the convergence behavior is abrupt, automatic time stepping will bisect the load increment until it is equal to a selected minimum load step size. The maximum and minimum load step sizes are required for automatic time stepping. Considering the slowly converging element that is reinforced concrete, large maximum number of substeps are chosen to apply the load in small enough increments to ensure that analysis closely follow the structures load-response curve.

As first cracking occurs, the solution becomes difficult to converge. If a load applied on the model is not small enough, the automatic time stepping will bisect the load until it is equal to the minimum load step size. After the first cracking load, the solution becomes easier to converge. Therefore the automatic time stepping increases the load increment up to the defined maximum load step size. If the load step size is too large, the solution either needs a large number of iterations to converge, which increases computational time considerably, or it diverges. Failure for each of the models is defined when the solution for

the smallest load increment still does not converge. The program then gives a message specifying that the models have a significantly large deflection, exceeding the displacement limitation of the ANSYS programme.

#### **4.2.4 Shear Transfer Coefficient**

In a nonlinear reinforced concrete analysis, the shear transfer coefficient needs to be assumed to avoid numerical difficulties. The shear transfer coefficient,  $\beta_t$ , represents conditions of crack face transmitting shear due to aggregate interlock. The value of  $\beta_t$  ranges from 0.0 to 1.0, with 0.0 representing a smooth crack (complete loss of shear transfer) and 1.0 representing a rough crack (no loss of shear) (ANSYS 1997). For closed cracks, the coefficient is assumed to be 1.0, while for open cracks it should be in the suggested range of 0.05 to 0.5, rather than 0.0 [Barzegar, et al. (1997)]. In this study, a value of 0.35 was used, which resulted in fairly accurate predictions. Values less than 0.30 were tried, but they caused divergence problems at very low loading levels.

#### **4.3 Mesh Sensitivity (Nonlinear)**

At the beginning of FE model development, a reasonable mesh and a convergence study are needed to obtain a reliable solution. In other words, the structure is divided into a number of small elements, and after loading, stress and strain are calculated at integration points of these small elements (Bathe 1996). An important step in finite element modeling is the selection of the mesh density. A convergence of results is obtained when an adequate number of elements are used in a model. This is practically achieved when an increase in the mesh density has a negligible effect on the results (Adams and Askenazi 1998). In chapter 3 a mesh sensitivity analysis was carried out for the model within elastic limit. In the nonlinear solution of the problem, mesh sensitivity is again

checked to see if a relatively coarser mesh can give an acceptable result to save CPU time. Figure 4.3.1 shows complete load-deflection response of a square slab (A-7b plate) for varying element size i.e. number of elements. The element size ranged between 2.5"x 2.5"x1" to 5"x 5"x1". It appears that numerical solutions are not so sensitive to the element size effect.

For reinforced concrete models in a nonlinear analysis, however, too fine of a mesh may cause numerical instability. On the other hand, if the mesh is too coarse, the analysis will not be sufficiently accurate. Generally, when an actual crack or groups of cracks occur in concrete, the width of the crack band is many times larger than the maximum aggregate size [Shah, et al. (1995)]. As a result, the concrete element size should be two to five times greater than the maximum aggregate size to correctly and realistically model the actual cracks using the smeared cracking approach [Barzegar, et al. (1997) and Shah, et al. (1995)]. In this study, the maximum nominal aggregate size used in the experimental slabs was 1½", and the minimum FE element size was 3.33" x 3.33" x 1".

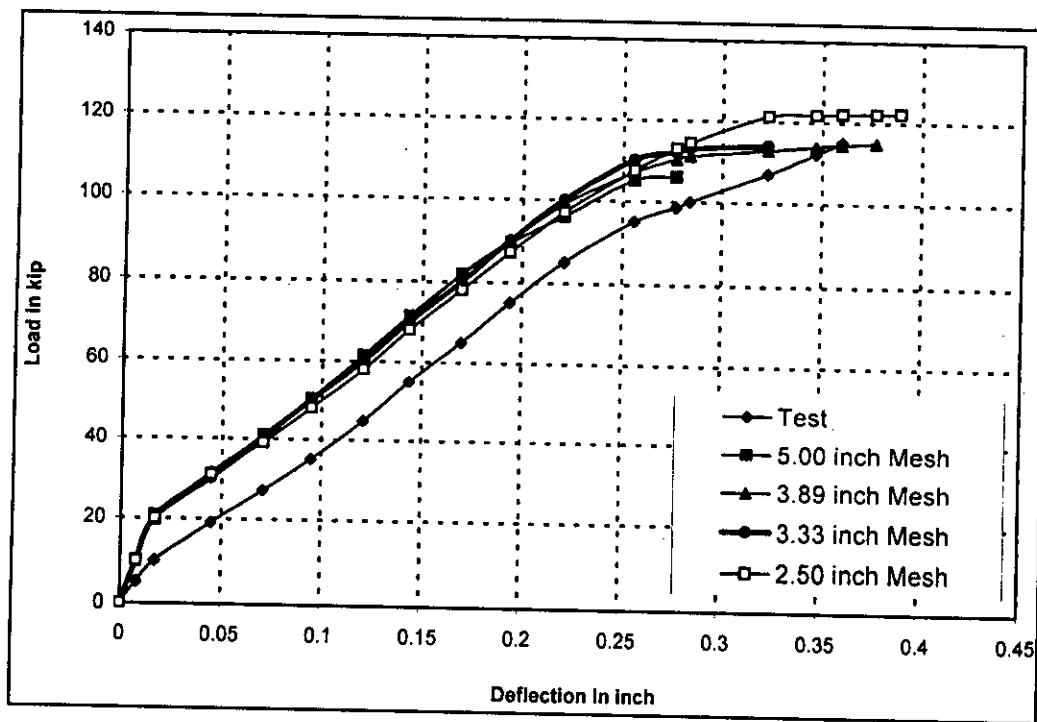


**Figure 4.3.1** Load-deflection Curve for Mesh Sensitivity (Nonlinear)

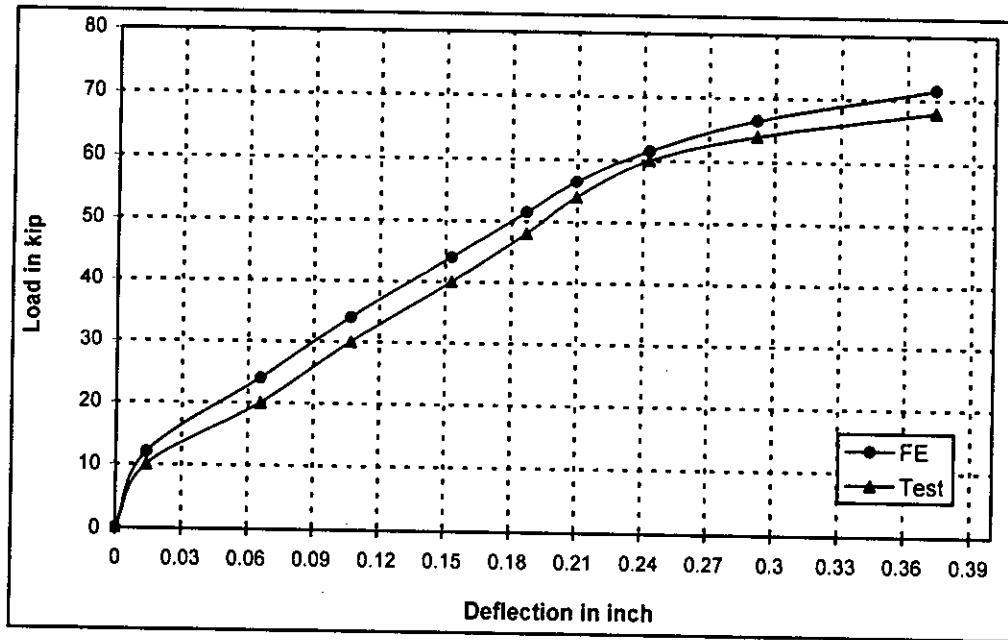
#### 4.4 Comparison of Numerical Results with Experimental data

To carry out finite element analysis in order to predict the behaviour of any structure, it is essential to verify the developed model against some well-established theoretical solutions or experimental results to ensure that the developed model is tracing the actual response closely. Results of the nonlinear finite element analysis carried out here are compared with the test results obtained from Elstner and Hognestad (1956) to ensure the acceptability of the numerical results. For this purpose five slabs from Elstner and Hognestad (1956) were taken as reference. Material properties for these plates were presented in Table 3.4.1. Other parameters of the test slabs and the corresponding FE model plates are listed in Table 4.4.1. These five test slabs cover a wide range of concrete strength, flexural reinforcement ratio, strength of reinforcement, support condition and effect of shear reinforcement.

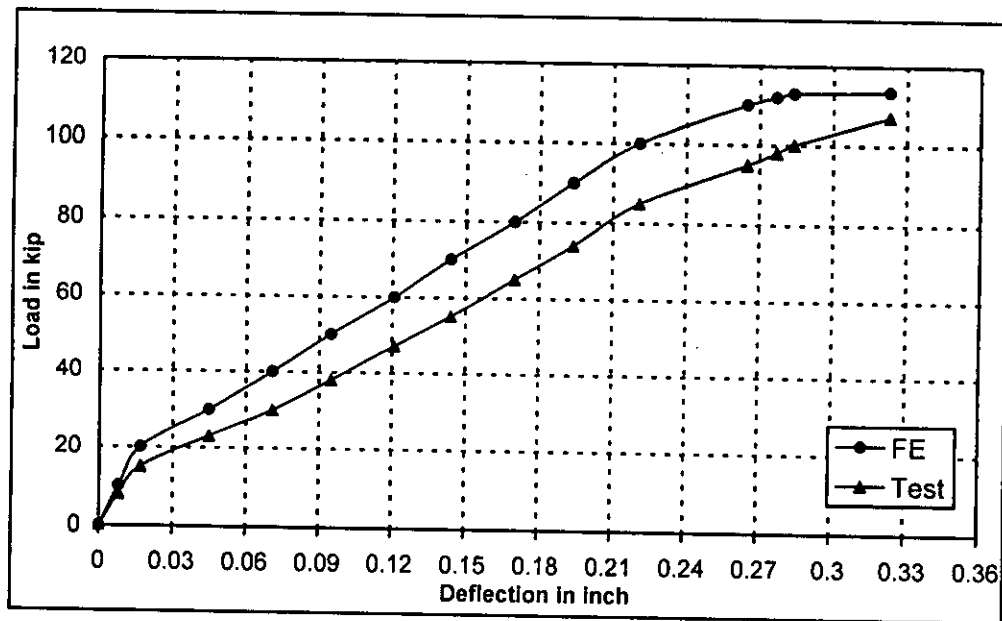
**Table 4.4.1:** Comparison of Numerical with Experimental Results

Plate No	Tension Mat $\rho$ percent	Compression Mat $\rho$ percent	Shear Reinforcement $A_v$ sq in	Support Condition	Plate Dimension (in)		$d$ (in)		Ultimate Load (k)	
					Test	FE	Test	FE	Test	FE
A-1a	1.15	0.56	-	Symmetrical support on four Edges	72x72x6	70x70x6	4.63	5	68	71.5
A-7b	2.47	1.15	-	do	do	do	4.50	5	115	116
A-7	2.47	1.15	-	Symmetrical support on two opposite edges	do	do	4.50	5	90	98
B-14	3.00	-	-	Symmetrical support on four Edges	do	do	4.50	5	130	144
B-16	3.00	-	1.60	do	do	do	4.50	5	168	190

Comparative load-deflection response for the test and FE results are shown in Figure 4.4.1 through 4.4.5 for A-1a, A-7, A-7b, B-14 and B-16 slabs of Elstner and Hognestad (1956) respectively.



**Figure 4.4.1** Comparative Load-Deflection Response for A-1a



**Figure 4.4.2** Comparative Load-Deflection Response for A-7b



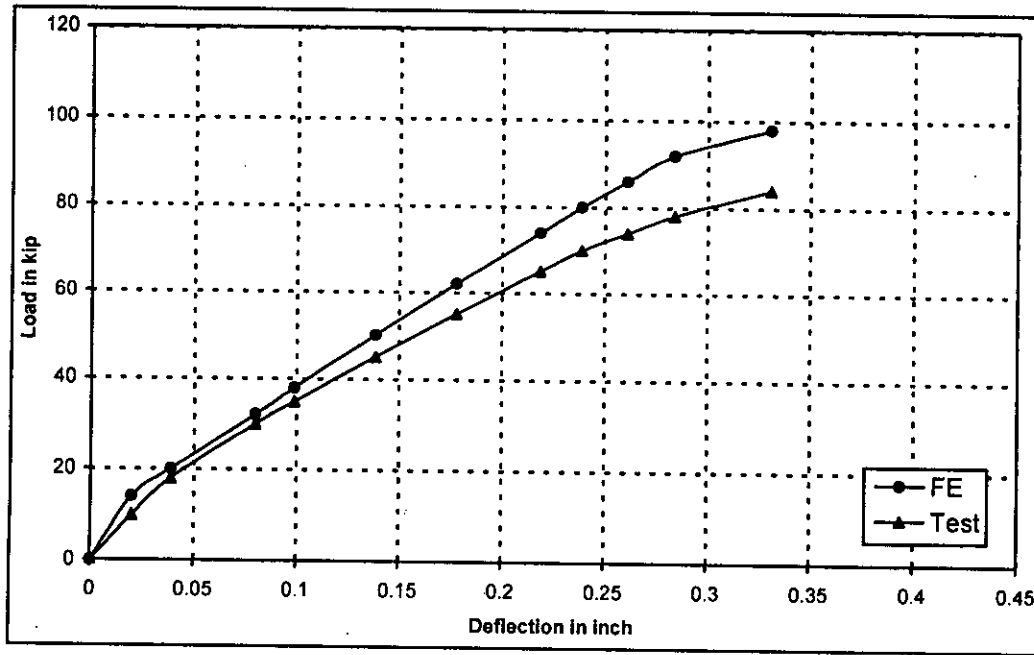


Figure 4.4.3 Comparative Load-Deflection Response for A-7

99597

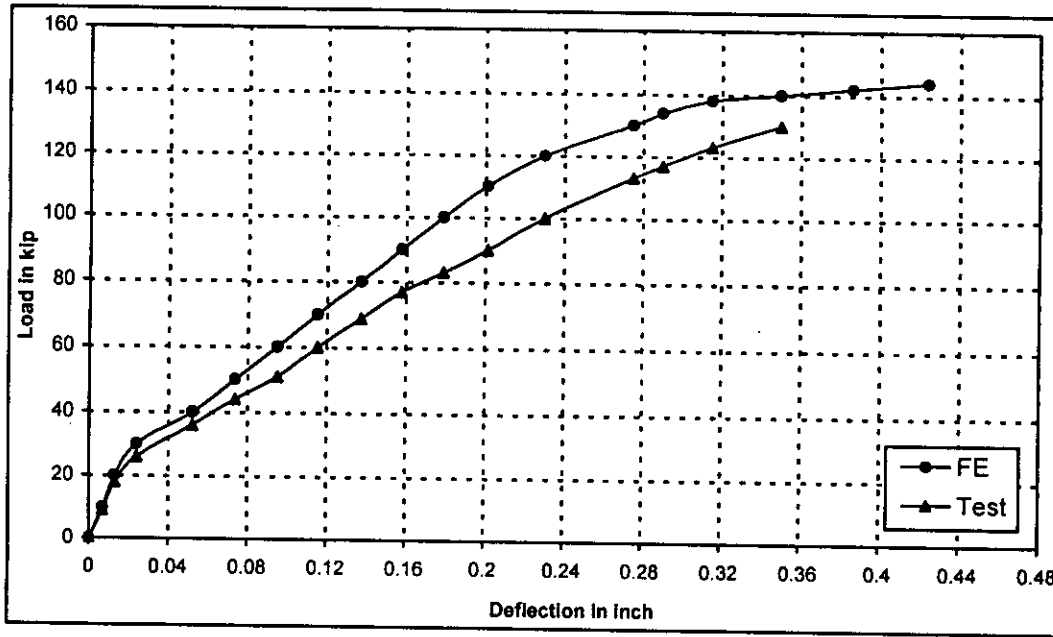
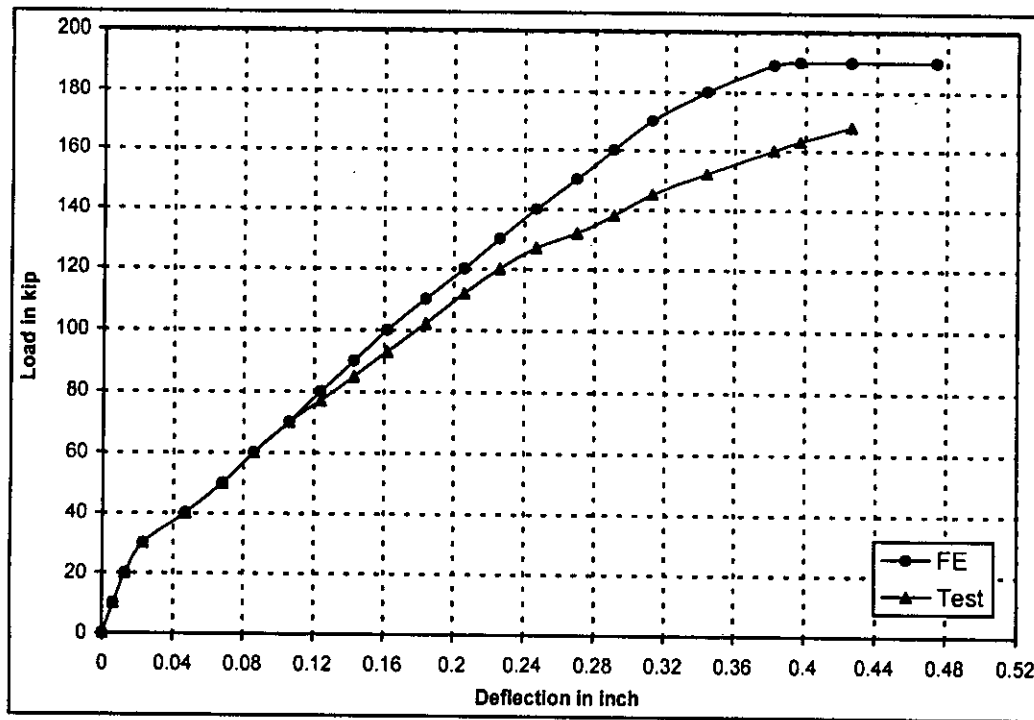


Figure 4.4.4 Comparative Load-Deflection Response for B-14



**Figure 4.4.5** Comparative Load-Deflection Response for B-16

It is observed that Non-linear load-deflection curves show very close results at every stages of load history of the slab up to failure. The FE analysis can trace the test results closely. The initially linear relation experience a small jump with a sudden loss of stiffness, when cracking in concrete begins followed by a nearly linear curve. At the end of nearly linear response during progressive cracking of concrete, the nonlinear response of the finite element model is consistent with the test data as steel starts yielding. Hence it may be concluded that the present FE-programme can be used to simulate the whole load-deformation curve, i.e., the elastic part, the initiation of cracking, shear cracks, the yielding of the steel bars and up to the initiation of crushing of concrete at failure.

#### 4.5 Discussions

The general behavior of the finite element models represented by the load-deflection plots at centre of plate show good agreement with the test data. However, the finite element models show slightly more stiffness than the test data in both the linear and nonlinear ranges. The effects of bond slip (between the concrete and steel reinforcing) and microcracks occurring in the actual plates were excluded in the finite element models, contributing to the higher stiffness of the finite element models. The final loads from the finite element analyses are higher than the ultimate loads from the experimental results by 5% to 15%. The agreement may be considered to be excellent for any reinforced concrete problem.

Clearly the correlation of test and numerical data depends on the assignment of accurate linear and non-linear material properties as appropriate. In general given the compressive strength of the concrete it is thus usually possible to arrive at a sensible set of material data for inclusion in the nonlinear numerical model. The situation is not as clear in the context of the reinforcing bars. Generally the nominal strength of the reinforcement is specified and it is assumed in design that it behaves in an elastic-perfectly plastic manner.

For nonlinear analysis of a reinforced concrete plate, the total load applied to a model must be divided into a number of load steps. Properly defining minimum and maximum incremental sizes for each load step, depending upon the behavior of the reinforced concrete structure, convergence of the solutions can be quickly achieved that reduces computational time significantly.

In view of good correlation between the nonlinear finite element analysis model and the experimental data, it would seem that this numerical

package can be used with confidence in studying, both quantitatively and qualitatively, problems of punching in RC plates.

The present results indicate that the key to the understanding of mechanics of punching failure is a proper modeling of triaxial conditions that govern the behaviour of such structures. There is no need to invoke factors usually associated with shear-failure modes such as aggregate interlock and dowel action; instead, it is the very high principal stresses (often well in excess of  $f'_c$ ), achieved through triaxial conditions, that are capable of equilibrating the applied load at failure, and, also, of determining the degree of ductility attained.

## Chapter 5

# INFLUENCE OF MATERIAL AND GEOMETRIC PARAMETERS ON PUNCHING SHEAR STRENGTH

### 5.1 Introduction

In chapter 4 the developed model was verified against test results to ensure that the model is tracing the actual response closely to ensure the acceptability of the obtained results. This chapter is dedicated to a thorough parametric study to identify the effects of concrete material and geometric parameters on the punching shear capacity of flat plates. The general idea of parametric study for a number of independent parameters embodies the fact that at a single instance only one variable should be allowed to vary while all other parameters are fixed at some initial value. If two or more parameters were allowed to vary at the same time it would cause confusion in the results of the parametric study and their interpretation. Another point that is worth mentioning is the range of different variables, as the parameters were varied one at a time it is expected that they remain within certain bounds. This is due to the fact that exceptionally large or small values, which are not likely to occur in real-life problems, would cause wastage of computational effort. Hence investigation at hand specifies a fixed range for all the variables within which the actual work of parametric study is carried out. Investigation conducted in this chapter leads to a recommendation on the choice of structure parameters to enhance the punching shear strength.

### 5.2 Material Parameters

Reinforced concrete plate, speaking in a very common sense, is a mass of hardened concrete with steel reinforcement embedded within it.

Material details of concrete like cement, aggregate, water-cement ratio etc would not be included in FE analysis like experimental research. Of material parameters mainly concrete cylinder strength, flexural reinforcement ratio and the yield strength of reinforcement are considered. Shear reinforcement is discussed in a separate chapter.

### 5.2.1 Concrete Strength

At the initial step, five square slabs (6'x6') of Elstner and Hognestad (1956) were taken as reference. These were slab number A-1a through A-1e of series I. Keeping other parameters constant concrete compressive strength was varied from 2040 psi to 5340 psi. The model plates were considered 70 inches square, supported along the edges, and loaded with a central load uniformly distributed over an area of 10" x 10" and applied through a column stub. The thickness of the slabs was 6 inches. The orthogonal longitudinal reinforcement was provided in the tension and compression zone. The distance from the centroid of the longitudinal reinforcement to the top of the compression face was taken to be 5 inches though it varied slightly for the test slabs. Figure 5.2.1 shows the variation of ultimate load capacity (punching strength) of the test and FE analysis with varying compressive strength of concrete. Figure 5.2.2 shows the load-deflection response of FE analysis for five slabs (A-1a through A-1e). It is observed that for the given reinforcement ratio ( $\rho = 1.15\%$ ) and yield strength of steel ( $f_y = 48.2$  ksi) highest ultimate load is obtained for concrete strength,  $f'_c = 3660$  psi. Further increase in concrete strength  $f'_c$  does not increase the ultimate load capacity of the slab, rather slight decrease in ultimate load is observed.

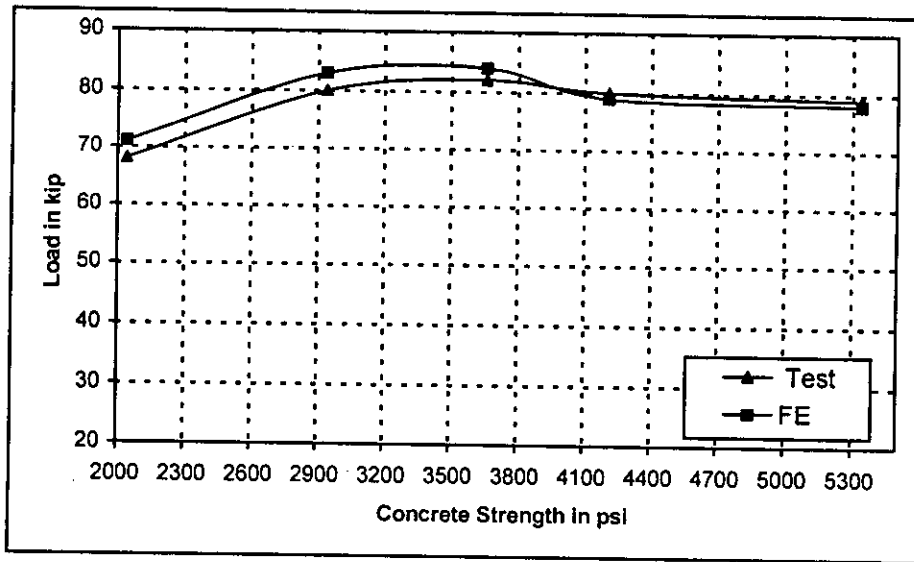


**Figure 5.2.1** Variation of Ultimate Load Capacity of the Test and FE Analysis with Varying Compressive Strength of Concrete

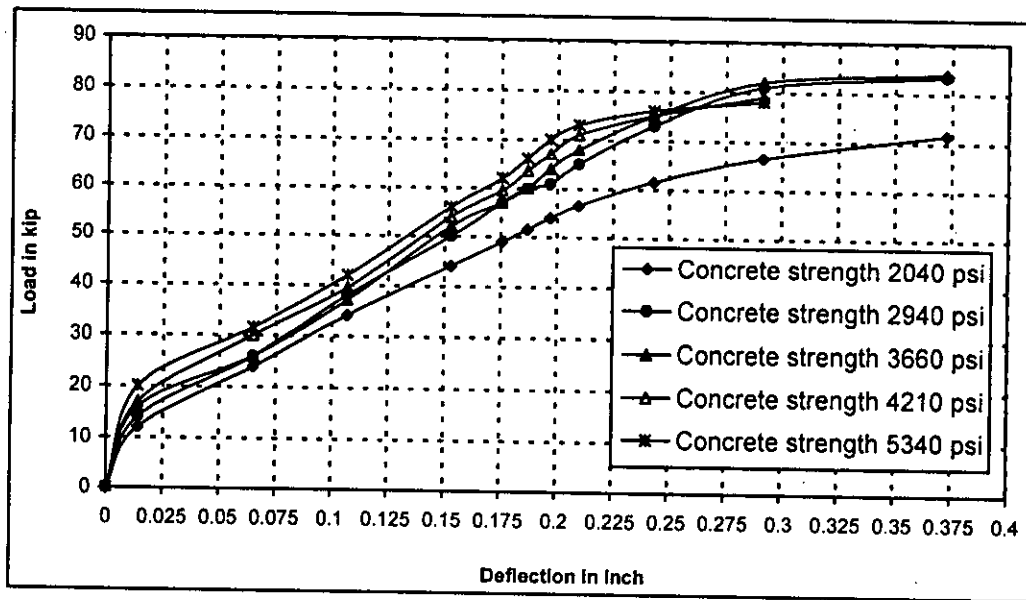
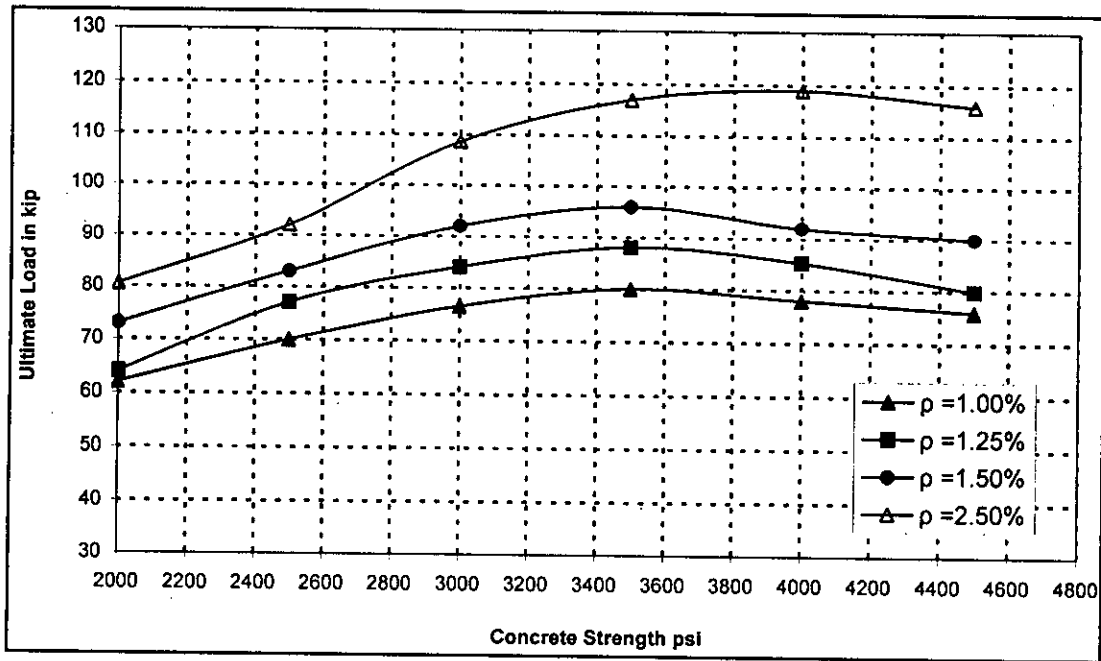


**Figure 5.2.2** Load-deflection Response of FE Analysis for Slabs A-1a through A-1e

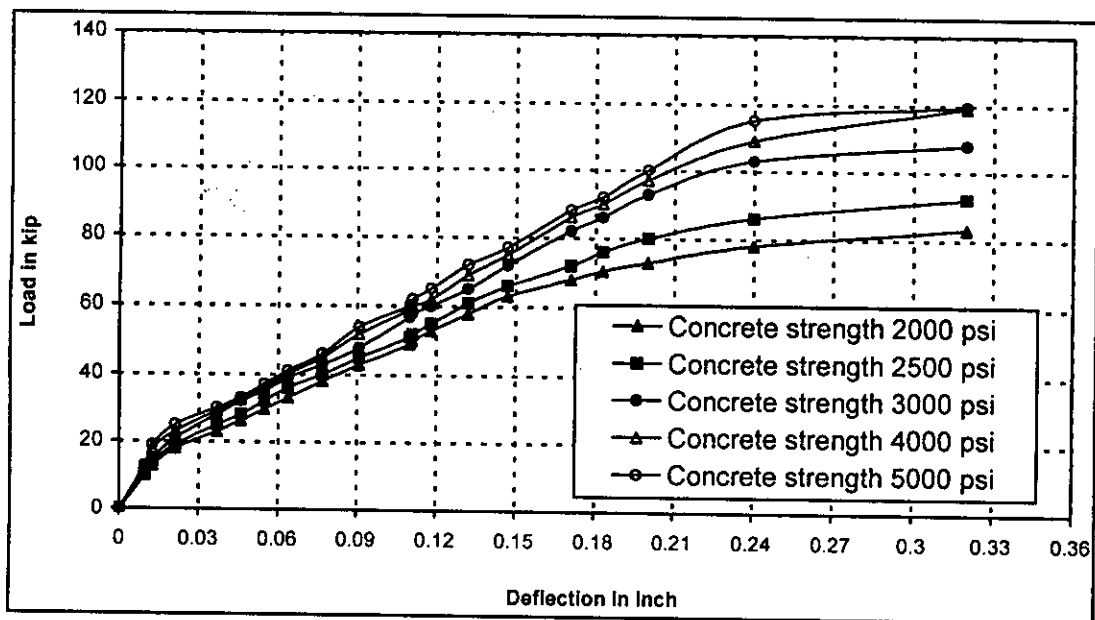
Next, a series of similar plates with concrete strengths varying from 2000 psi to 5000 psi with increment of 500 psi were analyzed with tension reinforcement percentages of 1, 1.25, 1.5, and 2.5. Variation of the ultimate loads for these slabs with variation in concrete strength are graphically shown in Figure 5.2.3. It is seen that increase in ultimate load is more prominent with higher strength concrete compared to lower strength concrete. It is also seen that the load-carrying capacity of the plates increased with the addition of steel reinforcement, changing significantly as the reinforcement ratio increased from 1 to 2.5 percent. For reinforcement ratio up to 1.5 %, the highest ultimate load is obtained at about 3500 psi concrete compressive strength. Beyond this point, ultimate load capacity falls, though the compressive strength is increased. This highest ultimate load point is shifted to 4000 psi compressive strength for reinforcement ratio 2.5 %. After which it reduces with the increase of compressive strength but the rate of reduction is less than that at low reinforcement ratio. Hence it may be concluded that concrete compressive strength increases the ultimate capacity up to certain limit for particular reinforcement ratio.

Figure 5.2.4 shows the load-deflection response with varying concrete compressive strength for reinforcement ratio of 2.5 %. This figure shows that the slope of the deflection curve gradually increases with increase in ultimate concrete strength.





**Figure 5.2.3** Variation of Ultimate Load with Varying Compressive Strength of Concrete for Different Reinforcement Ratio



**Figure 5.2.4** Load-deflection Response with Varying Concrete Compressive Strength for Reinforcement Ratio of 2.5%

### 5.2.2 Flexural Reinforcement

Flexural reinforcement for both tension and compression face was considered. Parametric study was conducted to observe the effect of tension and compression mat on model slab A-7b of Elstner and Hognestad (1956). Load-deflection response of this is shown in Figure 5.2.5. From the figure, it can be seen that the influence of compression mat on the ultimate load is not so significant. Hence for subsequent study with flexural reinforcement, the tension face steel is considered.

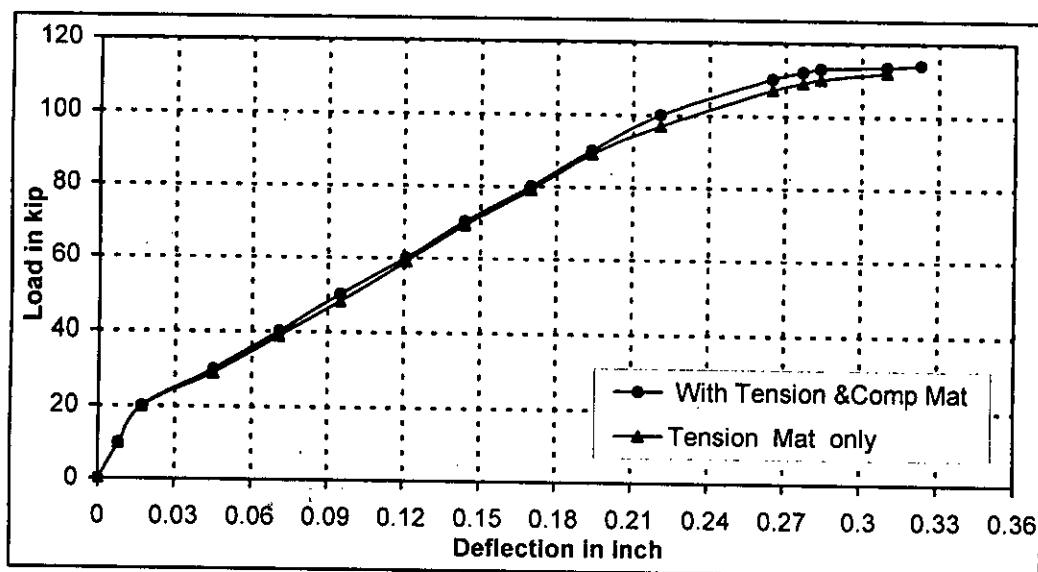


**Figure 5.2.5** Influence of Flexural Reinforcement on Load-deflection Response

#### 5.2.2.1 Reinforcement Ratio

This effect is already highlighted in article 5.2.1 and in Figure 5.2.3 where the variation of ultimate load with respect to change in the compressive strength and percentage of flexural reinforcement are illustrated. Figure 5.2.6 shows the influence of reinforcement ratio on punching shear for varying concrete compressive strength. The change in behaviour with the change in the reinforcement ratio was particularly

noticeable for higher values of compressive strength. For compressive strength less than 3000 psi the increase in punching strength with increasing reinforcement ratio is relatively gradual and flat compared to  $f'_c = 3000$  psi and above. This indicates that steel reinforcement has an important effect on the punching shear strength for reinforced concrete plates and more so with higher strength concrete.

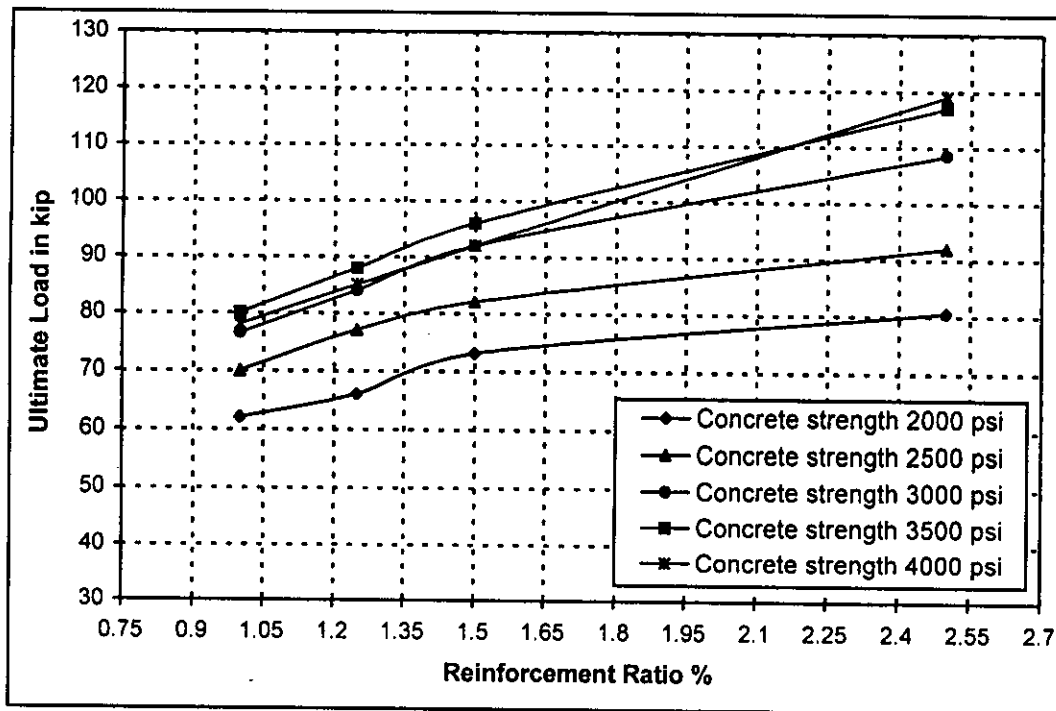


**Figure 5.2.6** Influence of Reinforcement Ratio on Punching Shear for varying Concrete Compressive Strength

#### 5.2.2.2 Yield Strength

To study the effect of yield strength of steel on the punching shear, reference plate A-1b was taken with reinforcement ratio 1.5 % and concrete compressive strength 3500 psi. Yield strength was varied from 40 ksi to 60 ksi (40, 45, 50, and 60 ksi). Figure 5.2.7 represents the variation of ultimate strength due to change in yield strength of the steel. The nature of the curve conforms to the general understanding. It is

seen that the ultimate strength is increased with the increase of yield strength of the reinforcement. But for given condition, the rate of increase in ultimate load decreased for yield strength greater than 50 ksi. Similar curve was obtained for concrete compressive strength 3000 psi as shown in the figure. It is also observed that at lower yield strength of steel, increase of ultimate load with increasing concrete strength is comparatively less than that of higher strength steel.

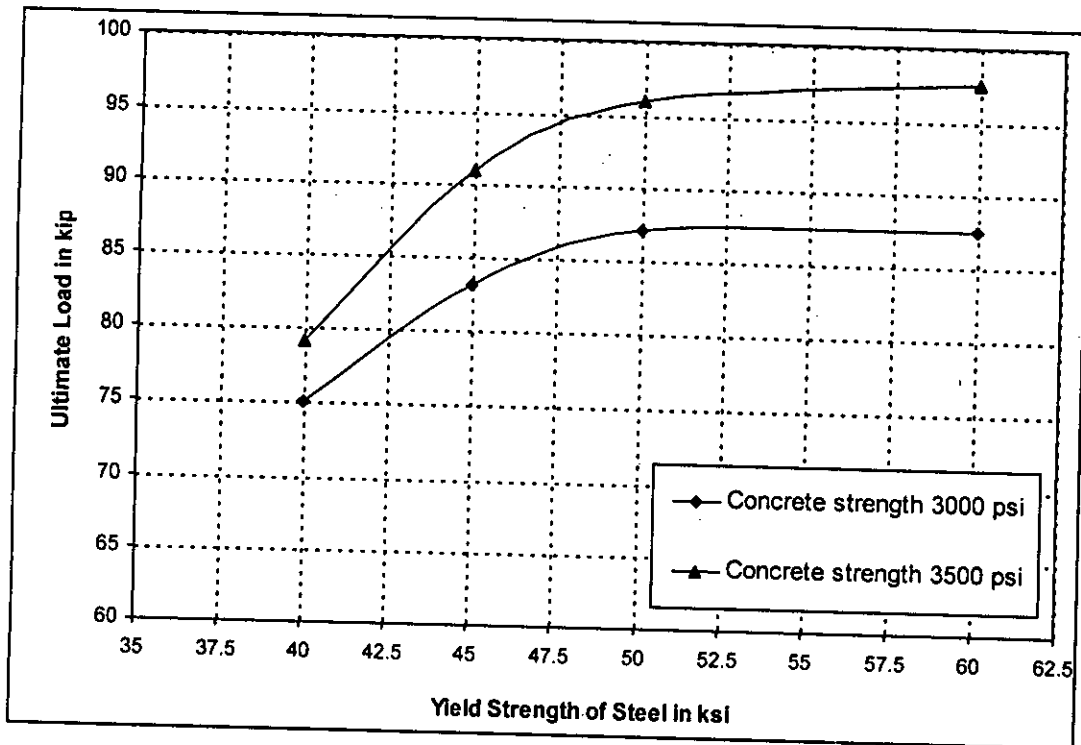


**Figure 5.2.7** Variation of Ultimate Strength due to change in Yield Strength of Reinforcement

### 5.3 Geometric Parameters

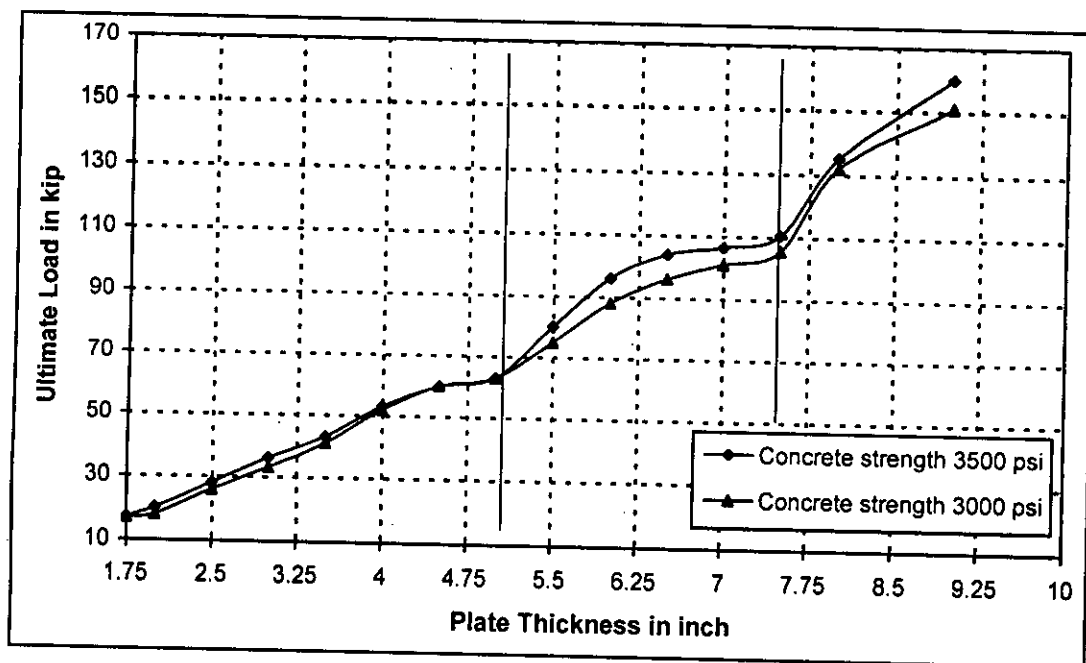
In the geometric parameters mainly the size effect like span-depth ratio, the column size that is the load or the concentrated reaction area and the support or boundary condition is considered. The model plates were 70" square on supports in planer dimension while the plate thickness,

column or loading area and support conditions were varied. A suitable material property was chosen for the study of geometric parameters.

### 5.3.1 Plate Thickness (Span-Depth Ratio)

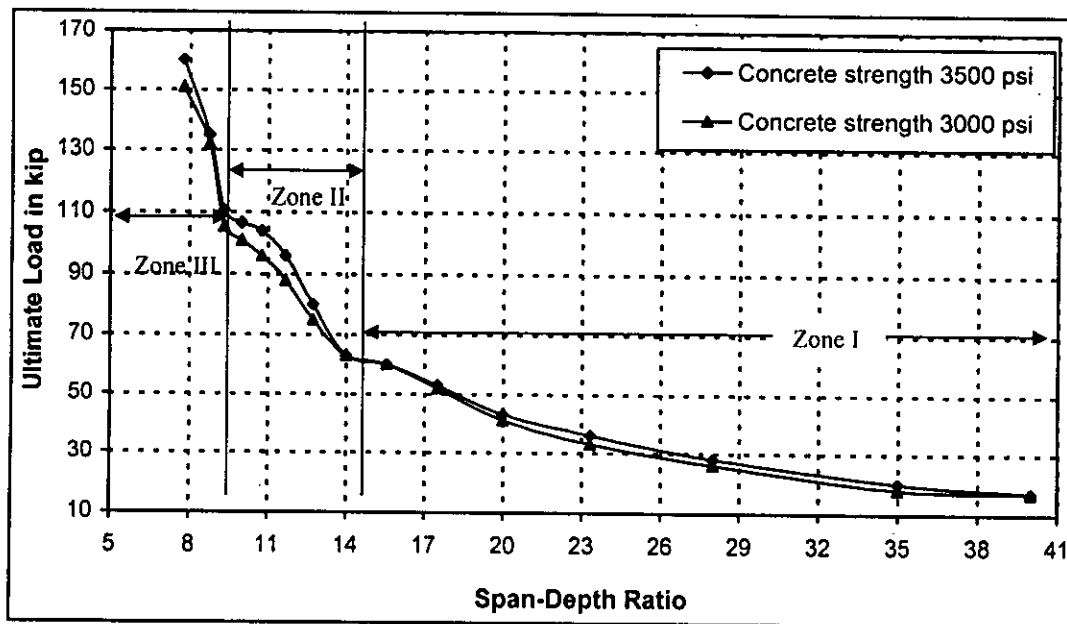
Different span-depth ratios were achieved by varying plate thickness of the model. The thickness varied from 1.75-in to 9-in. with span-depth ratio varies from 40 to 7.777. For this, reinforcement ratio 1.5 %,  $f'_c = 3500$  psi and  $f_y = 48.2$  ksi were chosen. Figure 5.3.1 shows that the thicker the slabs, the higher the punching shear strength, thus it appears that the thickness is an important factor affecting the punching load capacity of a reinforced concrete flat plate. Similar curves were obtained with concrete compressive strength of 3000 psi.

Figure 5.3.2 shows the plot of ultimate load vs. span-depth ratio that can be divided into three zones. First span-depth ratio above 15, where a flatter slope of the curve indicates gradual increase of ultimate load with decrease in span-depth ratio. This is the zone where actual plate action takes place. But is no test data available for this range of span-depth ratio. Next zone, span-depth ratio 15 to 9, where slope of the curve is comparatively steeper than the first zone but it becomes flatter around span-depth ratio 10, and the variation of ultimate load is comparatively less. Last but not the least, span-depth ratio below 9, where steepest curve with rapid increase of ultimate load is observed. The strength increase with small span-depth ratios may be due to the development of compression struts forming a tied-arch mechanism similar to that observed in deep beams and the interaction of in-plane compressive forces resulting from friction at the support.



**Figure 5.3.1** Variation of Punching Shear Strength with Plate Thickness

Similar behaviour as mentioned above was reported by Lovrovich and McLean (1990). They have observed for the test series with circular slabs, the normalized punching shear strength remained relatively constant for span-depth ratios of 6, 8 and 12. However, the specimen strengths significantly increased as span-depth ratios decreased from 6 to 2. There was some evidence of the formation of compression struts between the point of application of the load and the support as the specimens approached failure. Thus, a tied-arch mechanism similar to that observed in deep beams are developed. Additionally, in-plane compressive forces resulting from friction between the slab and the supports may have interacted with the arch mechanism. This interaction may have also contributed to the increased strengths observed in the specimens with small span-depth ratios.



**Figure 5.3.2** Influence of Span-Depth Ratio on Ultimate Load

From this observation it may be concluded that span-depth ratio has direct influence on the ultimate load carrying capacity of the flat plate with slightly varying response in different zones. For higher strength, span-depth ratio should be below 9 but restriction on the thickness of the plate/slabs and increased material cost should be taken into consideration.

### 5.3.2 Column Size

Column size or the loading area is related to the mesh size. Using 3.333 inch mesh size for the 70 inch square plate, column or loading area at the centre of the plate can be 3.333 inch, 10 inch, 16.666 inch or 23.33 inch square. Using 3.89 inch mesh size the size of the column can be 3.89 inch, 7.78 inch, 15.56 inch etc. To study the effect of column size on punching shear 7.78, 10 and 15.56 inch size column was used while all other parameters were constant. Plate A-7b was taken as reference.

Though two different mesh sizes are used, their load-deflection response is very close to each other (Figure 4.3.1). Figure 5.3.3 shows the load-deflection curves for varying column size. As would be expected, the increase in column size increased the slab stiffness and there by increased the slopes of the load-deflection curves. Figure 5.3.4 shows the variation of ultimate load with varying column size. It is observed that by doubling the column size, ultimate load is increased over 30 %. It may be concluded that to enhance punching shear strength column size be increased to a maximum permissible limit.

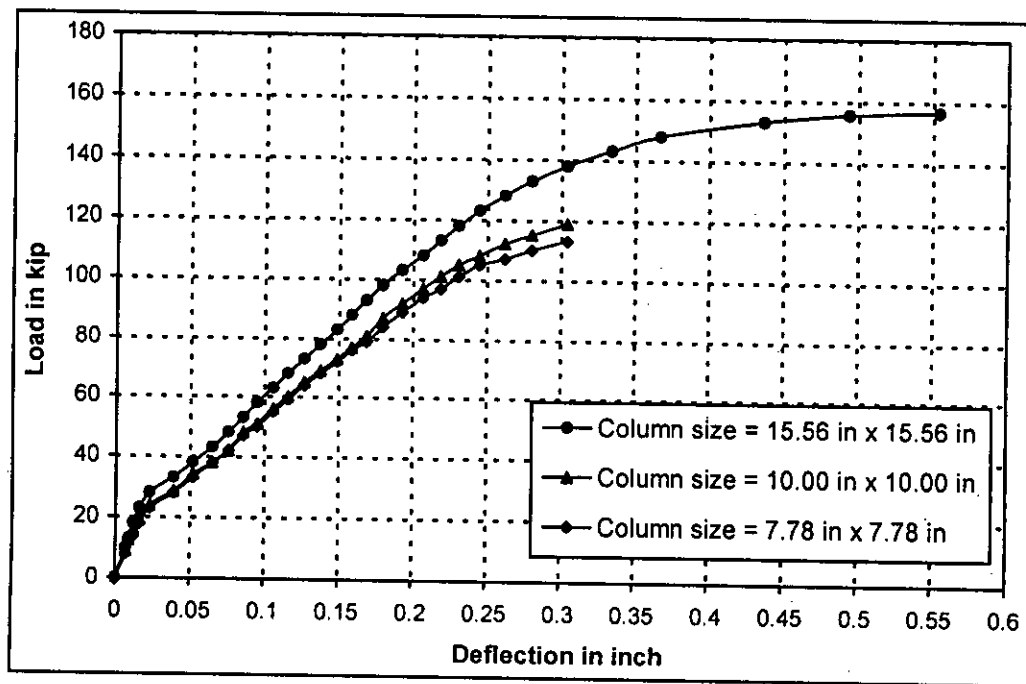


**Figure 5.3.3** Comparative Load-deflection Response for Different Column size



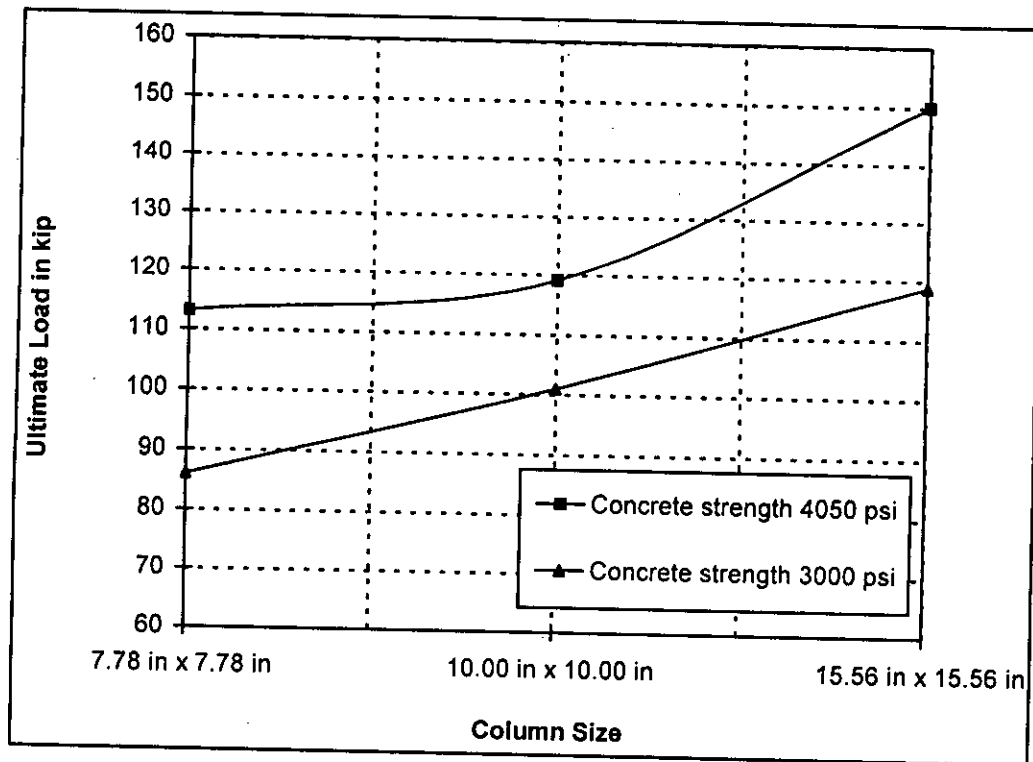


**Figure 5.3.4** Variation of Punching Shear Strength with Column Size

### 5.3.3 Support Condition

To study the effect of edge condition, three slabs of Elstner and Hognestad (1956) were taken as reference. The slabs selected are A-7, A-7a and A-7b. The model plates were square (70" x 70") and loaded with a central load uniformly distributed over an area of 10" x 10" and applied through a column stub. The thickness of the slabs were 6 inch. The orthogonal longitudinal reinforcement was provided in the tension and compression zone. The distance from the centroid of the longitudinal reinforcement to the top of the compression face was 5 inch. Keeping other parameters constant three different support conditions were applied: symmetrical support on four edges, symmetrical support on two opposite edges and symmetrical support (each 10" square) on

four corners. Corresponding load-deflection response is plotted in Figure 5.3.5.

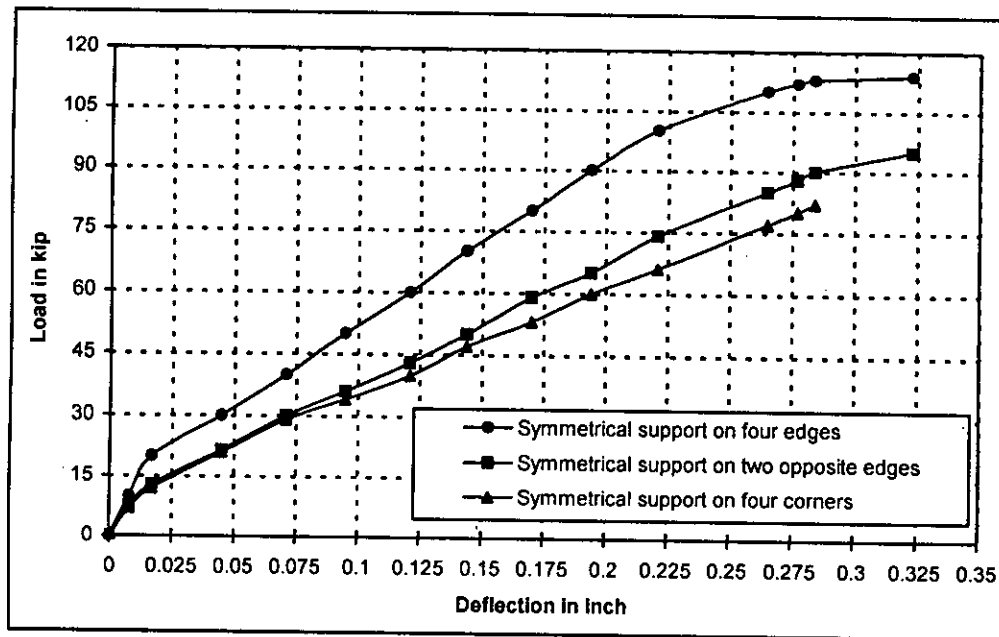


**Figure 5.3.5** Comparative Load-deflection Response for Different Edge Condition of the Plate

#### 5.4 Remarks

The available finite element model (from ANSYS) was used to investigate the influence of several factors on the behaviour of plate subjected to transverse load. The factors studied were the slab thickness, the amount of longitudinal reinforcement, and concrete compressive strength. The dimensions, boundary conditions, and loading type for the plates analyzed as part of this parametric study were identical to the slabs of a Test Series.

The results of the analysis confirm the general understanding of the behaviour of slabs in punching shear. As the concrete compressive

strength, longitudinal reinforcement ratio, and slab thickness increases so does the shear strength of the slabs. This study shows that both span-depth ratio and the type of support condition have significant influence on the punching shear strength of concrete slabs. However, the test slabs selected had a span-depth ratio of 12, which is far short of the practical ranges. So, further test programme may be undertaken for span-depth ratio 20 to 40 to compare the test results with numerical predictions.

From the graphical presentation of the various parameters, a designer can visualize and choose the suitable plate parameters to enhance the punching shear strength.

## Chapter 6

# INFLUENCE OF SHEAR REINFORCEMENT ON PUNCHING SHEAR STRENGTH

### 6.1 Introduction

The use of shear reinforcement in the form of stirrups can increase the shear strength of the connections. However, the difficulty of installing such reinforcement in relatively thin plate is a problem. The vertical branches of a stirrup represent the only part of this element contributing to the shear strength. In thin slabs, the vertical part of the stirrup is not sufficiently anchored to produce a force equal to the yield strength of the stirrup. For a stirrup to be effective it must enclose the flexural reinforcement. To maintain the required concrete cover above and below the stirrup, the effective depth of the flexural reinforcement must be reduced. Thus, increased amount of flexural reinforcement will be necessary. In this chapter various types of shear reinforcement as proposed by different researchers have been discussed and the influence of some of those on punching shear have been numerically studied and relative effectiveness compared.

### 6.2 Shear Reinforcement

At the design stage, there are several ways of avoiding punching shear failure, such as; reducing the effective length of the slab, increasing the overall thickness of the slab, increasing the thickness of the slab locally with a drop panel or an inverted cone (column capital), increasing the column head dimensions and providing some kind of shear reinforcement [Pilakoutas and Li (2003)]. The first four solutions either increase the overall floor height, or are impractical, sometimes architecturally unacceptable, or expensive. Consequently, very often, to

achieve an elegant thin flat slab, shear reinforcement is required. Properly designed shear reinforcement can prevent brittle punching failure and increase the strength and ductility of the slab-column connection.

Traditionally, to prevent shear failure, reinforcement is provided either at an angle or perpendicular to the main flexural reinforcement as shown in Figure 6.2.1.

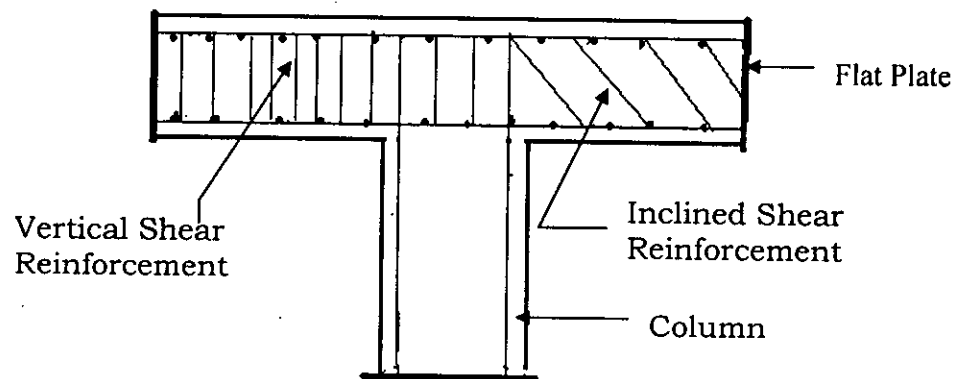


**Figure 6.2.1** Typical Vertical and Inclined Shear Reinforcement

However, in thin structural elements, such as slabs, anchoring short lengths of perpendicular reinforcement is difficult, because full anchorage should be provided to develop the yield strength of shear reinforcement within the depth of slab. This problem is further aggravated by the fact that conventional shear reinforcement, due to its cross-sectional dimensions, cannot be placed in the cover region above the top layer of flexural reinforcement without reducing durability or the efficiency of flexural reinforcement.

Stirrup shear reinforcement was investigated by Elstner and Hognestad (1956), Olivera et al. (2000), Pillai et al. (1982) and others. Much of the experimental work reported until now led to the conclusion that, shear

reinforcement consisting of bars is not fully effective, because it does not reach its yield strength before slab failure.

### **6.2.1 Types of Shear Reinforcement**

Special shear reinforcement is often used at the supports for flat plates, and some times for flat slabs as well. It may take several forms. Based on the orientation, it can be broadly classified as vertical and inclined shear reinforcement, besides there are some special forms like shear heads, shear studs etc.

#### **6.2.1.1 Vertical Shear Reinforcement**

A few common types of vertical shear reinforcement are open links, closed hoops, sausage links, and shear studs etc. Yamada et al. (1992) tested hat type and hook type shear reinforcement (Figure 6.2.2). Broom (1990) tested different types of shear reinforcement from ordinary stirrup and bent bars. The test results showed that ordinary shear reinforcement in the form of open links (Figure 6.2.2b) enclosing only the tension flexural reinforcement was not effective enough to give flat slabs desired ductility [Pilakoutas and Li (2003)]. Closed hoops, as shown in Figure 6.2.2d are best suited for shear reinforcement; however, their integration involves building up reinforcement cages from individual bars. This increases the costs and time required for fixing reinforcements. Sausage links as shown in Figure 6.2.2c are relatively easy to install, although these involve additional labour with shade of doubts regarding their effectiveness.

A more recent development is the shear stud reinforcement shown in Figure 6.2.2e. Stud type reinforcement is an efficient solution involves the use of shear studs welded on a metal strip. The use of shear reinforcement in the form of vertical rods (studs) is simple because it

does not interfere with the placement of the flexural reinforcement at the slab-column connection. To be fully effective, the studs should be mechanically anchored at each end by a plate or head capable of developing the yield strength of the studs. Tests verified that stud type reinforcement substantially increases the strength and ductility of slabs. Shear-stud reinforcement can transform the failure mode from a brittle punching shear failure to a more ductile flexural failure [Mortin and Ghali (1991)].

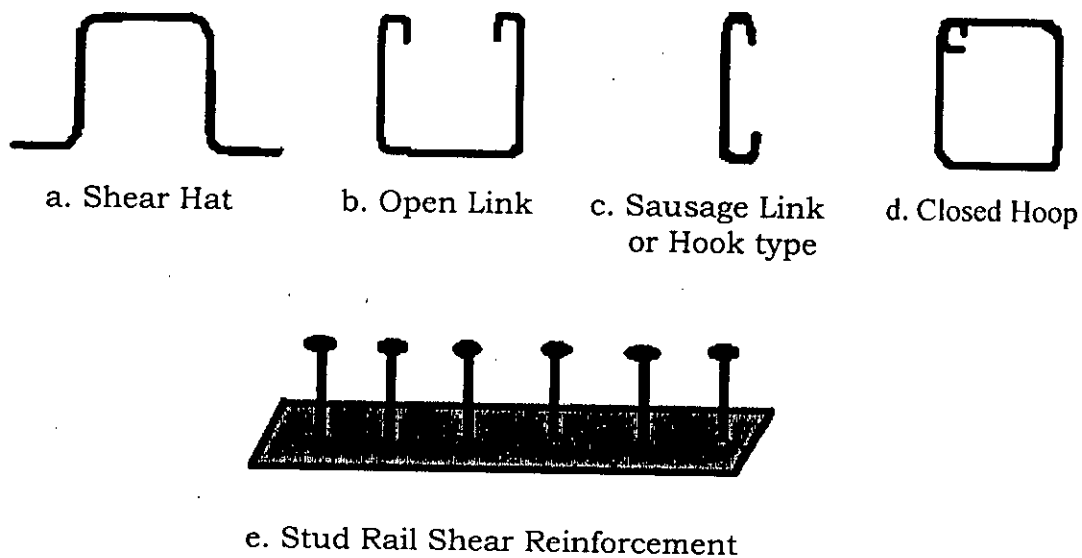


**Figure 6.2.2** Various Types of Vertical Shear Reinforcement

### 6.2.1.2 Inclined Shear Reinforcement

Inclined reinforcement, though effective, is difficult to design, manufacture, and place. It is not well suited for earthquake resistant design, where a reversal of movement may occur. There are several forms like; bent bars, inclined stirrup, and shearband reinforcement etc.

The bent-bar arrangement of Figure 6.2.3 is suited for use with concrete columns. The bars are usually bent at  $45^\circ$  across the potential diagonal tension crack, and extend along the bottom of the slab a distance sufficient to develop their strength by bond.

Shearband reinforcement system (Figure 6.2.4.) is made of steel strip of high ductility. The strip is punched with holes, because this has been demonstrated experimentally to increase its anchoring characteristics over short lengths [Pilakoutas and Li (2003)]. The strip can be bent to a variety of shapes.

This shear reinforcement system differs from all existing systems. Due to its small thickness, the reinforcement can be placed from the top after all flexural reinforcement is in place with minimal loss of cover. This system is adaptable and can accommodate greater tolerances in placement and enables quick addition of extra reinforcement where required at a later stage. In addition, on the practical side, since it is light it is easy to store and transport.

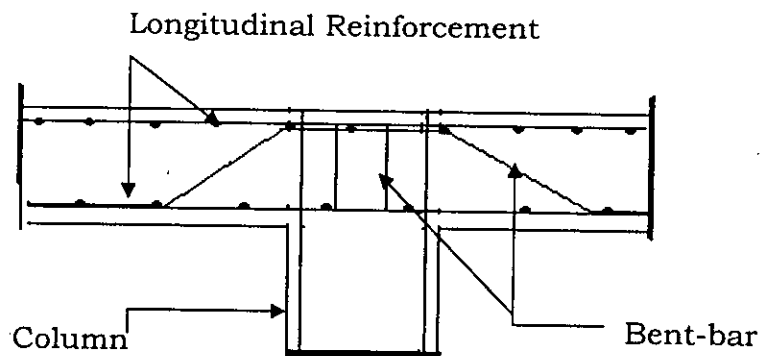


**Figure 6.2.3** Bent-bar Shear Reinforcement



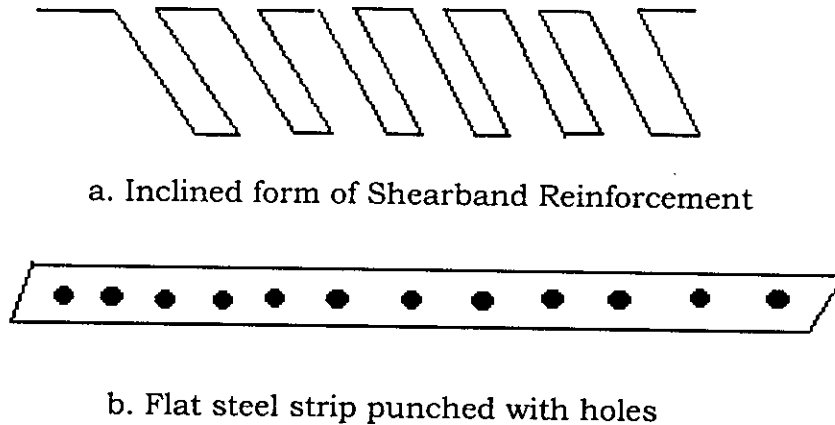


**Figure 6.2.4** Shearband Reinforcement

### 6.2.1.3 Non conventional Shear Reinforcement

Due to the difficulties with conventional reinforcement, there have been many attempts to develop easy to place and effective shear reinforcement for flat slabs. All current types of shear reinforcement have advantages and disadvantages concerning ease of detailing, anchorage effectiveness, cost effectiveness, and ease of placement. However, many of the existing systems increase not only the shear capacity of the connection, but also the flexural capacity. Two types of nonconventional reinforcement are worth mentioning: stud type reinforcement as shown in Figure 6.2.2.e and steel section shear head reinforcement. Shearhead reinforcement includes the use of I sections, channel sections, D collars, or steel plates. Shearheads provide effective but cumbersome way of reinforcing against shear. Steel sections tend to be heavy, expensive relative to conventional reinforcement, and normally require welding at the intersection right above the column. They can be difficult to integrate with conventional reinforcement and may obstruct passage of the column bars through the connection. Due to their high stiffness, they attract extra moment to the connection, which can lead to problems at the ends of the steel sections.

### **6.3 Limitations and Assumptions in FE Modeling of Various forms of Shear Reinforcement**

Like flexural reinforcement shear reinforcements are also modeled using Link 8 element. With Link 8 element exact shape of the shear reinforcement cannot be modeled. For example, anchorage hooks and bends of conventional shear reinforcement and the heads for shear studs cannot be appropriately modeled. However, in this study, the effect of anchorage hooks or bends are assumed by connecting the link element for shear reinforcement between nodes of each adjacent concrete solid element, so that the two materials share the same nodes. Perfect bond is also assumed between materials as mentioned in Chapter 3. Besides, since the shear reinforcement will be modeled by connecting the nodes of the adjacent concrete element, inclination angle of the inclined shear reinforcement will depend on the element mesh size. Exact angle of the test specimen may not be possible to maintain if same size mesh is used for the entire plate. With all these assumptions and limitations influence of few selected types of shear reinforcement is studied in the following sections.

### **6.4 Effects of Bent bar Shear Reinforcement**

To study the effect of bent bar reinforcement slabs B-14, B-16 and A-7b of Elstner and Hognestad (1956) were taken as reference. B-14 and B-16 slabs are having all the material and geometric parameters identical except that in B-16 shear reinforcement was provided. The model plates were square (70" x 70"), supported along the edges, and loaded with a central load uniformly distributed over an area of 10" square and applied through a column stub. The thickness of the slabs was 6 inch. The orthogonal longitudinal reinforcement was provided in the tension zone. The distance from the centroid of the longitudinal reinforcement to the top of the compression face was 5 inch. The shear reinforcement was

additional steel and not bent-up tension reinforcement. The bend in these added bars was generally directly under the column edges. The second bend was at 3.333 inch from the column edges details of which are shown in Figure 6.4.1. Numerical results of slab B-14 and B-16 were verified with test results in chapter 4 (Figure 4.4.4 and 4.4.5). Effect of shear reinforcement is observed by plotting the load-deflection curve of plate B-14 and B-16 together as shown in Figure 6.4.2. It is observed that, the punching shear strength and the ductility of the slab increased with the addition of shear reinforcement. The ultimate load capacity of slab B-14 without shear reinforcement is 144 kip and that of B-16 with shear reinforcement is 188 kip. An increase in strength of about 30 % is found from the numerical solutions. Test results also indicate similar increase in strength with shear reinforcement compared to the slab without shear reinforcement (168 kip with shear reinforcement as against 130 kip without it).

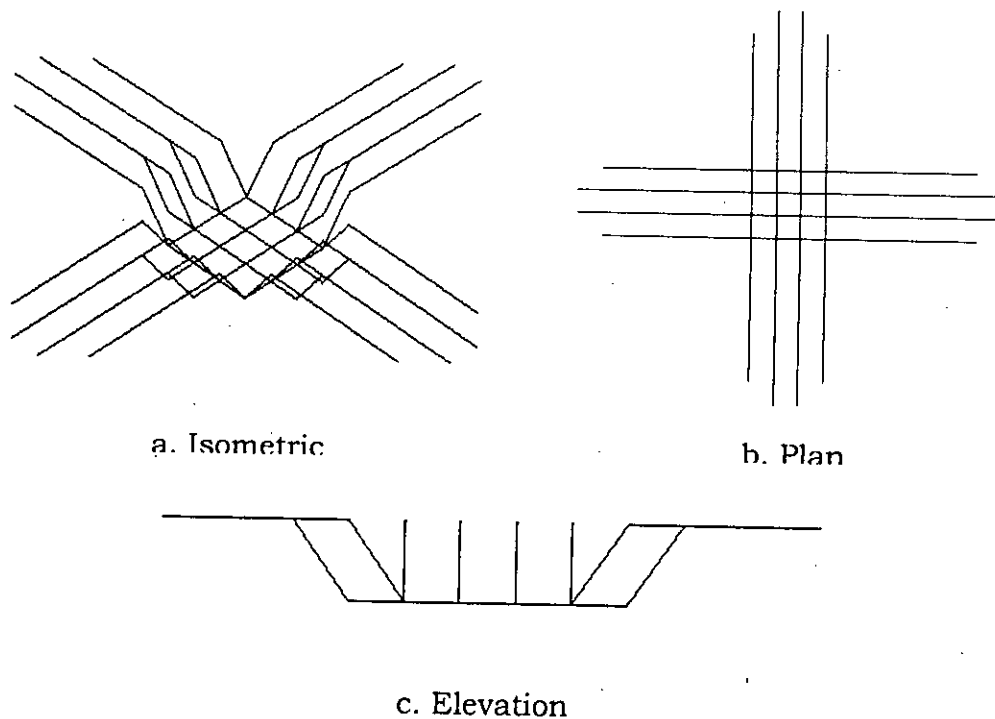


**Figure 6.4.1** Bent-bar Shear Reinforcement

On the basis of the case studies, it seems that the introduction of stirrups may considerably enhance the ultimate load of even over reinforced slabs (3.00 %); the main reason for this is that the vertical steel takes up some of the axial stresses in the concrete and controls the spread of the associated strains towards adjacent areas.

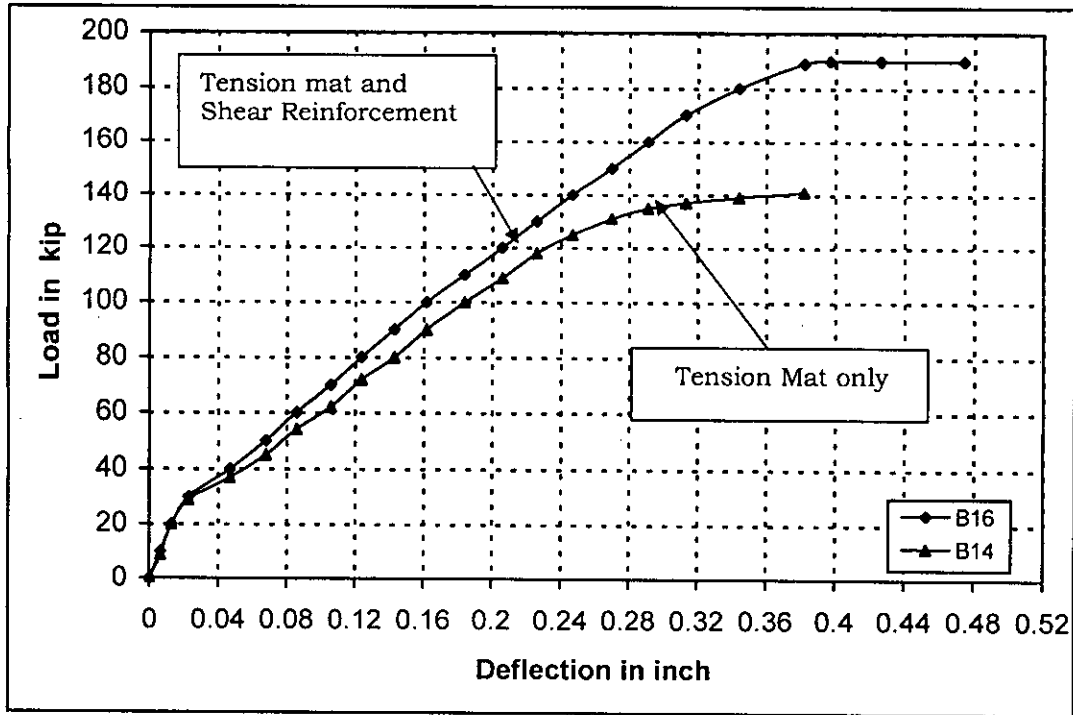


**Figure 6.4.2** Influence of Bent-bar Shear Reinforcement on Load-deflection Response of Flat Plate

Next a parametric study was conducted to observe the effect of shear reinforcement on model A-7b. First group of 8 bars was bend directly under the column edge. In the second group additional 4 bars was bend at 3.333 inch from the column edge. Comparative load-deflection response is shown in Figure 6.4.3. It is observed that bending the bars directly under column edge has no significant effect on the strength enhancement. Bending of shear bars at certain distance from the column edge has considerable effect on the ultimate strength.

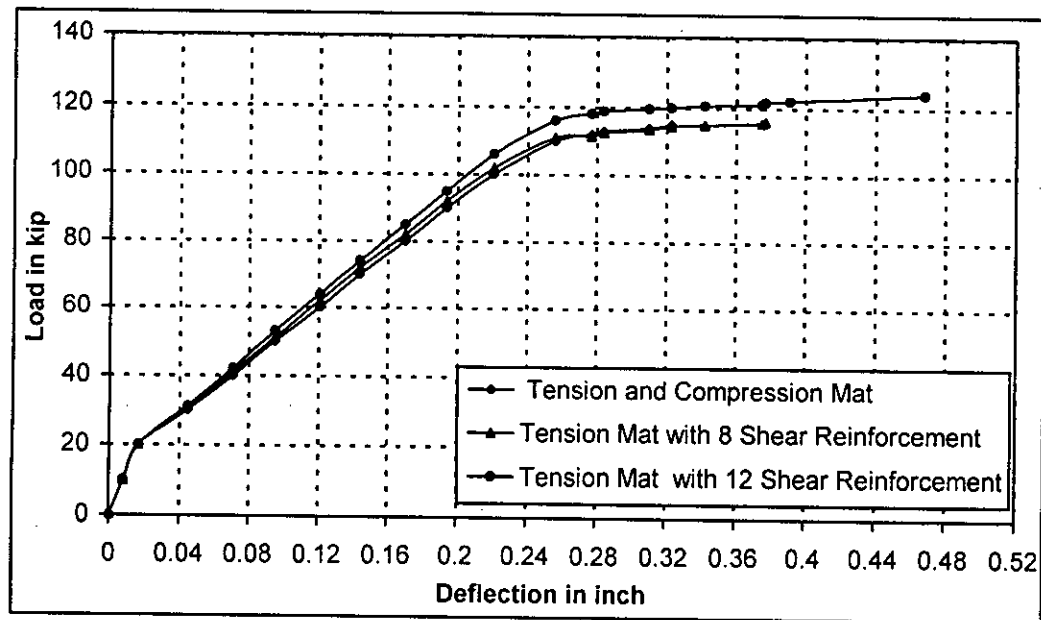


**Figure 6.4.3** Comparative Load-deflection Response of Bent-bar Shear Reinforcement

### 6.5 Effects of Closed hoop Shear Reinforcement

Closed hoop shear reinforcement both vertical and inclined form were studied. Control plate was taken without shear reinforcement as A-7b of Elstner and Hognestad (1956). Shear reinforcements were placed in the same way as Olivera et al. (2001) and shown in Figure 6.5.1 and Figure 6.5.2. Number 4 bar was considered as stirrup. Total six loops were placed on all four sides of the column at 3.333 inch spacing covering 16.66 inch. Load-deflection curves for these slabs (with shear reinforcement) are compared with the slab (without shear steel) in Figure 6.5.3. As one would expect, slabs with inclined shear reinforcement exhibited increased stiffness and higher ultimate load compared to the slab with vertical shear reinforcement. It may be noted from the figure that the shear reinforcement comes into play only after first cracking has occurred. As expected, the punching shear strength and the ductility of the specimens increased with the addition of shear reinforcement and so is the ultimate load.

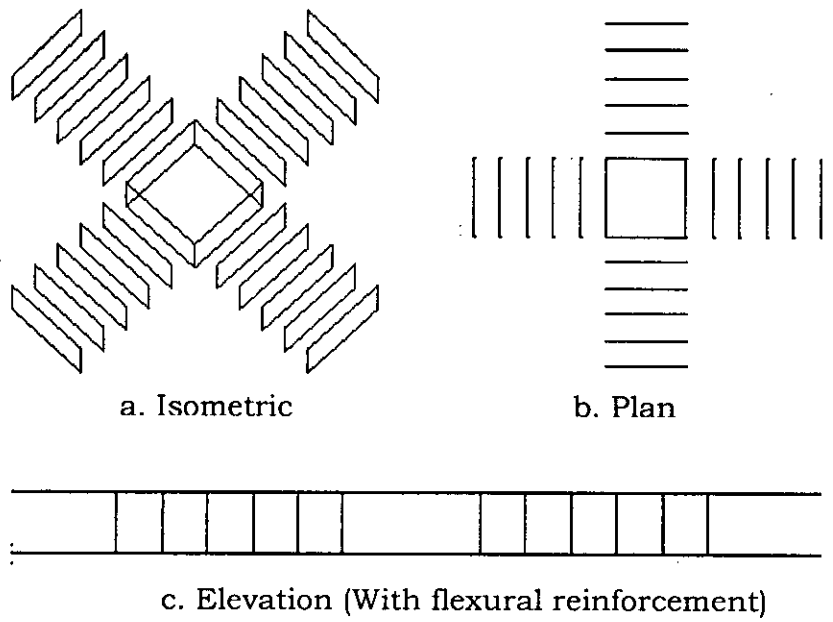


**Figure 6.5.1** Closed hoop Shear Reinforcement (Vertical)

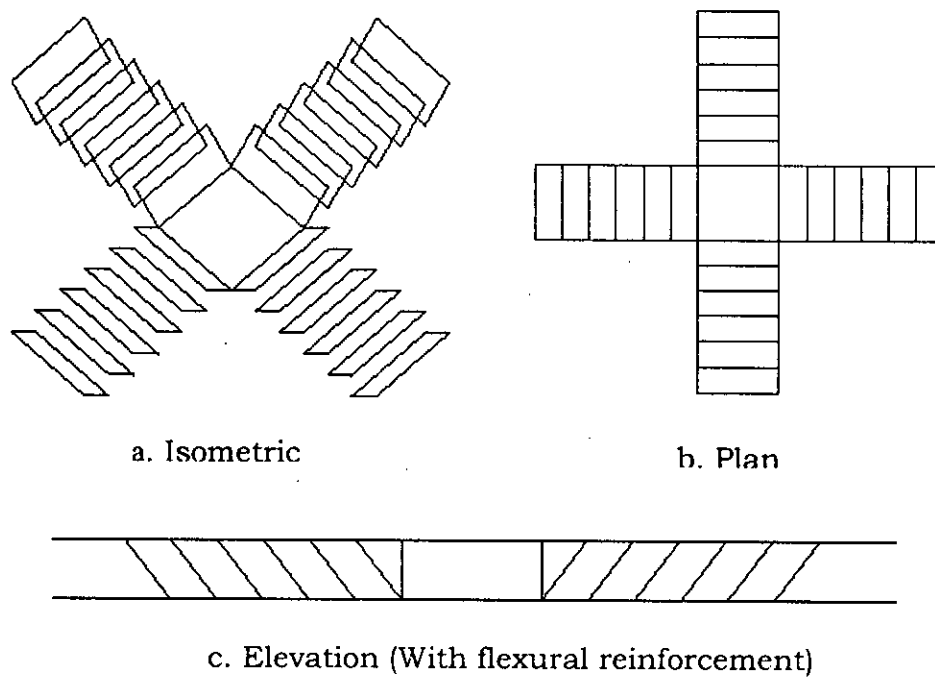


**Figure 6.5.2** Closed hoop Shear Reinforcement (Inclined)

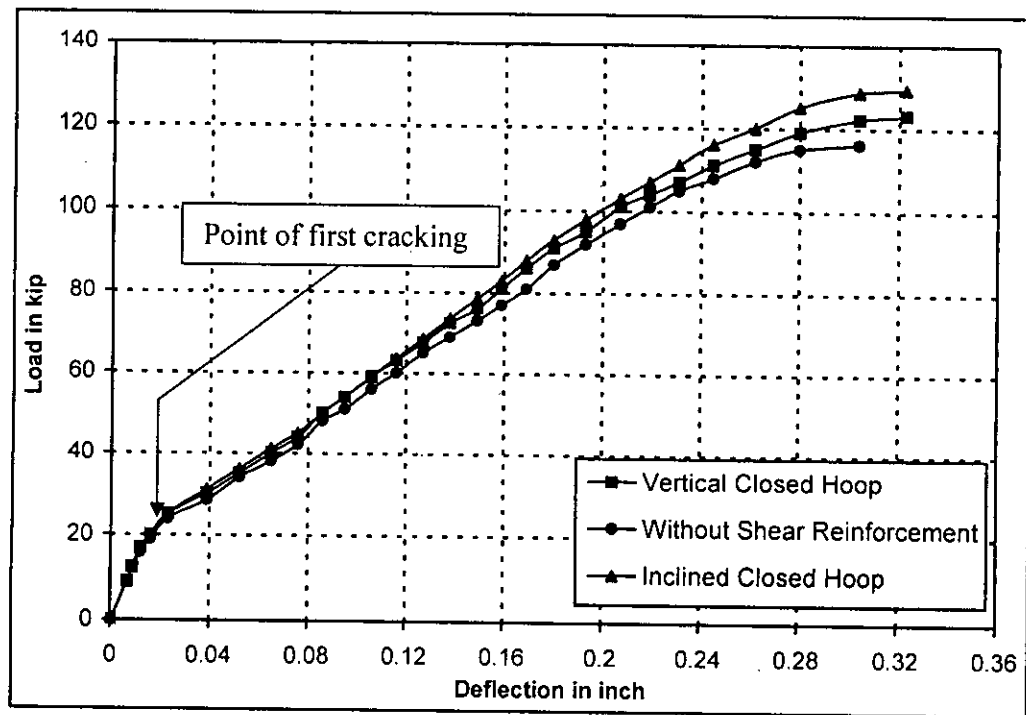


**Figure 6.5.3** Effect of Closed hoop Shear Reinforcement

The results indicate that the inclined stirrups are technically superior. They are easy to install, and would thus seem to be a promising form of shear reinforcement for flat plates.

### 6.6 Effects of Open Link Shear Reinforcement

Open link shear reinforcement both vertical and inclined were considered and placed in the same way as closed hoop reinforcement mentioned above. Shear reinforcements were placed in the same way as shown in Figure 6.6.1 and 6.6.2. Number 4 bar was considered as stirrup. Total six loops were placed on all four sides of the column at 3.333 inch spacing. Load-deflection curves for the slabs are compared with the slab without shear reinforcement in Figure 6.6.3.

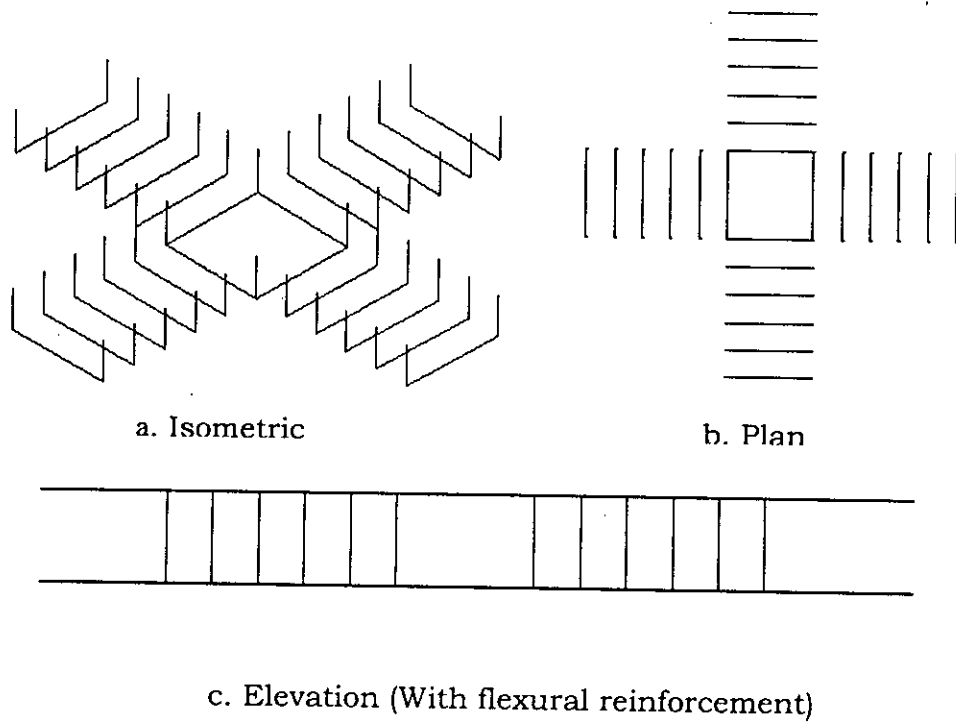


**Figure 6.6.1** Open link Shear Reinforcement (Vertical)

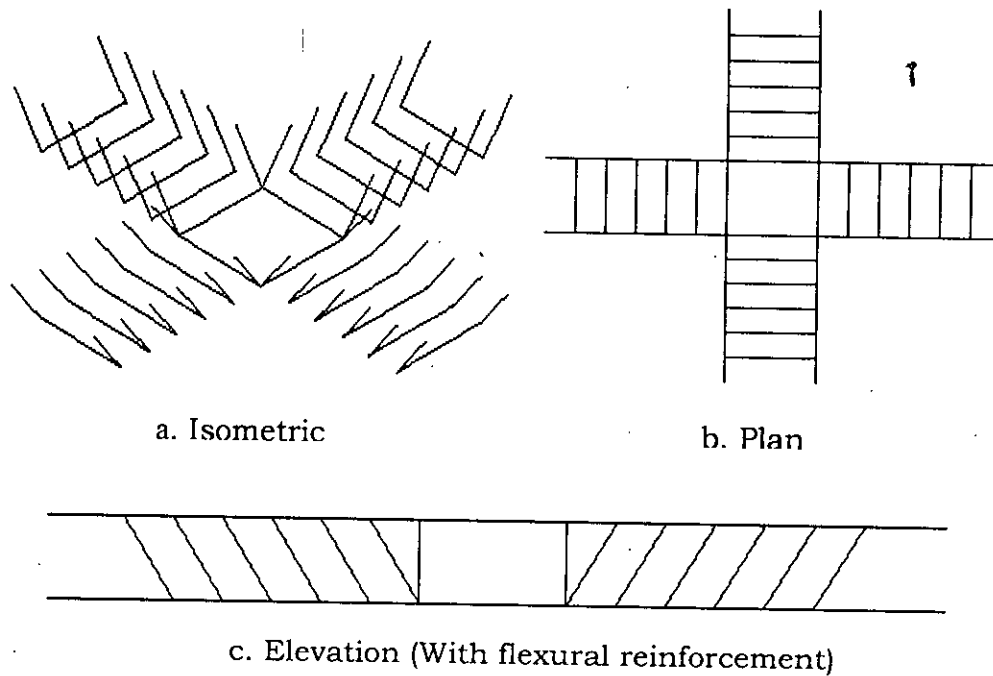


**Figure 6.6.2** Open link Shear Reinforcement (Inclined)



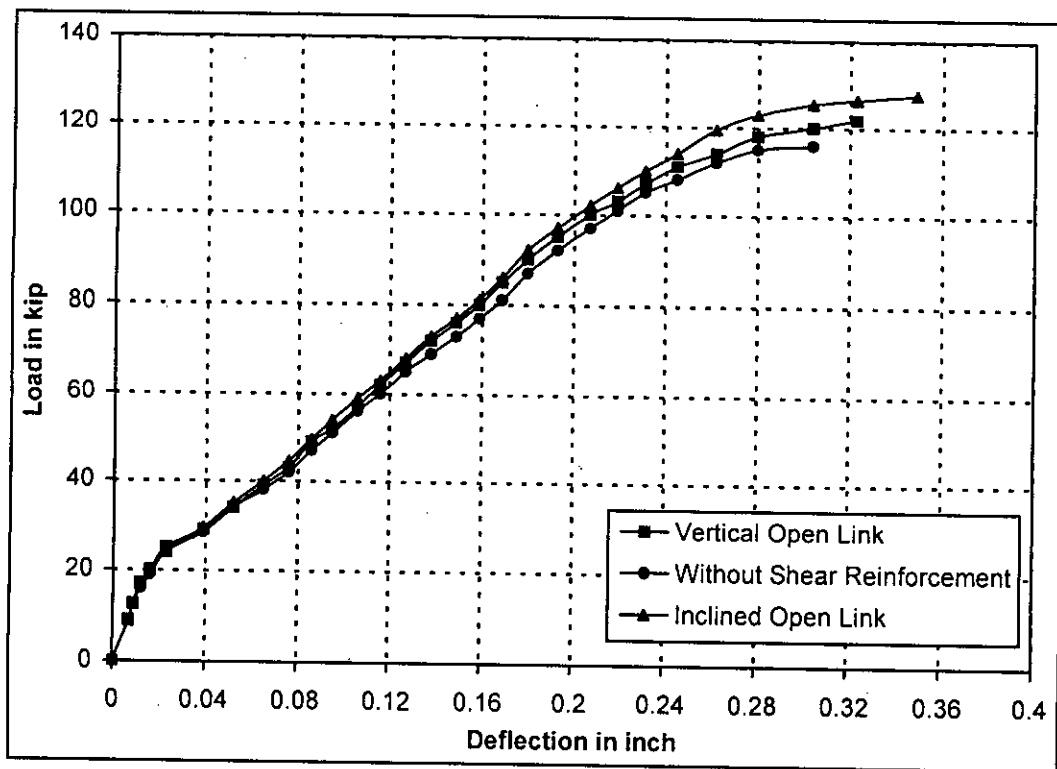


**Figure 6.6.3** Effect of Open link Shear Reinforcement

### 6.7 Effects of Hat type Shear Reinforcement

Hat type shear reinforcement both vertical and inclined form were considered and placed in the same fashion as closed hoop reinforcement. Shear reinforcements were placed in the same way as shown in Figure 6.7.1 and 6.7.2. Number 4 bar was considered as shear hat. The hats are placed on the tension face with the arm in the compression face extending outwards like a hat. Total six hats were placed on all four sides of the column at 3.333 inch spacing. Load-deflection curves for slabs are compared with the slab without any shear reinforcement in Figure 6.7.3. Here, it is also observed that inclined hat types are more effective compared to the vertical hat type shear reinforcement.

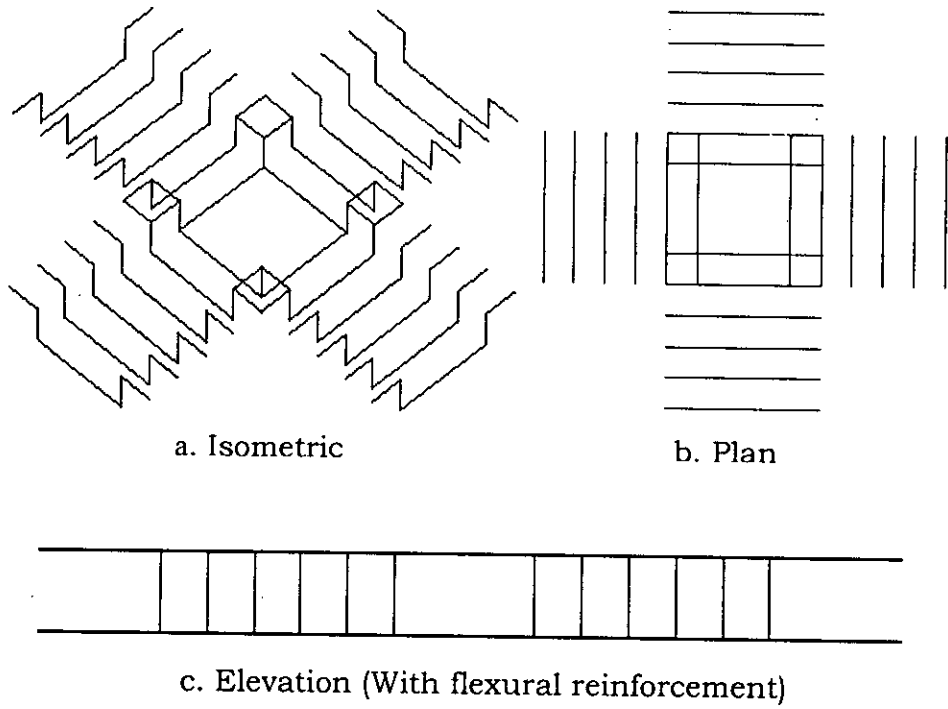


**Figure 6.7.1** Hat type Shear Reinforcement (Vertical)

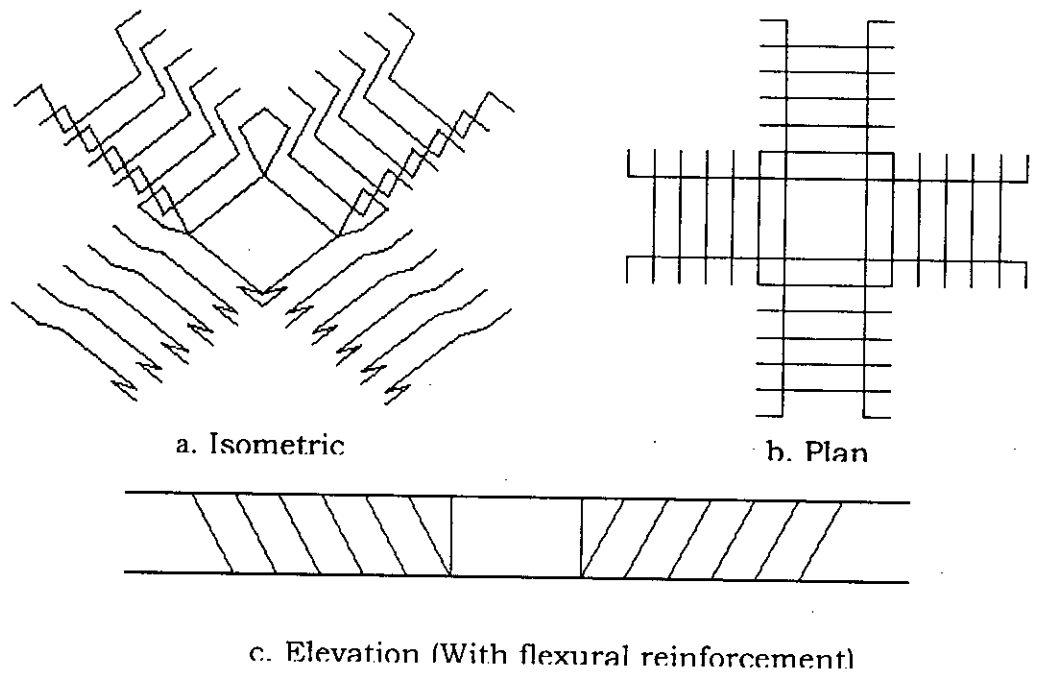


**Figure 6.7.2** Hat type Shear Reinforcement (Inclined)

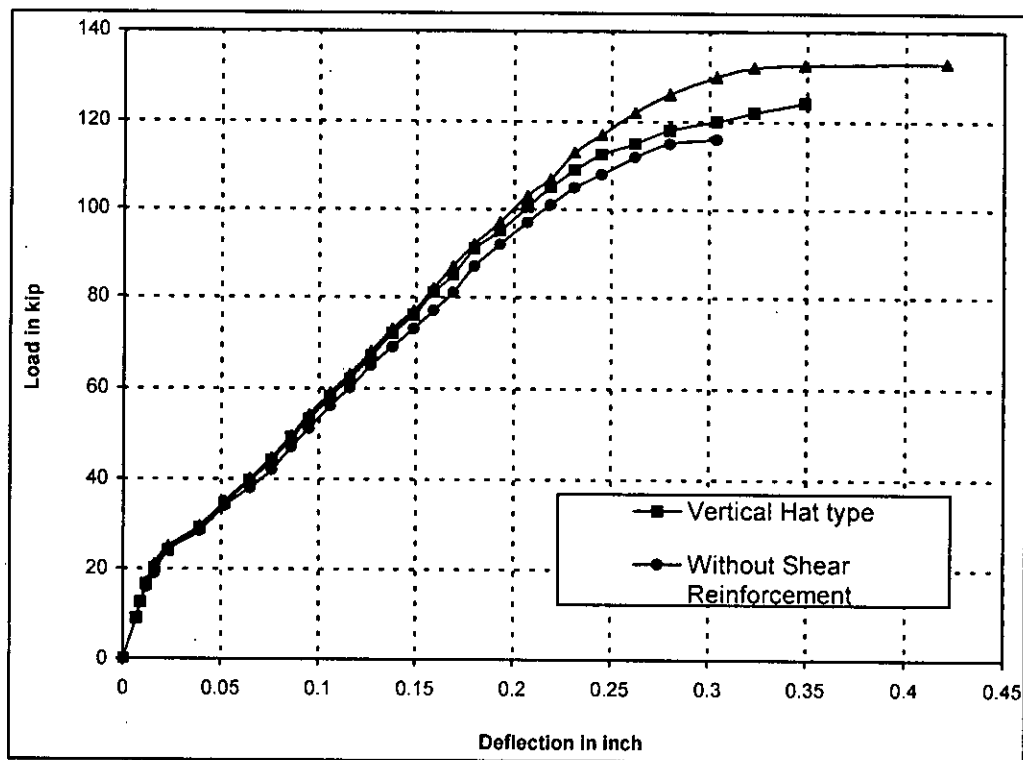


**Figure 6.7.3** Effect of Hat type Shear Reinforcement

### 6.8 Discussion on Effective Shear Reinforcement

Figures 6.8.1 and 6.8.2 shows the comparative effect of various types of shear reinforcement with vertical and inclined alignment. As can be seen from the figures that for all types of shear reinforcement their inclined orientation has better strength enhancement compared to vertical placement. Ultimate strength increases 5 to 7 % with vertical alignment whereas for inclined orientation the increase in strength is about 10 to 15 %. In the previous chapter (Figure 5.3.1) it was observed that with the increase of plate thickness ultimate strength increases. Hence, lower plate thickness may be possible if some shear reinforcement is included. However, more studies are required to correlate the percentage of shear reinforcement with corresponding change of plate thickness.

Among the three types of shear reinforcement hat type appears to give the highest strength in numerical computation for inclined orientation. Though experimental results showed that the hat-shaped shear reinforcement was not so effective compared to the closed hoop because of the lack of proper anchorage [Yamada et al. (1992)]. A hat-shaped unit is very advantageous from prefabrication and field installation points of view. Better effect of hat shaped reinforcement in FE analysis may be due to the present modeling technique which considered full and perfect bond in bent tails. Thus a hat shaped unit consists of five element connecting six nodes, whereas, open link unit consists of three elements connecting four nodes and closed hoop unit consists of four elements connecting four nodes. Here, hat shaped unit may have the actual effect of a hat with anchorage hook, which resulted in the highest strength contribution. However, hat shaped unit with anchorage hook may cost some extra labour and time for field installation compared to plain hat type.

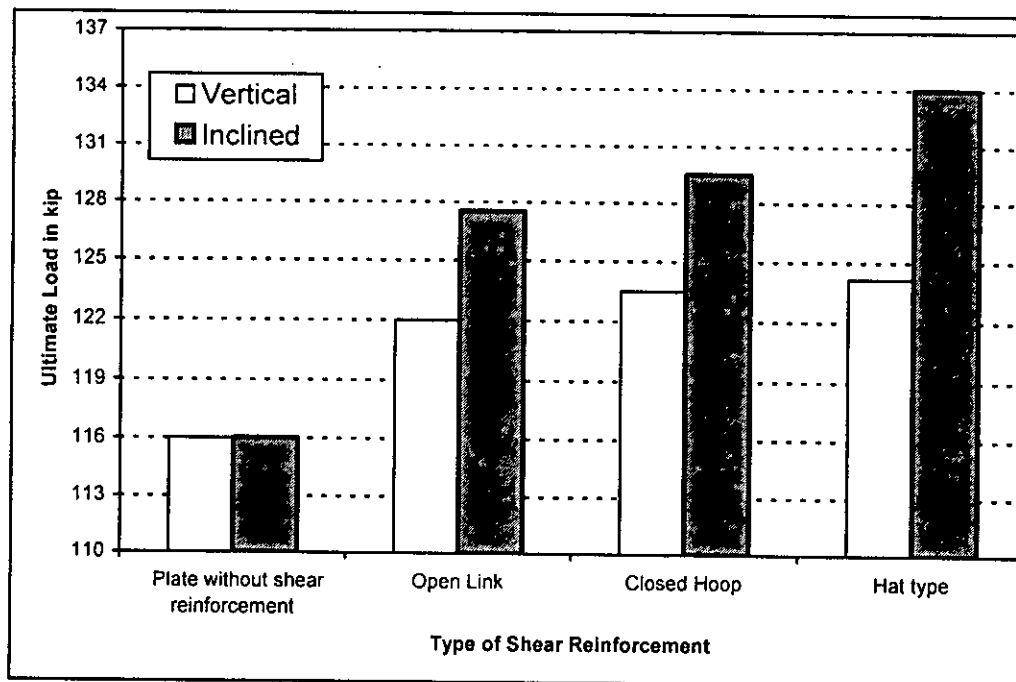


**Figure 6.8.1** Relative Performance of Various types of Shear Reinforcement

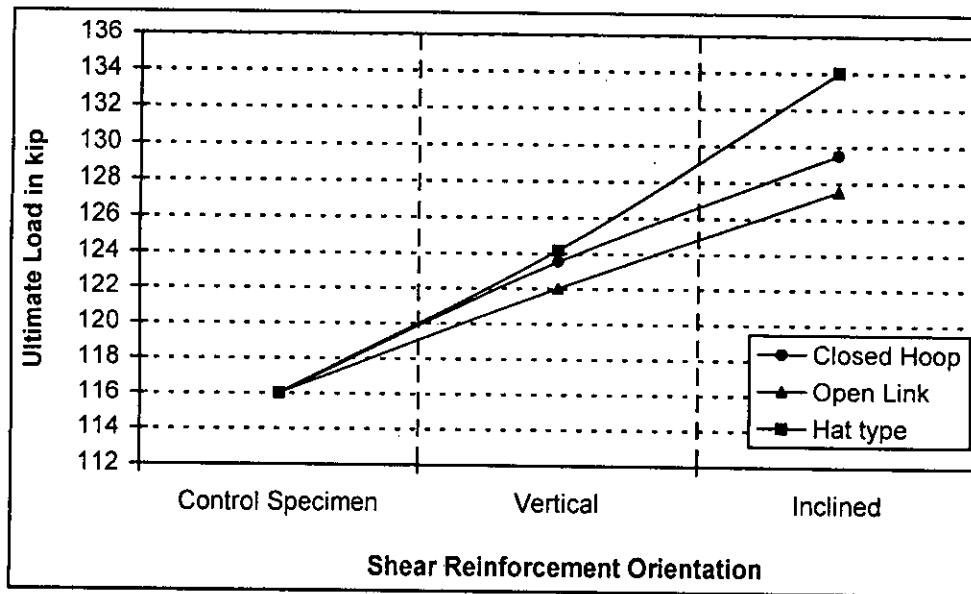


**Figure 6.8.2** Effect of Inclination of Shear Reinforcement for three Different Types

The experimental literature states that the bar spacing less than  $d/2$  is needed to intercept inclined cracks. But in the FE model the reinforcements are placed connecting the nodes, as such the minimum spacing was the size of the mesh, which is 3.333 inch in this case. For all practical purposes inclination of the shear reinforcement should be  $45^\circ$  and spacing should be less than  $d/2$ .

### 6.9 Final Remarks

The addition of shear reinforcement had a significant effect on the punching shear strength of the reinforced concrete plates. The models with shear reinforcement showed a more ductile behavior than those without shear reinforcement. The ultimate load increased too. The results indicate that the inclined stirrups are more efficient in increasing the ductility and strength. They are also easy to install, and would thus be classed as technically superior class of shear reinforcement for flat plates. Further experimental and numerical study may be carried out with inclined shear reinforcement.

## Chapter 7

### A RATIONALE FOR PUNCHING SHEAR PREDICTION EQUATION

#### 7.1 General

For the design of flat plates, flat slabs and column footings punching shear strength of concrete in the vicinity of columns, concentrated loads or reaction is one of the design criterion which often governs the design. Thus, the critical shear section for this type of shear should be located so as the perimeter of critical section is a minimum, but need not approach closer than a certain distance from edge or corners of columns, concentrated load or reaction areas. Different Code provisions provide the location of this critical section differently. But for all the Codes, when this is done, the shear strength is taken almost independent of the edge condition, reinforcement ratio and span-depth ratio. There are scopes of modification within the method. The purpose of this chapter, therefore, is to identify these scopes of modifications and propose changes. Efforts are then made to test the performance of the suggested proposition.

In Chapter 2, various code provisions along with few individual researchers' prediction equations are presented. Among the code predictions British Code appears to be less conservative as critical shear perimeter is taken as a rectangle located at a distance of  $1.5d$  from the edge of column, for all other codes this perimeter is taken at  $d/2$  from the column face. This code also considers the effect of reinforcement ratio. It is to be further noted that BNBC (1993) adopted ACI Code (S.I. unit) with minor modification. As such all the succeeding discussions are mainly related to ACI Code.

**7.2 ACI 318-02 Code Provision**

Provisions in ACI 318 are based on the assumption that the punching shear failure surface will develop at an angle of 45 deg. The permissible nominal shear stresses in the concrete are empirically derived based on a critical section located at half the effective depth of the slab away from the perimeter of the load. The ACI equation for predicting punching shear mentioned in Chapter 2 is reiterated here. According to this Code, for non-prestressed slabs and footing, nominal punching shear strength provided by concrete ( $V_c$  in pound) shall be smallest of the following three equations:

In F.P.S. Unit:

$$V_c = (2 + 4/\beta_c) \sqrt{f'_c} b_o d \quad (7.2.1)$$

$$V_c = (2 + \alpha_s d/b_o) \sqrt{f'_c} b_o d \quad (7.2.2)$$

$$V_c = 4 \sqrt{f'_c} b_o d \quad (7.2.3)$$

Here,

$\beta_c$  = ratio of long side to short side of concentrated load or reaction area.

$f'_c$  = uniaxial cylinder (compressive) strength of concrete in psi.

$b_o$  = perimeter of critical section of slab or footing at a distance of  $d/2$  away from the column faces in inch.

$d$  = Effective depth (distance from extreme compression fiber to centroid of longitudinal tension reinforcement) in inch.

$\alpha_s$  = 40 for interior column, 30 for edge column, 20 for corner column.

According to ACI 318-02 Code, the critical section for shear in slabs subjected to bending in two directions follow the perimeter ( $b_0$ ) located at a distance  $d/2$  from the periphery of the concentrated load. It further assumes that the shear capacity of the concrete is proportional to the square root of the concrete strength. The other parameters considered are the aspect ratio of the column or reaction area ( $\beta_c$ ), effective depth ( $d$ ) and location of the column ( $\alpha_c$ ).

As can be seen, ACI Building Code does not recognize the effect of restraining action at the support when treating punching shear in reinforced concrete slabs. The expression for  $V_c$  does not include terms considering the ratio of main steel or the slab depth. Effects of span-depth ratio are not addressed in the current punching shear provisions. Analysis performed in Chapter 5 reveals that reinforcement ratio and span-depth ratio has a significant influence on punching shear strength. Though effective depth may be somehow related to the slab thickness, but it does not relate to the span-depth ratio in any way. For a particular thickness of slab, span-depth ratio may be varied by changing the span of the slab. Though in this study, span-depth ratio was varied by changing the slab thickness keeping the span constant.

### **7.3 Comparison of Analytical and Experimental results with ACI 318-02 Code Provision**

Some of the analytical results are already compared with test data in Table 4.1 and some are graphically compared in Figure 5.2.1. Here, Table 7.1 shows further a comparison among the experimental results, FE analysis and predicted values according to ACI 318-02 Code without  $\phi$  factor for slabs having no shear reinforcement.



**Table 7.1** Comparison of Results

Slab No.	$\rho$ per cent	$d$ (in) test	$d$ (in) FE	$f'_c$ (psi)	$f_y$ (ksi)	$P_{test}$ (kip)	$P_{FE}$ (kip)	ACI 318 $V_c$ (kip)	$\frac{P_{FE}}{V_c}$	$\frac{P_{test}}{V_c}$	Difference in % ( $P_{FE}$ & $V_c$ )
A-1a	1.15	4.63	5	2040	48.2	68	71	54	1.32	1.26	24
A-1b	1.15	4.63	5	3660	48.2	82	84	72	1.16	1.14	14
A-1c	1.15	4.63	5	4210	48.2	80	79	77	1.03	1.04	2.50
A-1d	1.15	4.63	5	5340	48.2	79	78	87	0.89	0.90	-11
A-1e	1.15	4.63	5	2940	48.2	80	83	65	1.27	1.23	21
A-7	2.47	4.50	5	4050	46.6	90	98	76	1.29	1.18	22
A-7b	2.47	4.50	5	4050	46.6	115	116	76	1.53	1.51	34.50
B-14	3.00	4.50	5	7330	47.2	130	144	103	1.39	1.26	28

It is observed from the table that for most of the cases, ACI 318-02 prediction are conservative, giving predicted values about 15 to 40 percent lower than the test results. Two exceptions are slabs A-1d and A-1e. Experimentally and numerically it is observed that for a particular reinforcement ratio, progressive increase in shear strength with increase in compressive strength nearly stops for concrete strength beyond some higher value. Results of slabs A-1b, A-1c and A-1d may be compared to see the effect. This decrease of ultimate strength for high strength concretes may be related to the fact that for a given steel ratio, there is a limit to the concrete strength upto which more or less a ductile failure occurs. When concrete strength exceeds that limit brittle failure is encountered with no appreciable change in ultimate load. ACI Code addresses this fact for flexural analysis but neglects it for punching shear prediction. As such ACI prediction of punching shear increases with the increase in compressive strength and it overestimates the strength for A-1d slab. Application of  $\phi$  factor will bring the load on conservative side. Further, it may be noticed that ACI prediction gives same ultimate load value for A-7 (opposite edges simply supported) and

A-7b (four edges simply supported). Thus it is independent of the edge condition effect. It can be seen from Figure 5.2.6 that for a particular compressive strength with all other parameters left constant ultimate strength increases with increase in reinforcement ratio. But this effect cannot be accommodated in the ACI 318 provision.

#### **7.4 Scope of Modification**

From the above discussion, it is evident that to eliminate the problem of underestimation or overestimation of punching strength by ACI 318 Code, a modification is required to attain a level of accuracy that can reasonably be compared with the test results (or finite element solution). This study, therefore, identifies that the code provisions may be reviewed taking into consideration the influence of the following:

- Effects of span-depth ratio on punching shear strength.
- Influence of reinforcement ratio (flexural).
- Type, amount and alignment of the shear reinforcement.
- Influence of edge restraint.

The complete investigation is a trial and error process. Once the final value of the items of modification are decided, depending on the proximity of test data, attempts would be made to suggest a modified form of prediction equations incorporating the required changes.

#### **7.5 Suggested Modification to the ACI Method**

From the several parameters studied in Chapter 5, reinforcement ratio and concrete strength are the two included for the proposed modification. Keeping similarity with the flexural formula modifiers ( $\alpha$  and  $\beta$ ),  $\lambda$  and  $\gamma$  are proposed for reinforcement ratio and concrete compressive strength respectively. Increasing the reinforcement ratio increases the punching strength of the plate as shown in Figure 5.2.6.

This increase in strength with reinforcement ratio is more pronounced with higher strength concrete and higher reinforcement ratio. Since reinforcement ratio directly increases ultimate strength, value of the factor of contribution  $\lambda$  should be greater than unity and assumed to be multiplier of  $f'_c$ . To maintain similarity with the value of  $\alpha$ , starting value of  $\lambda$  is assumed to be 0.72 and inverse of  $\lambda$  is multiplied with  $f'_c$ . As observed experimentally and numerically, ultimate strength reduces for very high values of concrete compressive strength. Hence, value of  $\gamma$  is assumed to be unity for normal strength concrete and reduces with the increase in compressive strength, and used as a direct multiplier to the prediction equation. Considering these aspects, the proposed modifications to ACI 318 Code equations are as follows:

In F.P.S. Unit:

$$V_{cm} = (2 + 4/\beta_c) \sqrt{\frac{1}{\lambda} f'_c} \gamma b_0 d \quad (7.5.1)$$

$$V_{cm} = (2 + \alpha_s d/b_0) \sqrt{\frac{1}{\lambda} f'_c} \gamma b_0 d \quad (7.5.2)$$

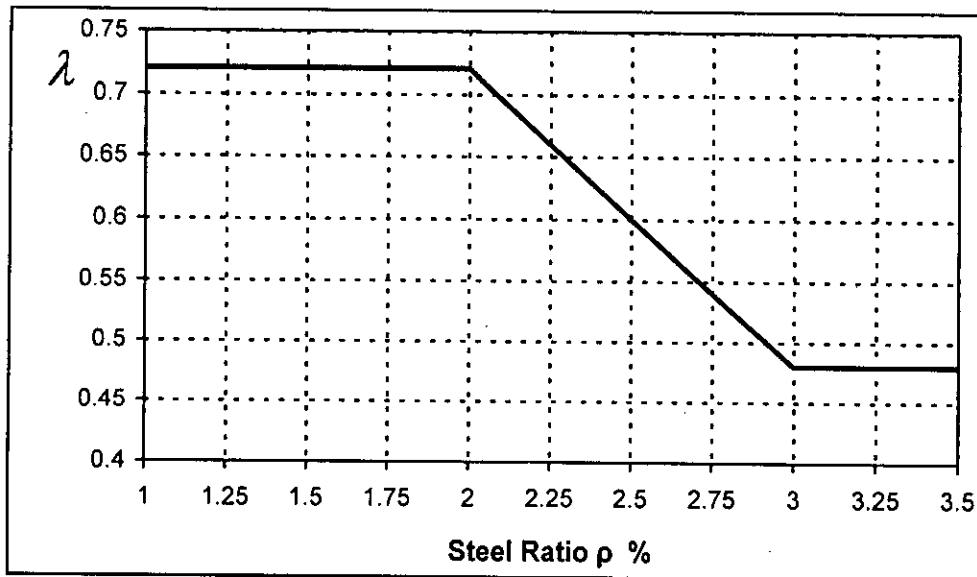
$$V_{cm} = 4 \sqrt{\frac{1}{\lambda} f'_c} \gamma b_0 d \quad (7.5.3)$$

Through a number of trials, the following values of  $\lambda$  and  $\gamma$  are found to be satisfactory and conservative.

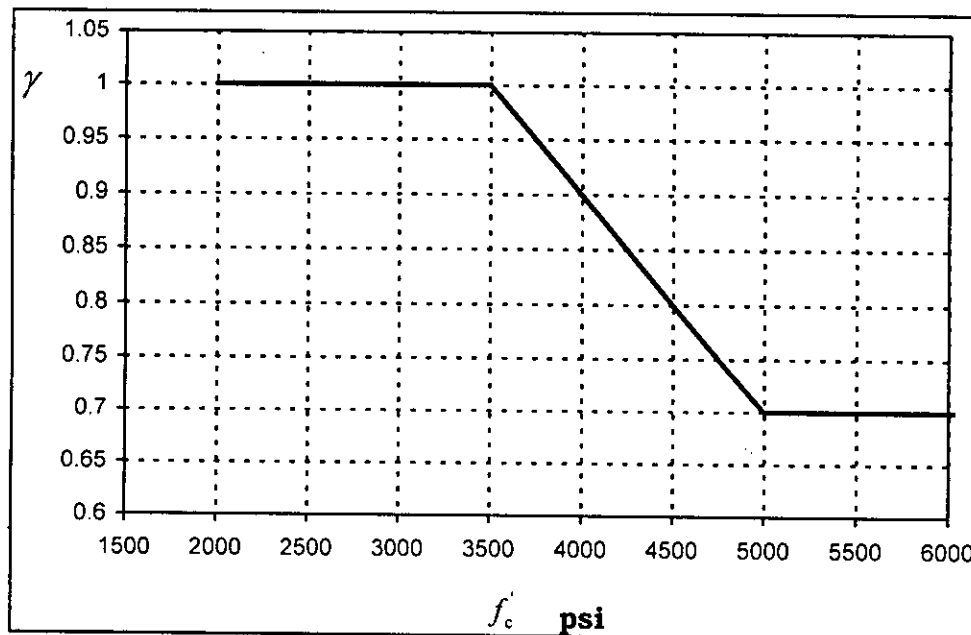
$\lambda$  equals 0.72 for  $\rho \leq 2\%$  and decreases by 0.06 for every 0.25% above 2 up to 3%. For  $\rho > 3\%$ ,  $\lambda = 0.48$ .

$\gamma$  equals 1.00 for  $f'_c \leq 3500$  psi and decreases by 0.10 for every 500 psi above 3500 up to 5000 psi. For  $f'_c \geq 5000$  psi,  $\gamma = 0.70$  applicable for  $\rho \leq 2.50\%$ .

Figure 7.5.1 and 7.5.2 shows these simple relations.



**Figure 7.5.1** Variation of  $\lambda$  with Steel Ratio



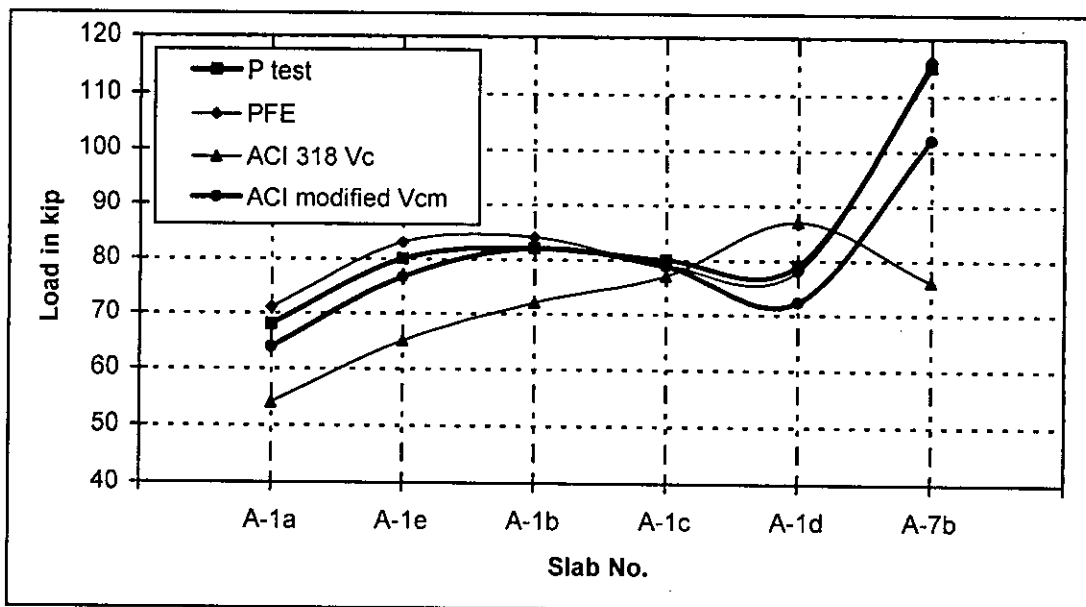
**Figure 7.5.2** Variation of  $\gamma$  with Concrete strength  $f_c'$  for  $\rho \leq 2.50$  %.

Table 7.2 compares the experimental results with the ultimate loads obtained from FE analysis and as predicted by ACI 318 Code formula and the modified ACI equations.

**Table 7.2** Comparison of Test Results with FE, ACI and Modified ACI Formula (6 Test Slabs)

Slab No.	$\rho$ percent	$f'_c$ (psi)	$f_y$ (ksi)	$P_{test}$ (kip)	$P_{FE}$ (kip)	ACI 318 $V_c$ (kip)	ACI modified $V_{cm}$ (kip)	$\frac{P_{test}}{V_c}$	$\frac{P_{test}}{V_{cm}}$	$\frac{P_{FE}}{V_{cm}}$
A-1a	1.15	2040	48.2	68	71	54	63.87	1.26	1.05	1.11
A-1b	1.15	3660	48.2	82	84	72	82	1.14	1.00	1.03
A-1c	1.15	4210	48.2	80	79	77	78.73	1.04	1.02	1.01
A-1d	1.15	5340	48.2	79	78	87	72.34	0.91	1.09	1.08
A-1e	1.15	2940	48.2	80	83	65	76.68	1.23	1.04	1.08
A-7b	2.47	4050	46.6	115	116	76	102	1.51	1.13	1.14

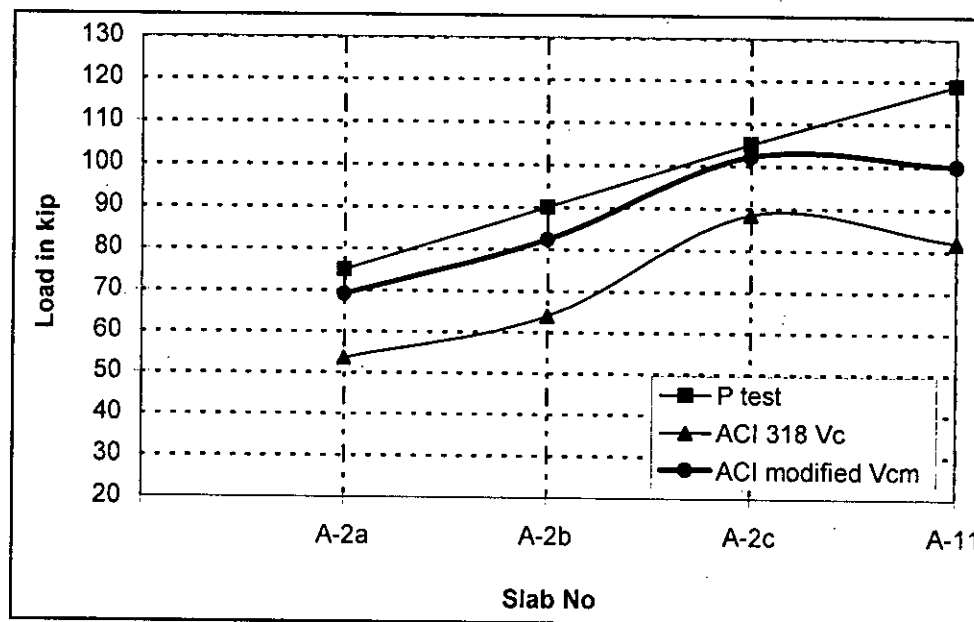
The comparison is better interpreted in Figure 7.5.3. As can be seen from the figure, modified prediction is very close to test results compared to ACI 318 prediction. The problem of overestimation of strength by ACI formula is overcome and underestimation is also well addressed.

**Figure 7.5.3** Comparison of Results of Test, FE, ACI and Modified Formula (6 Test Slabs)

To confirm the acceptability of the modified equations, more test results from Elstner and Hognestad (1956) and Moe (1961) are compared in Tables 7.3 and 7.4 respectively. These are plotted in Figures 7.5.4 and 7.5.5.

**Table 7.3** Comparison of Results of Test, ACI and Modified Formula (Further 4 Test Slabs)

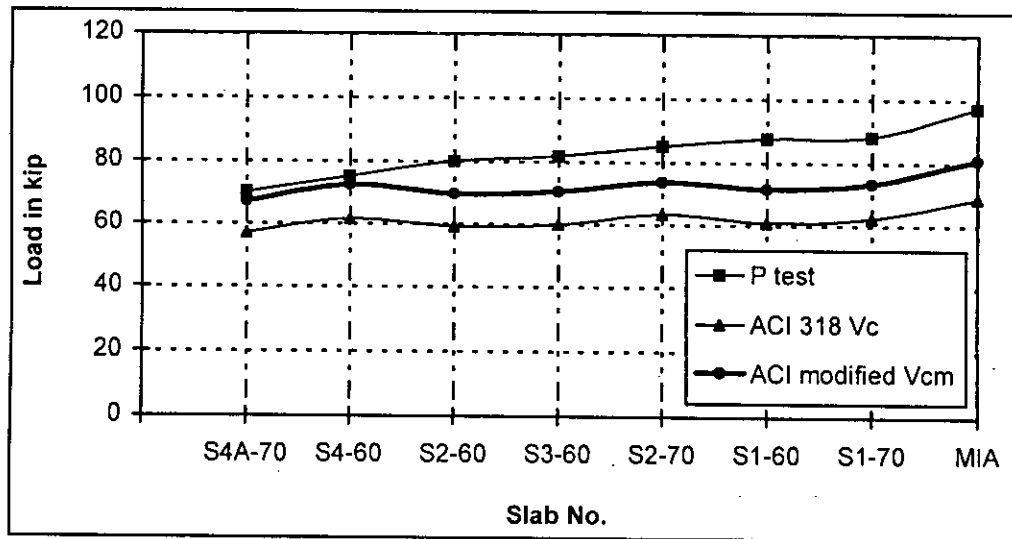
Slab No.	$\rho$ percent	$f'_c$ (psi)	$f_y$ (ksi)	$P_{test}$ (kip)	ACI 318 $V_c$ (kip)	ACI modified $V_{cm}$ (kip)	$\frac{P_{test}}{V_c}$	$\frac{P_{test}}{V_{cm}}$
A-2a	2.47	1980	46.6	75	53.40	69	1.41	1.09
A-2b	2.47	2830	46.6	90	63.84	82.40	1.41	1.09
A-2c	2.47	5430	46.6	105	88.42	102	1.19	1.03
A-11	2.47	3760	46.6	119	82	100	1.45	1.19



**Figure 7.5.4** Comparison of Results of Test, ACI and Modified Formula (Further 4 Test Slabs)

**Table 7.4** Comparison of Results of Test, ACI and Modified Formula (Moe's Test Slabs)

Slab No.	$\rho$ percent	$f'_c$ (psi)	$d$ inch	$d_{punch}$ in x in	$P_{test}$ (kip)	ACI 318 $V_c$ (kip)	ACI modified $V_{cm}$ (kip)	$\frac{P_{test}}{V_c}$	$\frac{P_{test}}{V_{cm}}$
S4A-70	1.13	2970	4.5	10x10	70	56.89	67.05	1.23	1.04
S4-60	1.13	3460	4.5	10x10	75	61.41	72.37	1.22	1.04
S2-60	1.03	3200	4.5	10x10	80	59.06	69.6	1.36	1.15
S3-60	1.02	3280	4.5	10x10	81.75	59.74	70.46	1.36	1.16
S2-70	1.02	3680	4.5	10x10	85	63.33	73.51	1.34	1.16
S1-60	1.06	3380	4.5	10x10	87.5	60.69	71.53	1.44	1.22
S1-70	1.06	3550	4.5	10x10	88.2	62.2	73.31	1.42	1.20
MIA	1.5	3340	4.5	12x12	97.3	68.65	80.91	1.43	1.20

**Figure 7.5.5** Comparison of Test Results with ACI and Modified ACI Formula (Moe's Test Slabs)

Finally a comparison is also made with the prediction of Gardener's Equation, British Code and Canadian Code provisions taking some of the test data from Elstner and Hognestad (1956) and Moe (1961). These are presented in Table 7.5 and Figure 7.5.6.

**Table 7.5** Comparison of Results with Gardener's Equation, British Code and Canadian Code provisions

Slab No.	Gardener's Equation $V$ (kip)	BS 8110 $V_p$ (kip)	CAN3-A23.3-M84 $V_{pc}$ (kip)	ACI 318 $V_c$ (kip)	ACI modified $V_{cm}$ (kip)	$P$ test (kip)	$\frac{P_{test}}{V}$	$\frac{P_{test}}{V_p}$	$\frac{P_{test}}{V_{pc}}$	$\frac{P_{test}}{V_c}$	$\frac{P_{test}}{V_{cm}}$
A-1a	47	64	59	54	63.87	68	1.45	1.06	1.15	1.26	1.05
A-1b	57.10	78	79	72	82	82	1.44	1.04	1.04	1.14	1.00
A-1c	59.82	81.73	84.76	77	78.73	80	1.34	0.98	0.94	1.04	1.02
A-1d	65	84.43	95.46	87	72.34	79	1.22	0.94	0.83	0.91	1.09
A-1e	53.78	72.51	70.84	65	76.68	80	1.49	1.10	1.13	1.23	1.04
A-2a	60	78.97	56	53.40	69	75	1.25	0.95	1.34	1.41	1.09
A-2b	67	88.95	67	63.84	82.40	90	1.34	1.01	1.34	1.41	1.09
A-2c	84	104.89	92.73	88.42	102	105	1.25	1.00	1.13	1.19	1.03
S4A-70	51	69.65	68.58	56.89	67.05	70	1.37	1.00	1.02	1.23	1.04
S2-60	50.67	69.24	71.19	59.06	69.6	80	1.58	1.16	1.12	1.36	1.15
S2-70	52.90	72.3	76.34	63.33	73.51	85	1.60	1.18	1.11	1.34	1.16
S1-60	52.10	71.19	73	60.69	71.53	87.5	1.68	1.23	1.20	1.44	1.22
S1-70	53	72.36	75	62.2	73.31	88.2	1.66	1.22	1.18	1.42	1.20



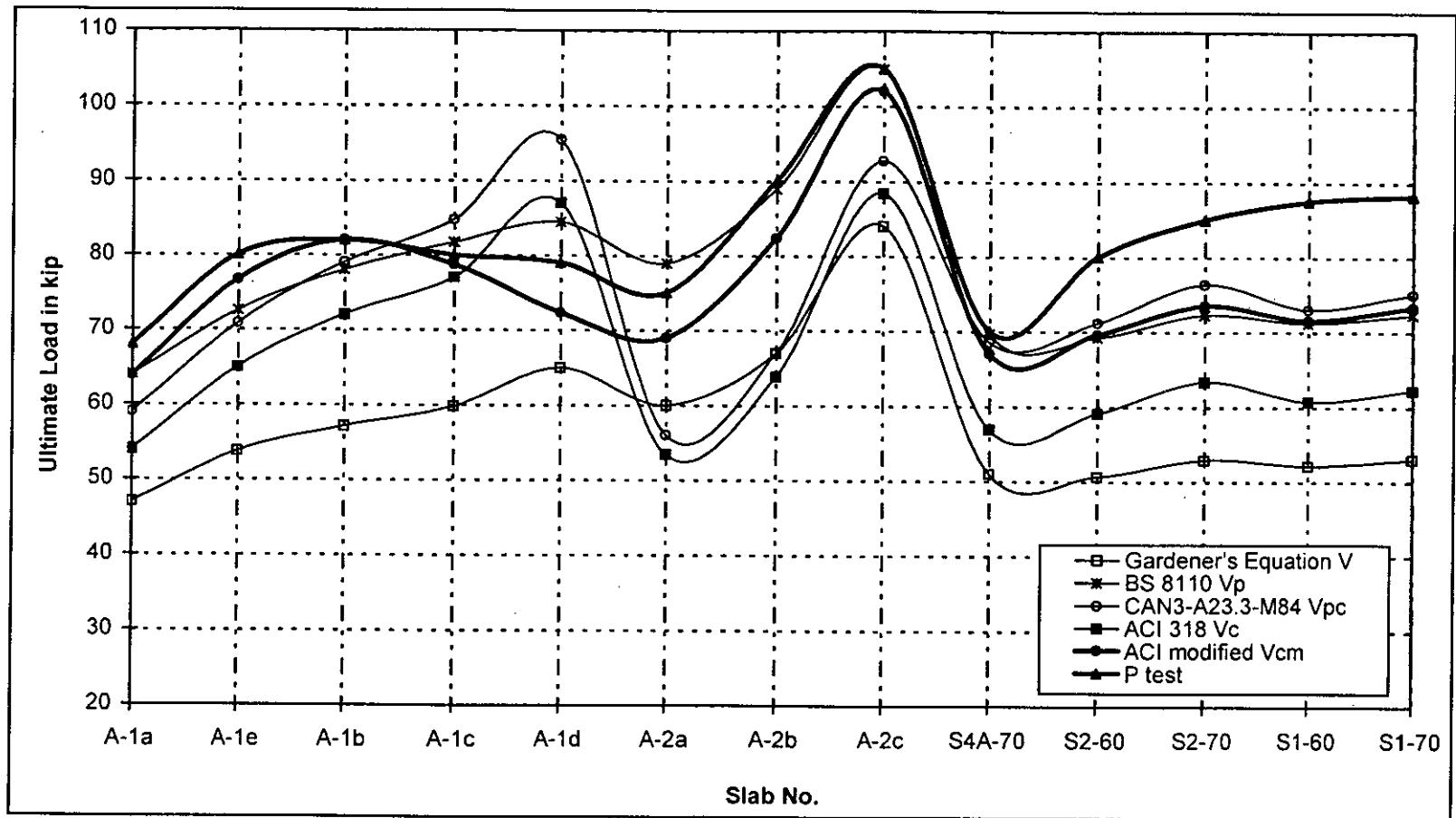


Figure 7.5.6 Comparison of Results with Gardener's Equation, British, Canadian and ACI Code Provisions

From these tabular and graphical comparisons, it is observed that the Gardener's equation is very conservative. British and Canadian Codes are less conservative compared to ACI Code and still overestimates the ultimate loads like ACI Code. Among all these options, the modified form of ACI Code prediction appears to be moderately conservative and overestimation is to a low level. As such these equations may be adopted by the designer with reasonable safety applying appropriate  $\phi$  factor.

### 7.6 Provision for Shear Reinforcement

As specified in the ACI Code, the punching shear strength provided by the concrete in a slab with shear reinforcement is taken as one-half that of the strength provided by the concrete in a slab without shear reinforcement. Reduction of the concrete component of resistance to  $2\sqrt{f'_c}b_0d$  that is  $0.5V_c$  in the presence of shear reinforcement is too conservative. The maximum allowable shear stress in a critical section at a distance  $d/2$  from the column face is  $6\sqrt{f'_c}$  psi allowed by ACI 318, the code gives this upper limit as the maximum permitted stress when shear reinforcement is provided. This study also highlighted the varying effect of different types of shear reinforcement. This suggests that maximum allowable shear stresses may be made dependent on type and layout of shear reinforcement and may be set differently.

### 7.7 Concluding Remarks

ACI 318 codes of practice appear to be conservative in predicting the punching resistance of concrete slabs and underestimate the contribution of shear reinforcement. ACI code is more conservative

when it comes to calculate the resistance of reinforced concrete slabs with shear steel, because it reduces the contribution of the concrete shear resistance to half. The proposed modified formula may be adopted for predicting punching shear without shear reinforcement. However, still there are scopes to review the code provisions taking into consideration the influence of the following:

- Effects of span-depth ratio on punching shear strength.
- Type, amount and alignment of the shear reinforcement.
- Influence of edge restraint.

## Chapter 8

### CONCLUSION

#### 8.1 General

This study was intended to investigate the possibilities of performing nonlinear finite element analysis of reinforced concrete plates using concrete model with 3-D brick element of ANSYS Package software. The dedicated element employs a smeared crack model to allow for concrete cracking with the option of modeling the reinforcement in a distributed or discrete manner. Only nonlinear stress-strain relations for concrete in compression have made it possible to reach the ultimate load and determine the entire load-deflection diagram. In view of the good correlation between the nonlinear finite element analysis model and experimental data, it would seem that this numerical package can be used with confidence in studying, both quantitatively and qualitatively, the problems of punching in RC plates.

#### 8.2 Summary of Conclusions

From the investigations carried out the following deductions can be made for linear and nonlinear analyses of reinforced concrete plates:

- (i) The good agreement between the numerical and the experimental results establish the validity and acceptability of the computational models. Load-deflection curves show very close results at the early stages of load history for all the test slabs. The initially linear relation experiences a small jump, with a sudden loss of stiffness, when cracking in concrete begins, followed by a nearly linear curve with flatter slope than the initial.

- (ii) The finite element models show slightly stiffer response than the test data in both the linear and nonlinear ranges. The effects of bond slip (between the concrete and steel reinforcing) and microcracks occurring in the actual plates are not included in the finite element model, contributing to higher stiffness of the model.
- (iii) Convergence criteria and tolerances are to be achieved through a number of trial run. With load adjustment, tolerances for both force and displacement criteria may need to be relaxed to avoid a divergence of solution. After the load range that produces a diverged solution is revealed from a previous ANSYS trial run, either the tolerance or load adjustments or both have to be made to prevail over the divergence problem at that loading level.
- (iv) In a nonlinear reinforced concrete analysis, the shear transfer coefficient needs to be assumed to avoid any numerical instability. In this study, a value of 0.35 is assumed for shear transfer coefficient on trial and error basis, which resulted in fairly accurate predictions.
- (v) For nonlinear analysis of a reinforced concrete plate, the total load applied to a model must be divided into a number of load steps. Sufficiently small load step sizes are required, particularly at change points in behavior of the reinforced concrete plate, i.e., major cracking of concrete, yielding of steel, and approaching failure of the reinforced concrete plate. Defining minimum and maximum sizes for each load step, depending upon the actual behavior of the reinforced concrete plate, will assist in convergence of the solutions and reduce computational time.
- (vi) For a given reinforcement ratio and yield strength of steel, ultimate load increases with the increase in concrete compressive strength

upto certain limit. After that further increase in concrete strength does not increase the ultimate capacity of the slab, rather slight decrease in ultimate load takes place. Increase in ultimate load is more prominent with higher strength concrete compared to lower strength concrete for different steel ratios. Hence, concrete compressive strength increases the ultimate capacity upto certain limit for particular reinforcement ratio.

- (vii) The influence of flexural reinforcement on compression face is not so significant on the ultimate load. However, reinforcement on tensile face has positive influence. The change in behaviour with the change in the reinforcement ratio is particularly noticeable for higher values of concrete compressive strength. Flexural steel ratio has an important effect on the punching shear strength for reinforced concrete plates and more so with higher strength concrete.
- (viii) The ultimate punching shear strength increases with the increase in yield strength of reinforcement. But for a given condition, the rate of increase in ultimate load is significantly reduced for yield strength beyond 50 ksi. Increase of ultimate load with increase in concrete strength is comparatively less for lower grade steel compared to higher grades.
- (ix) As the thickness of the plate increases so does the shear strength of the slabs. Both span-depth ratio and the type of support condition have a significant influence on the punching shear strength of reinforced concrete flat plates. Span-depth ratio effect has different prominence in different range of the ratio. Plate action takes place for span-depth ratio between 20 to 40. For very low span-depth ratio below 9, the plate behaviour almost ceases and a deep beam action dominates failure mechanism.

- (x) Increase in column size or loading area increases the ultimate load capacity. By doubling the column size, ultimate load is increased over 30 %.
- (xi) Addition of shear reinforcement has a significant effect on the punching shear strength of the plates. Shear reinforcement increases the ductility of the plate. For bent-bar shear reinforcement, bending the bars at certain distance from the column edge has better effect than bending directly under column edges.
- (xii) The inclined orientation of shear reinforcement has better strength enhancement compared to vertical placement. Among various types of shear reinforcement hat type appears to give the highest strength in numerical computation for inclined orientation. They are also easy to install, and would thus seem to be a promising form of shear reinforcement for flat plates. From practical consideration the inclined hat type may be fabricated with anchorage hook for field installation.
- (xiii) There is scope for improvement of shear strength computation formula of ACI-02, steel percentage, support condition, concrete strength and plate dimension that is size effect may be included.
- (xiv) Proposed modification to ACI 318 Code appears to be conservative and safe with appropriate  $\phi$  factor of 0.75 for shear.

### **8.3 Recommendations for Future Studies**

The following recommendations are made for future investigations:

- (i) The proposed system is only meant for a typical interior column. The analytical model may be extended to incorporate the analysis

of punching shear at corner and edge column connections with or without edge beam or torsion strip.

- (ii) Improvement to the analytical model may be made to study the punching behavior with column capital and drop panel.
- (iii) Further improvement to the analytical model may be made to study and analyze the punching behaviour for skew plates, circular plates with circular column or loading.
- (iv) Punching behaviour of flat plates with openings subjected to uniform load/ or point loads may be investigated
- (v) Suitable nonlinear finite element model may be employed to study the effect of other forms of shear strengthening technique for example carbon fiber reinforced polymer (CFRP).
- (vi) Punching behaviour of flat plates with additional percentage of longitudinal reinforcement in the column strips and their varying effects may be investigated.
- (vii) The analytical model may be extended to incorporate the analysis of punching shear for dynamic loads.
- (viii) More research may be carried out to review the code provision and arrive at suitable formulation of the empirical equations.



## REFERENCES

**ACI 318(1995)**, "Building Code Requirements for Reinforced Concrete (ACI 318-95)," American Concrete Institute, Detroit.

**ACI 318(1999)**, "Building Code Requirements for Reinforced Concrete," American Concrete Institute, Farmington Hills, Michigan.

**ACI 318(2002)**, "Building Code Requirements for Reinforced Concrete," American Concrete Institute, Farmington Hills, Michigan.

**Adams, V. and Askenazi, A. (1998)**, Building Better Products with Finite Element Analysis, On Word Press, Santa Fe, New Mexico.

**Aghayere, A. O. and MacGregor, J. G. (1990a)**, "Analysis of Concrete Plates Under Combined In Plane and Transverse Loads", ACI Structural Journal, Vol. 87, No.5, pp.539-547.

**Aghayere, A. O. and MacGregor, J. G. (1990b)**, "Tests of Reinforced Concrete Plates under Combined In plane and Transverse Loads", ACI Structural Journal, Vol. 87, No.6, pp. 615-622.

**Alam, A. K. M. J. (1997)**, "Punching Shear Behaviour of Reinforced Concrete Slabs", M: Sc Engineering Thesis, B U E T, pp. 1-12.

**Alexander, S. D. B. and Simmonds, S. H. (1992)**, "Tests of Column-Flat Plate Connections", ACI Structural Journal, Vol. 89, No.5, pp. 495-502.

**ANSYS, ANSYS version 5.4 Manual Set (1997)**, ANSYS Inc., Southpointe, 275 Technology Drive, Canonsburg, PA 15317, USA.

**Bangash, M. Y. H. (1989)**, Concrete and Concrete Structures: Numerical Modeling and Applications, Elsevier Science Publishers Ltd., London, England.

**Bangladesh National Building Code (BNBC 1993)**, Housing and Building Research Institute and Bangladesh Standards and Testing Institution, Dhaka, Bangladesh.

**Banici, B. and Bayrak, O. B. (2003)**, "Punching Shear Strengthening of Reinforced Concrete Flat Plates Using Carbon Fiber Reinforced Polymers", ASCE Journal of Structural Engineering, Vol.129, No.9, pp.1173-1182.

**Barzegar, F. and Maddipudi, S. (1997)**, "Three-Dimensional Modeling of Concrete Structures. I: Plain Concrete." ASCE Journal of Structural Engineering, Vol.123, No.10, pp.1339-1346.

**Bathe, K. J. (1996)**, Finite Element Procedures, Prentice-Hall, Inc., Upper Saddle River, New Jersey.

**Bazant, Z. P. and Cao, Z. (1987)**, "Size Effect in Punching Shear Failure of Slabs", ACI Structural Journal, January-February 1987, pp. 44-53.

**Begum, M. (2001)**, "Analysis of Reinforced Concrete Beams with Ferrocement Overlay", M. Sc Engineering Thesis, B U E T.

**Bortolotti, L. (1990)**, "Punching Shear Strength in Concrete Slabs", ACI Structural Journal, Vol. 87, No. 2, pp. 208-219.

**Broms, C. E. (2000)**, "Elimination of Flat Plate Punching Failure Mode", ACI Structural Journal, Vol. 97, No.1, pp. 94-101.

**Broms, C. E. (1990a)**, "Punching of Flat Plates- A Question of Concrete Properties in Biaxial Compression and Size Effect", ACI Structural Journal, Vol. 87, No.3, pp. 292-304.

**Broms, C. E. (1990b)**, "Shear Reinforcement for Deflection Ductility of Flat Plates", ACI Structural Journal, Vol. 87, No.6, pp. 696-705.

**BS 8110 (1985)**, "Structural use of Concrete: Part 1: Code of Practice for Design and Construction," British Standard Institution, London.

**CAN3-A23.3-M84 (1984)**, "Design of Concrete for Buildings", Canadian Standards Association, Rexdale.

**CEB-FIP (1978)**, "Model Code for concrete Structures," Comite Euro-International du Beton, Cement and Concrete Association, London.

**Chen, W. F. (1982)**, Plasticity in Reinforced Concrete. McGraw-Hill Book Company, Inc. USA.

**Desayi, P. and Krishnan, S. (1964)**, "Equation for the Stress-Strain Curve of Concrete," Journal of the American Concrete Institute, 61, pp. 345-350.

**Di, S. and Cheung, Y. K. (1993)**, "Nonlinear Analysis of RC Shell Structures Using Laminated Element II," ASCE Journal of Structural Engineering, Vol. 119, No. 7, pp. 2074-2094.

**Elgabry, A. A. and Ghali, A. (1990)**, "Design of Stud-Shear Reinforcement for Slabs", ACI Structural Journal, Vol. 87, No. 3, pp. 350-361.

**El-Salakawy, E. F., Polak, M. A. and Soudki, K. A. (2003)**, "New Shear Strengthening Technique for Concrete Slab-Column Connections", ACI Structural Journal, Vol.100, No. 3, pp.297-304.

**Elstner, R. C. and Hognestad, E. (1956)**, "Shearing Strength of Reinforced Concrete Slabs", ACI Structural Journal, Vol. 28, No. 1, pp.29-58.

**Enam, M. B. (2001)**, "Investigation of the Sway Characteristics of Reinforced Concrete Frames Subjected to Lateral Loads", M. Sc Engineering Thesis, B U E T.

**Falamaki, M. and Loo, Y.C. (1992)**, "Punching Shear Tests of Half-Scale Reinforced Concrete Flat-Plate Model with Spandrel Beams", ACI Structural Journal, Vol. 89, No.3, pp. 263-271.

**Gardner, N. J. (1990)**, "Relationship of the Punching Shear Capacity of Reinforced Concrete Slabs with Concrete Strength", ACI Structural Journal, Vol. 87, No. 1, pp.66-71.

**Gere, J. M. and Timoshenko, S. P. (1997)**, Mechanics of Materials, PWS Publishing Company, Boston, Massachusetts.

**Ghonoim, M. G. and MacGregor, J. G. (1994a)**, "Tests of Reinforced Concrete Plates Under Combined In plane and Lateral Loads", ACI Structural Journal, Vol. 91, No.1, pp.19-30.

**Ghonoim, M. G. and MacGregor, J. G. (1994b)**, "Behaviour of Reinforced Concrete Plates Under Combined In plane and Lateral Loads", ACI Structural Journal, Vol. 91, No.2, pp.188-197.

- Gonzalez-Vidosa, F., Kotsovos, M. D. and Pavlovic, M. N. (1988)**, "Symmetrical Punching of Reinforced Concrete Slabs: An Analytical Investigation Based on Nonlinear Finite Element Modeling", ACI Structural Journal, May-Jun 1988, pp.241-250.
- Hammill, N. and Ghali, A. (1994)**, "Punching Shear Resistance of Corner Slab-Column Connections", ACI Structural Journal, Vol. 91, No.6, pp.697-707.
- Harmon, T. G. and Zhangyuan, N. (1989)**, "Shear Strength of Reinforced Concrete Plates and shells Determined by Finite Element Analysis Using Layered Elements", ASCE Journal of Structural Engineering, Vol. 115, No. 5, pp. 1141-1157.
- Hueste, M. B. D. and Wight, J. K. (1999)**, "Nonlinear Punching Shear Failure Model for Interior Slab-Column Connections," ASCE Journal of Structural Engineering, Vol. 125, No. 9, pp. 997-1008.
- Huyse, L., Hemmaty, Y., and Vandewalle, L. (1994)**, "Finite Element Modeling of Fiber Reinforced Concrete Beams," Proceedings of the ANSYS Conference, Vol. 2, Pittsburgh, Pennsylvania.
- Irons, B. and Ahmad, S. (1979)**, Techniques of Finite Elements, Ellis Horwood, Chichester, U.K.
- Kachlakev, D., Millar, T. and Yim, S. (2001)**, "Finite Element Modeling of Reinforced Concrete Structures Strengthened with FRP Laminates", Oregon Department of Transportation, Salem, Oregon.
- Kuang, J. S. and Morley, C. T. (1992)**, "Punching Shear Behaviour of Restrained Reinforced Concrete Slabs," ACI Structural Journal, Vol. 89, No. 1, pp. 13-19.
- Loo, Y. C. and Chiang, C. L. (1993)**, "Methods of Punching Shear Strength analysis of Reinforced Concrete Flat Plates- A Comparative Study", Structural Engineering and Mechanics, Vol.1. No.1, pp.75-86.
- Loo, Y.C. and Falamaki, M. (1992)**, "Punching Shear Strength Analysis of Reinforced Concrete Flat Plates with Spandrel Beams", ACI Structural Journal, Vol. 89, No.4, pp. 375-383.

**Loo, Y.C., and Guan, H. (1997)**, "Cracking and Punching Shear Failure Analysis of RC Flat Plates" ASCE Journal of Structural Engineering, Vol. 123, No.10, pp. 1321-1330.

**Lovrovich, J.S. and McLean, D.I. (1990)**, "Punching Shear Behaviour of Slabs with varying Span-Depth Ratios", ACI Structural Journal, Vol. 87, No. 5, pp.507-511.

**Marti, P. (1990)**, "Design of Concrete Slabs for Transverse Shear", ACI Structural Journal, Vol. 87, No.2, pp. 180-190.

**Mitchell, D. and Cook, W. D. (1984)**, "Preventing Progressive Collapse of Slab Structures", ASCE Journal of Structural Engineering, Vol. 110, No.7, pp. 1513-1531.

**Moe, J. (1961)**, "Shear Strength of Reinforced Concrete Slabs and Footings Under Concentrated Load," Development Department Bulletin No. D47, Portland Cement Association, Stokie, pp.135.

**Mortin, J. D. and Ghali, A. (1991)**, "Connection of Flat Plates to edge Columns", ACI Structural Journal, Vol. 88, No.2, pp. 191-198.

**Murray, K. A., Cleland, D. J., Gilbert, S. G. and Scott, R. H. (2003)**, "Improved Equivalent Frame Analysis Method for Flat Plate Structures in Vicinity of Edge Columns", ACI Structural Journal, Vol. 100, No.4, pp. 454-464.

**Najjar, S., Pilakoutas, K., and Waldran, P. (1997)**, "Finite Element Analysis of GFRP Reinforced Concrete Beams." Proceedings of the Third International Symposium, Sapporo, Japan, 2, 519-526.

**Nilson, A. H (1997)**. Design of Concrete structures, 12<sup>th</sup> Edition, McGraw- Hill Book Co. Singapore.

**Noor, M. A., and Ahsan, M. S. U. (2003)**, "Effect of Opening Location on Reinforced Concrete beam", Proceedings of the Second Annual Paper meet and International Conference on Civil Engineering, The Institution of Engineers (Bangladesh) Dhaka, pp. 235-241.

**Olivera, D.R., Milo, G. S. and Regan, P. E. (2000)**, "Punching Strengths of Flat Plates with Vertical or Inclined Stirrups", ACI Structural Journal, Vol. 97, No.3, pp.485-491.

- Pilakoutas, K. and Li, X. (2003)**, "Alternative Shear Strengthening of Reinforced Concrete Flat Slabs", ASCE Journal of structural Engineering, Vol. 129, No. 9, pp.1164-1172.
- Pillai, S. U., Kirk, W. and Scavuzzo, L. (1982)**, "Shear Reinforcement at Slab-Column Connections in a Reinforced Concrete Flat Plate Structure", ACI Structural Journal, January-February 1982, pp.36-42.
- Polak, M.A. (1998)**, "Modeling Punching Shear of Reinforced Concrete Slabs using Layered Finite Elements", ACI Structural Journal, Vol. 95, No.1, pp. 71-80.
- Rangan, B. V. (1990)**, "Punching Shear Design in the New Australian Standard for Concrete Structures", ACI Structural Journal, Vol. 87, No. 2, pp. 140-144.
- Regan, P. E. (1981)**, "Behaviour of reinforced Concrete Flat Slabs", CIRIA Report No. 89, Construction Industry Research and Information Association, London.
- Regan, P. E., Jorabi, H. R. (1988)**, "Shear Resistance of One-Way Slabs under Concentrated Loads", ACI Structural Journal, pp. 150-157.
- Robertson, I. N. (1997)**, "Analysis of Flat Slab Structures Subjected to Combined Lateral and gravity Loads", ACI Structural Journal, Vol. 94, No. 6, pp. 723-729.
- Salim, W. and Sebastian, W. M. (2002)**, "Plasticity Model for Predicting Punching Shear Strengths of Reinforced Concrete Slabs", ACI Structural Journal, Vol. 99, No. 6, pp.827-835.
- Salim, W. and Sebastian, W. M. (2003)**, "Punching Shear Failure in Reinforced Concrete Slabs with Compressive Membrane Action", ACI Structural Journal, Vol. 100, No. 4, pp.471-479.
- Shaaban A. M. and Gesund, H. (1994)**, "Punching Shear Strength of Steel Fiber Reinforced Concrete Flat Plates", ACI Structural Journal, Vol. 91, No.3, pp.406-414.
- Shah, S. P., Swartz, S. E., and Ouyang, C. (1995)**, Fracture Mechanics of Concrete, John Wiley & Sons, Inc., New York, New York.

**Siao, W. B. (1994)**, "Punching Shear Resistance of Flat Slabs: A Beam-Strip Analogy", ACI Structural Journal, Vol. 91, No .5, pp.594-604.

**Timoshenko, S. and Krieger, S.W. (1959)**, Theory of Plates and Shells, McGraw-Hill Book Company, New York.

**William, K. J. and Warnke, E. P. (1975)**, "Constitutive Model for the Triaxial Behavior of Concrete," Proceedings, International Association for Bridge and Structural Engineering, Vol. 19, ISMES, Bergamo, Italy, pp. 174.

**Yamada, T., Nanni, A. and Endo, K. (1992)**, "Punching Shear Resistance of Flat Slabs: Influence of Reinforcement Type and Ratio", ACI Structural Journal, Vol. 88, No. 4, pp.555-563.

**Zienkiewicz, O.C. (1979)**, The Finite Element Method. TMII edition, McGraw-Hill Publishing Company Limited, New Delhi.

# **APPENDIX A**



## TYPICAL ANSYS SCRIPT FILE

```
KEYW, PR_STRUC, 1
KEYW, PR_FLUID, 0
KEYW, PR_MULTI, 0
```

```
/prep7
```

```
/TITLE,NLFEA OF RC PLATES IN PUNCHING SHEAR
```

```
ANTYPE, STATIC !STATIC NONLINEAR STRUCTURAL ANALYSIS
```

```
!MODEL FOR SLAB A-7B WITHOUT COMPRESSION MAT AND WITH !SHEAR
!REINFORCEMENT
```

```
| *****
```

```
!Defining UNITS
```

```
/units,bin
!/units,si
!Defining Element Types
```

```
!et,ITYPE,ename,keyopt1,keyopt2,keyopt3,.....
```

```
et,1,SOLID65,0,,,,,1      !Concrete Plate
et,2,LINK8                !Reinforcement
```

```
!Defining Real Constants
!r,nset,area
```

```
r,1,
r,2,.74      !Flexural reinforcement
r,3,.74
!r,4,.40
!r,5,.40
r,6,.2      !Shear reinforcement
!r,7,
r,8,.32     !Reinforcement for column stub
```

```
!Defining Material Properties
!IMP,Lab,Mat,C0,C1,C2,C3,C4
```

```
mp,ex,1,3659277.5 !Concrete
mp,dens,1,.0839
mp,nuxy,1,.17
```

```
mp,ex,2,29e6      !Reinforcement tension mat x direction
mp,dens,2,.293
mp,prxy,2,.3
```

mp,ex,3,29e6      !Reinforcement tension mat z direction  
 mp,dens,3,.293  
 mp,prxy,3,.3

!mp,ex,4,29e6      !Reinforcement Top mat  
 !mp,dens,4,.293  
 !mp,prxy,4,.3

!mp,ex,5,29e6      !Reinforcement Top mat  
 !mp,dens,5,.293  
 !mp,prxy,5,.3

mp,ex,6,29e6      ! Shear Reinforcement  
 mp,dens,6,.293  
 mp,prxy,6,.3

mp,ex,8,29e6      !Column reinforcement  
 mp,dens,8,.293  
 mp,prxy,8,.3

!TB, Lab, MAT, NTEMP, NPTS, TBOPT — Activates a data table for !nonlinear  
 !material properties or special element input.

!Defining Concrete Properties

TB,CONCR,1,,

!TBDATA, STLOC, C1, C2, C3, C4, C5, C6 — Defines data for the data !table

TBDATA,1,.35,.35,477.29707,4050,,,, !Concrete crushing capability is !turned  
 !off

TB,MISO,1,,

!TBPT, Oper, X, Y — Defines a point on a stress-strain or B-H curve.  
 !Defining Stress- Strain curve for concrete

TBPT,,.0003320327578,1215  
 TBPT,,.0004,1417.4085  
 TBPT,,.0005,1740.7979  
 TBPT,,.0006,2045.2723  
 TBPT,,.0007,2328.6  
 TBPT,,.0008,2589.2022  
 TBPT,,.0009,2826.13  
 TBPT,,.0010,3039.02  
 TBPT,,.0011,3228.02  
 TBPT,,.0012,3393.73  
 TBPT,,.0013,3537.07  
 TBPT,,.0014,3659.2328  
 TBPT,,.0015,3761.5895  
 TBPT,,.0016,3845.6291

TBPT,,.0017,3912.89  
 TBPT,,.0018,3964.92  
 TBPT,,.0019,4003.2293  
 TBPT,,.002,4029.27  
 TBPT,,.0021,4044.41  
 TBPT,,.0022136,4050

!TBPLOT,MISO,1

!Defining Steel Properties

TB,BKIN,2,,  
 TBDATA,,46600,0  
 TB,BKIN,3,,  
 TBDATA,,46600,0  
 !TB,BKIN,4,,  
 !TBDATA,,46600,0  
 !TB,BKIN,5,,  
 !TBDATA,,46600,0  
 TB,BKIN,6,,  
 TBDATA,,46600,0  
 !TB,BKIN,7,,  
 !TBDATA,,60000,0  
 TB,BKIN,8,1,  
 TBDATA,,46600,0

!Generation of Keypoints

K,1,0,0,0  
 K,2,30,0,0  
 K,3,40,0,0  
 K,4,70,0,0

!KGEN, !TIME, NP1, NP2, NINC, DX, DY, DZ, KINC, NOELEM, IMOVE —  
 !Generates additional keypoints from a pattern of keypoints.

KGEN,2,1,4,1,,,30,4,1, !Copy key point in the xz plane  
 KGEN,2,5,8,1,,,10,4,1,  
 KGEN,2,9,12,1,,,30,4,1,

KGEN,2,1,16,1,,6,,16,1, !Copy key point in the Y direction

!KGEN,2,22,23,,,2,,,1, !Key point for for column plate  
 !KGEN,2,26,27,,,2,,,1,

!Generation of Volumes

V,1,5,6,2,17,21,22,18  
 V,2,6,7,3,18,22,23,19  
 V,3,7,8,4,19,23,24,20  
 V,5,9,10,6,21,25,26,22  
 V,6,10,11,7,22,26,27,23

V,7,11,12,8,23,27,28,24  
 V,9,13,14,10,25,29,30,26  
 V,10,14,15,11,26,30,31,27  
 V,11,15,16,12,27,31,32,28  
 IV,22,26,27,23,33,35,36,34

! Generate new volumes by "gluing "Volumes

VGLUE,ALL

!Meshing the vertical lines in 6 layers

!LESIZE, NL1, SIZE, ANGSIZ, NDIV, SPACE, KFORC, LAYER1, LAYER2,  
 !KYNDIV ! Specifies the divisions and spacing ratio on unmeshed lines.

LESIZE,5,1,,,,,  
 LESIZE,7,1,,,,,  
 LESIZE,9,1,,,,,  
 LESIZE,11,1,,,,,  
 LESIZE,17,1,,,,,  
 LESIZE,19,1,,,,,  
 LESIZE,25,1,,,,,  
 LESIZE,27,1,,,,,  
 LESIZE,32,1,,,,,  
 LESIZE,35,1,,,,,  
 LESIZE,40,1,,,,,  
 LESIZE,45,1,,,,,  
 LESIZE,50,1,,,,,  
 LESIZE,53,1,,,,,  
 LESIZE,58,1,,,,,  
 LESIZE,63,1,,,,,

!Meshing the Volumes

!TYPE, ITYPE — Sets the element type attribute pointer.

TYPE,1  
 MAT,1  
 REAL,1  
 ESIZE,3.333333  
 MSHAP,0,3d  
 VMESH,1,9,1

!TYPE,1  
 !MAT,7  
 !REAL,7  
 !ESIZE,3.333333  
 !MSHAP,0,3d  
 !VMESH,10,,

!GENERATION OF LINK8 ELEMENT

TYPE,2 !Bottom reinforcement x direction  
 MAT,2  
 REAL,2

!x1\*\*\*\*\*  
E,120,277  
\*DO,i,277,307,5  
E,i,i+5  
\*ENDDO  
E,312,228  
E,228,805  
E,805,810  
E,810,762  
E,762,1117  
\*DO,i,1117,1147,5  
E,i,i+5  
\*ENDDO  
E,1152,1068

!x3\*\*\*\*\*  
E,126,421  
\*DO,i,421,451,5  
E,i,i+5  
\*ENDDO  
E,456,234  
E,234,841  
E,841,846  
E,846,768  
E,768,1261  
\*DO,i,1261,1291,5  
E,i,i+5  
\*ENDDO  
E,1296,1074

!x5\*\*\*\*\*  
E,136,501  
\*DO,i,501,531,5  
E,i,i+5  
\*ENDDO  
E,536,244  
E,244,861  
E,861,866  
E,866,778  
E,778,1341  
\*DO,i,1341,1371,5  
E,i,i+5  
\*ENDDO  
E,1376,1084

!x7\*\*\*\*\*  
E,146,581  
\*DO,i,581,611,5  
E,i,i+5  
\*ENDDO  
E,616,254

E,254,881  
E,881,886  
E,886,788  
E,788,1421  
\*DO,i,1421,1451,5  
E,i,i+5  
\*ENDDO  
E,1456,1094  
!x9\*\*\*\*\*  
E,156,661  
\*DO,i,661,691,5  
E,i,i+5  
\*ENDDO  
E,696,264  
E,264,901  
E,901,906  
E,906,798  
E,798,1501  
\*DO,i,1501,1531,5  
E,i,i+5  
\*ENDDO  
E,1536,1104

!x11\*\*\*\*\*  
E,1579,1671  
\*DO,i,1671,1701,5  
E,i,i+5  
\*ENDDO  
E,1706,1645  
E,1645,1794  
E,1794,1799  
E,1799,1780  
E,1780,1923  
\*DO,i,1923,1953,5  
E,i,i+5  
\*ENDDO  
E,1958,1897

!x12\*\*\*\*\*  
E,1584,1711  
\*DO,i,1711,1741,5  
E,i,i+5  
\*ENDDO  
E,1746,1650  
E,1650,1804  
E,1804,1809  
E,1809,1785  
E,1785,1963  
\*DO,i,1963,1993,5  
E,i,i+5  
\*ENDDO  
E,1998,1902

!x14\*\*\*\*\*  
E,2107,2313  
\*DO,i,2313,2343,5  
E,i,i+5  
\*ENDDO

E,2348,2209  
E,2209,2742  
E,2742,2747  
E,2747,2686  
E,2686,3069  
\*DO,i,3069,3099,5  
E,i,i+5  
\*ENDDO  
E,3104,2965

!x16\*\*\*\*\*  
E,2117,2393  
\*DO,i,2393,2423,5  
E,i,i+5  
\*ENDDO  
E,2428,2219  
E,2219,2762  
E,2762,2767  
E,2767,2696  
E,2696,3149  
\*DO,i,3149,3179,5  
E,i,i+5  
\*ENDDO  
E,3184,2975

!x18\*\*\*\*\*  
E,2127,2473  
\*DO,i,2473,2503,5  
E,i,i+5  
\*ENDDO  
E,2508,2229  
E,2229,2782  
E,2782,2787  
E,2787,2706  
E,2706,3229  
\*DO,i,3229,3259,5  
E,i,i+5  
\*ENDDO  
E,3264,2985

!x20\*\*\*\*\*  
E,2137,2553  
\*DO,i,2553,2583,5  
E,i,i+5  
\*ENDDO

E,2588,2239  
E,2239,2802  
E,2802,2807  
E,2807,2716  
E,2716,3309  
\*DO,i,3309,3339,5  
E,i,i+5  
\*ENDDO  
E,3344,2995

!x22\*\*\*\*\*  
E,2094,2161  
\*DO,i,2161,2191,5  
E,i,i+5  
\*ENDDO  
E,2196,2152  
E,2152,2668  
E,2668,2673  
E,2673,2665  
E,2665,2917  
\*DO,i,2917,2947,5  
E,i,i+5  
\*ENDDO  
E,2952,2908

!Bottom reinforcement in z direction

TYPE,2  
MAT,3  
REAL,3

!z1\*\*\*\*\*  
E,120,121  
\*DO,i,121,151,5  
E,i,i+5  
\*ENDDO  
E,156,102  
E,102,1579  
E,1579,1584  
E,1584,1572  
E,1572,2107  
\*DO,i,2107,2137,5  
E,i,i+5  
\*ENDDO  
E,2142,2094

!z3\*\*\*\*\*  
E,282,386  
\*DO,i,386,626,40  
E,i,i+40  
\*ENDDO  
E,666,180



E,180,1676  
E,1676,1716  
E,1716,1608  
E,1608,2318  
\*DO,i,2318,2558,40  
E,i,i+40  
\*ENDDO  
E,2598,2166

!z5\*\*\*\*\*  
E,292,396  
\*DO,i,396,636,40  
E,i,i+40  
\*ENDDO  
E,676,190  
E,190,1686  
E,1686,1726  
E,1726,1618  
E,1618,2328  
\*DO,i,2328,2568,40  
E,i,i+40  
\*ENDDO  
E,2608,2176

!z7\*\*\*\*\*  
E,302,406  
\*DO,i,406,646,40  
E,i,i+40  
\*ENDDO  
E,686,200  
E,200,1696  
E,1696,1736  
E,1736,1628  
E,1628,2338  
\*DO,i,2338,2578,40  
E,i,i+40  
\*ENDDO  
E,2618,2186

!z9\*\*\*\*\*  
E,312,416  
\*DO,i,416,656,40  
E,i,i+40  
\*ENDDO  
E,696,210  
E,210,1706  
E,1706,1746  
E,1746,1638  
E,1638,2348  
\*DO,i,2348,2588,40  
E,i,i+40  
\*ENDDO

E,2628,2196

!z11\*\*\*\*\*

E,805,831

\*DO,i,831,891,10

E,i,i+10

\*ENDDO

E,901,739

E,739,1794

E,1794,1804

E,1804,1768

E,1768,2742

\*DO,i,2742,2802,10

E,i,i+10

\*ENDDO

E,2812,2668

!z12\*\*\*\*\*

E,810,836

\*DO,i,836,896,10

E,i,i+10

\*ENDDO

E,906,744

E,744,1799

E,1799,1809

E,1809,1773

E,1773,2747

\*DO,i,2747,2807,10

E,i,i+10

\*ENDDO

E,2817,2673

!z14\*\*\*\*\*

E,1117,1221

\*DO,i,1221,1461,40

E,i,i+40

\*ENDDO

E,1501,1015

E,1015,1923

E,1923,1963

E,1963,1855

E,1855,3069

\*DO,i,3069,3309,40

E,i,i+40

\*ENDDO

E,3349,2917

!z16\*\*\*\*\*

E,1127,1231

\*DO,i,1231,1471,40

E,i,i+40

\*ENDDO  
E,1511,1025  
E,1025,1933  
E,1933,1973  
E,1973,1865  
E,1865,3079  
\*DO,i,3079,3319,40  
E,i,i+40  
\*ENDDO  
E,3359,2927

!z18\*\*\*\*\*  
E,1137,1241  
\*DO,i,1241,1481,40  
E,i,i+40  
\*ENDDO  
E,1521,1035  
E,1035,1943  
E,1943,1983  
E,1983,1875  
E,1875,3089  
\*DO,i,3089,3329,40  
E,i,i+40  
\*ENDDO  
E,3369,2937

!z20\*\*\*\*\*  
E,1147,1251  
\*DO,i,1251,1491,40  
E,i,i+40  
\*ENDDO  
E,1531,1045  
E,1045,1953  
E,1953,1993  
E,1993,1885  
E,1885,3099  
\*DO,i,3099,3339,40  
E,i,i+40  
\*ENDDO  
E,3379,2947

!z22\*\*\*\*\*  
E,1068,1069  
\*DO,i,1069,1099,5  
E,i,i+5  
\*ENDDO

E,1104,1006  
E,1006,1897  
E,1897,1902  
E,1902,1846  
E,1846,2965

\*DO,i,2965,2995,5  
E,i,i+5  
\*ENDDO  
E,3000,2908

## IShear Reinforcement

TYPE,2  
MAT,6  
REAL,6  
IX1\*\*\*\*\*  
\*DO,i,189,209,5  
E,i,i+5  
\*ENDDO  
E,214,166  
E,166,739  
E,739,744  
E,744,736  
E,736,1019  
\*DO,i,1019,1039,5  
E,i,i+5  
\*ENDDO

IX2\*\*\*\*\*  
\*DO,i,1685,1705,5  
E,i,i+5  
\*ENDDO  
E,1710,1645  
E,1645,1794  
E,1794,1799  
E,1799,1780  
E,1780,1927  
\*DO,i,1927,1947,5  
E,i,i+5  
\*ENDDO

IX3\*\*\*\*\*  
\*DO,i,1725,1745,5  
E,i,i+5  
\*ENDDO

E,1750,1650  
E,1650,1804  
E,1804,1809  
E,1809,1785  
E,1785,1967  
\*DO,i,1967,1987,5  
E,i,i+5  
\*ENDDO

IX4\*\*\*\*\*  
\*DO,i,1617,1637,5

E,i,i+5  
\*ENDDO  
E,1642,1594  
E,1594,1768  
E,1768,1773  
E,1773,1765  
E,1765,1859  
\*DO,i,1859,1879,5  
E,i,i+5  
\*ENDDO

IX22\*\*\*\*\*  
\*DO,i,1680,1700,5  
E,i,i+5  
\*ENDDO  
E,1705,1706  
E,1706,1645  
E,1645,1794  
E,1794,1799  
E,1799,1780  
E,1780,1923  
E,1923,1932  
\*DO,i,1932,1952,5  
E,i,i+5  
\*ENDDO

IX33\*\*\*\*\*  
\*DO,i,1720,1740,5  
E,i,i+5  
\*ENDDO  
E,1745,1746  
E,1746,1650  
E,1650,1804  
E,1804,1809  
E,1809,1785  
E,1785,1963  
E,1963,1972  
\*DO,i,1972,1992,5  
E,i,i+5  
\*ENDDO

IZ1\*\*\*\*\*  
\*DO,i,243,263,5  
E,i,i+5  
\*ENDDO  
E,268,166  
E,166,1645  
E,1645,1650  
E,1650,1594  
E,1594,2213  
\*DO,i,2213,2233,5  
E,i,i+5

\*ENDDO

!Z2\*\*\*\*\*!

\*DO,i,855,895,10

E,i,i+10

\*ENDDO

E,905,739

E,739,1794

E,1794,1804

E,1804,1768

E,1768,2746

\*DO,i,2746,2786,10

E,i,i+10

\*ENDDO

!Z3\*\*\*\*\*!

\*DO,i,860,900,10

E,i,i+10

\*ENDDO

E,910,744

E,744,1799

E,1799,1809

E,1809,1773

E,1773,2751

\*DO,i,2751,2791,10

E,i,i+10

\*ENDDO

!Z4\*\*\*\*\*!

\*DO,i,777,797,5

E,i,i+5

\*ENDDO

E,802,736

E,736,1780

E,1780,1785

E,1785,1765

E,1765,2690

\*DO,i,2690,2710,5

E,i,i+5

\*ENDDO

!Z2\*\*\*\*\*!

\*DO,i,845,885,10

E,i,i+10

\*ENDDO

E,895,901

E,901,739

E,739,1794

E,1794,1804

E,1804,1768

E,1768,2742

```
E,2742,2756
*DO,i,2756,2796,10
E,i,i+10
*ENDDO
```

```
!Z33*****
*DO,i,850,890,10
E,i,i+10
*ENDDO
E,900,906
E,906,744
E,744,1799
E,1799,1809
E,1809,1773
E,1773,2747
E,2747,2761
*DO,i,2761,2801,10
E,i,i+10
*ENDDO
```

```
!Reinforcement for column stub
```

```
TYPE,2
MAT,8
REAL,8
```

```
E,1544,1589
E,1751,1760
E,701,731
E,11,161
```

```
E,1544,1751
E,1751,701
E,701,11
E,11,1544
```

```
E,1589,1760
E,1760,731
E,731,161
E,161,1589
```

```
! The remaining command for solution and post processing is applied
!through GUI.
```

```
!Application of loads and boundary conditions
```

```
!/BATCH
```

```
!/COM,ANSYS RELEASE 5.4 UP19970828 07:15:22 03/11/2004
```

```
!/input,menust,tmp,,,,,,,,,,,,,1
```

```
!/GRA,POWER
```

```
!/GST,ON
```

```
!*use,VA7bEHO17s2.txt
```

```
!FINISH
```

```
! /SOLU
INLGEOM,0
INROPT,FULL, ,OFF
ILUMPM,0
IEQSLV,SPAR,1e-005,3,
ISSTIF
! PSTRES
!*
! FLST,2,44,1,ORDE,15
! FITEM,2,1
! FITEM,2,-10
! FITEM,2,911
! FITEM,2,920
! FITEM,2,-928
! FITEM,2,1541
! FITEM,2,-1543
! FITEM,2,1814
! FITEM,2,1823
! FITEM,2,-1824
! FITEM,2,2003
! FITEM,2,-2011
! FITEM,2,2822
! FITEM,2,2831
! FITEM,2,-2838
! D,P51X, ,0, , , ,UY
! /VIEW, 1 , 1
! /ANG, 1
! /REP,FAST
! FLST,2,44,1,ORDE,17
! FITEM,2,1
! FITEM,2,20
! FITEM,2,29
! FITEM,2,-36
! FITEM,2,704
! FITEM,2,713
! FITEM,2,-714
! FITEM,2,920
! FITEM,2,929
! FITEM,2,-936
! FITEM,2,2003
! FITEM,2,2012
! FITEM,2,-2020
! FITEM,2,2633
! FITEM,2,-2635
! FITEM,2,2822
! FITEM,2,-2830
! D,P51X, ,0, , , ,UY
! /VIEW, 1 , 1,1,1
! /ANG, 1
! /REP,FAST
! FLST,2,1,5,ORDE,1
! FITEM,2,25
```



```

!SFA,P51X,1,PRES,1500,
!*
!OUTRES,ALL,ALL,
!*
!TIME,150
!AUTOTS,1
!NSUBST,150,150000,30,1
!KBC,0
!*
!CNVTOL,U,,0.05,2,,
!*
!LNSRCH,1
!*
!PRED,ON,,ON
!NCNV,2,0,0,0,0,0,
!/STAT,SOLU
!SOLVE
!SAVE
!/POST1
!SET,FIRST
!AVPRIN,0,0,
!*
!PLNSOL,U,Y,0,1
!FINISH

```

**!An alternative modeling technique**

```
!*****
```

```

KEYW,PR_STRUC,1
KEYW,PR_FLUID,0
KEYW,PR_MULTI,0

```

```
/prep7
```

```
/TITLE,NLFEA OF RC PLATES IN PUNCHING SHEAR
```

```

ANTYPE,STATIC !STATIC NONLINEAR STRUCTURAL ANALYSIS
!MODEL FOR INCLINED HAT TYPE SHEAR REINFORCEMENT
!Defining UNITS

```

```

/units,bin
!/units,si

```

```
!Defining Element Types
```

```

!et,ITYPE,ename,keyopt1,keyopt2,keyopt3,.....
et,1,SOLID65,0,,,,,1 !Concrete Plate
et,2,LINK8 !Reinforcement

```

```
!Defining Real Constants
```

```
!r,nset,area
```

r,1,  
 r,2,.40  
 r,3,.40  
 r,4,.7458  
 r,5,.7458  
 r,6,.2  
 lr,7,  
 r,8,.32  
 lr,9,.33  
 lr,10,.62

lr,9,1 !Dummy link for slab edge

!Defining Material Properties

IMP,Lab,Mat,C0,C1,C2,C3,C4  
 mp,ex,1,3659277.5 !Concrete  
 mp,dens,1,.0839  
 mp,nuxy,1,.17

mp,ex,2,29e6       !Reinforcement Bottom mat  
 mp,dens,2,.293  
 mp,prxy,2,.3

mp,ex,3,29e6       !Reinforcement Bottom mat  
 mp,dens,3,.293  
 mp,prxy,3,.3

mp,ex,4,29e6       !Reinforcement Top mat  
 mp,dens,4,.293  
 mp,prxy,4,.3

mp,ex,5,29e6       !Reinforcement Top mat  
 mp,dens,5,.293  
 mp,prxy,5,.3

mp,ex,6,29e6       ! Shear Reinforcement  
 mp,dens,6,.293  
 mp,prxy,6,.3

lmp,ex,7,30e6       !Steel plate  
 lmp,dens,7,.293  
 lmp,prxy,7,.3

mp,ex,8,29e6       !Column reinforcement  
 mp,dens,8,.293  
 mp,prxy,8,.3

lmp,ex,9,29e6  
 lmp,dens,9,.293  
 lmp,prxy,9,.3

```
!mp,ex,10,29e6  
!mp,dens,10,.293  
!mp,prxy,10,.3
```

!TB, Lab, MAT, NTEMP, NPTS, TBOPT — Activates a data table for !nonlinear  
!material properties or special element input.

!Defining Concrete Properties

```
TB,CONCR,1,,  
!TBDATA, STLOC, C1, C2, C3, C4, C5, C6 — Defines data for the data !table  
TBDATA,1,.35,.35,477.29707,4050,,,,, !Concrete crushing capability is !turned  
!off  
TB,MISO,1,,
```

!TBPT, Oper, X, Y — Defines a point on a stress-strain or B-H curve.  
!Defining Stress- Strain curve for concrete

```
TBPT,,.0003320327578,1215  
TBPT,,.0004,1417.4085  
TBPT,,.0005,1740.7979  
TBPT,,.0006,2045.2723  
TBPT,,.0007,2328.6  
TBPT,,.0008,2589.2022  
TBPT,,.0009,2826.13  
TBPT,,.0010,3039.02  
TBPT,,.0011,3228.02  
TBPT,,.0012,3393.73  
TBPT,,.0013,3537.07  
TBPT,,.0014,3659.2328  
TBPT,,.0015,3761.5895  
TBPT,,.0016,3845.6291  
TBPT,,.0017,3912.89  
TBPT,,.0018,3964.92  
TBPT,,.0019,4003.2293  
TBPT,,.002,4029.27  
TBPT,,.0021,4044.41  
TBPT,,.0022136,4050
```

!TBPLOT,MISO,1

!Defining Steel Properties

```
TB,BKIN,2,,  
TBDATA,,46600,0  
TB,BKIN,3,,  
TBDATA,,46600,0  
TB,BKIN,4,,  
TBDATA,,46600,0
```

```
TB,BKIN,5,,  
TBDATA,,46600,0
```

```

TB,BISO,6,1,
TBDATA,,46600,0
ITB,BKIN,7,,
ITBDATA,,60000,0
TB,BKIN,8,1,
TBDATA,,46600,0

```

!Generation of Keypoints

```

K,1,0,0,0
K,2,70,0,0
K,3,0,0,70
K,4,70,0,70

```

!KGEN, ITIME, NP1, NP2, NINC, DX, DY, DZ, KINC, NOELEM, IMOVE —  
!Generates additional keypoints from a pattern of keypoints.  
KGEN,2,1,4,1,,6,,1, !Copy key point in the Y direction  
!Generation of Volumes

```

V,1,2,4,3,5,6,8,7
! Generate new volumes by "gluing "Volumes

```

!VGLUE,ALL

!Meshing the vertical lines in 6 layers

!LESIZE, NL1, SIZE, ANGSIZ, NDIV, SPACE, KFORC, LAYER1, LAYER2,  
KYNDIV ! Specifies the divisions and spacing ratio on unmeshed lines.

```

LESIZE,5,1,,,,,,,,
LESIZE,7,1,,,,,,,,
LESIZE,9,1,,,,,,,,
LESIZE,11,1,,,,,,,,

```

!Meshing the Volumes

!TYPE, ITYPE — Sets the element type attribute pointer.

```

TYPE,1
MAT,1
REAL,1
ESIZE,3.3333334
MSHAP,0,3d
VMESH,1,1,1

```

!GENERATION OF LINK8 ELEMENT

```

TYPE,2
MAT,2
REAL,2

```

!xt1\*\*\*\*\*

E,512,521  
\*DO,i,521,611,5  
E,i,i+5  
\*ENDDO  
E,616,490

!xt3\*\*\*\*\*  
E,898,1493  
\*DO,i,1493,1583,5  
E,i,i+5  
\*ENDDO  
E,1588,652

!xt5\*\*\*\*\*  
E,908,1693  
\*DO,i,1693,1783,5  
E,i,i+5  
\*ENDDO  
E,1788,662

!xt7\*\*\*\*\*  
E,918,1893  
\*DO,i,1893,1983,5  
E,i,i+5  
\*ENDDO  
E,1988,672

!xt9\*\*\*\*\*  
E,928,2093

\*DO,i,2093,2183,5  
E,i,i+5  
\*ENDDO  
E,2188,682

!xt11\*\*\*\*\*  
E,938,2293  
\*DO,i,2293,2383,5  
E,i,i+5  
\*ENDDO  
E,2388,692

!xt12\*\*\*\*\*  
E,943,2393  
\*DO,i,2393,2483,5  
E,i,i+5  
\*ENDDO  
E,2488,697

!xt14\*\*\*\*\*  
E,953,2593  
\*DO,i,2593,2683,5

E,i,i+5  
\*ENDDO  
E,2688,707

!xt16\*\*\*\*\*  
E,963,2793  
\*DO,i,2793,2883,5  
E,i,i+5  
\*ENDDO

E,2888,717

!xt18\*\*\*\*\*  
E,973,2993  
\*DO,i,2993,3083,5  
E,i,i+5  
\*ENDDO  
E,3088,727

!xt20\*\*\*\*\*  
E,983,3193  
\*DO,i,3193,3283,5  
E,i,i+5  
\*ENDDO  
E,3288,737

!xt22\*\*\*\*\*  
E,764,773  
\*DO,i,773,863,5  
E,i,i+5  
\*ENDDO  
E,868,618

!Top Mat z Direction

TYPE,2  
MAT,3  
REAL,3

!ZT1\*\*\*\*\*  
E,512,893  
\*DO,i,893,983,5  
E,i,i+5  
\*ENDDO  
E,988,764

!ZT3\*\*\*\*\*  
  
E,526,1398  
\*DO,i,1398,3198,100  
E,i,i+100  
\*ENDDO

E,3298,778

!ZT5\*\*\*\*\*

E,536,1408

\*DO,i,1408,3208,100

E,i,i+100

\*ENDDO

E,3308,788

!ZT7\*\*\*\*\*

E,546,1418

\*DO,i,1418,3218,100

E,i,i+100

\*ENDDO

E,3318,798

!ZT9\*\*\*\*\*

E,556,1428

\*DO,i,1428,3228,100

E,i,i+100

\*ENDDO

E,3328,808

!ZT11\*\*\*\*\*

E,566,1438

\*DO,i,1438,3238,100

E,i,i+100

\*ENDDO

E,3338,818

!ZT12\*\*\*\*\*

E,571,1443

\*DO,i,1443,3243,100

E,i,i+100

\*ENDDO

E,3343,823

!ZT14\*\*\*\*\*

E,581,1453

\*DO,i,1453,3253,100

E,i,i+100

\*ENDDO

E,3353,833

!zt16\*\*\*\*\*

E,591,1463

\*DO,i,1463,3263,100

E,i,i+100

\*ENDDO

E,3363,843

!zt18\*\*\*\*\*  
E,601,1473  
\*DO,i,1473,3273,100  
E,i,i+100  
\*ENDDO  
E,3373,853

!zt20\*\*\*\*\*  
  
E,611,1483  
\*DO,i,1483,3283,100  
E,i,i+100  
\*ENDDO  
E,3383,863

!zt22\*\*\*\*\*  
E,490,647  
\*DO,i,647,737,5  
E,i,i+5  
\*ENDDO  
E,742,618

!Bottom Mat

TYPE,2  
MAT,4  
REAL,4

!xb1\*\*\*\*\*  
E,516,517  
\*DO,i,517,607,5  
E,i,i+5  
\*ENDDO  
E,612,486

!xb3\*\*\*\*\*  
E,894,1489  
\*DO,i,1489,1579,5  
E,i,i+5  
\*ENDDO  
E,1584,648

!xb5\*\*\*\*\*  
E,904,1689  
\*DO,i,1689,1779,5  
E,i,i+5  
\*ENDDO  
E,1784,658

!xb7\*\*\*\*\*  
E,914,1889  
\*DO,i,1889,1979,5



E,i,i+5  
\*ENDDO  
E,1984,668

!xb9\*\*\*\*\*  
E,924,2089  
\*DO,i,2089,2179,5  
E,i,i+5  
\*ENDDO  
E,2184,678

!xb11\*\*\*\*\*  
E,934,2289  
\*DO,i,2289,2379,5  
E,i,i+5  
\*ENDDO  
E,2384,688

!xb12\*\*\*\*\*  
E,939,2389  
\*DO,i,2389,2479,5  
E,i,i+5  
\*ENDDO  
E,2484,693

!xb14\*\*\*\*\*  
E,949,2589  
\*DO,i,2589,2679,5  
E,i,i+5  
\*ENDDO  
E,2684,703

!xb16\*\*\*\*\*  
E,959,2789  
\*DO,i,2789,2879,5  
E,i,i+5  
\*ENDDO  
E,2884,713

!xb18\*\*\*\*\*  
E,969,2989  
\*DO,i,2989,3079,5  
E,i,i+5  
\*ENDDO  
E,3084,723

!xb20\*\*\*\*\*  
E,979,3189  
\*DO,i,3189,3279,5  
E,i,i+5  
\*ENDDO  
E,3284,733

!xb22\*\*\*\*\*  
E,768,769  
\*DO,i,769,859,5  
E,i,i+5  
\*ENDDO  
E,864,622

!Bottom Mat z Direction

TYPE,2  
MAT,5  
REAL,5

!Zb1\*\*\*\*\*  
E,516,889  
\*DO,i,889,979,5  
E,i,i+5  
\*ENDDO  
E,984,768

!Zb3\*\*\*\*\*  
E,522,1394  
\*DO,i,1394,3194,100  
E,i,i+100  
\*ENDDO  
E,3294,774

!Zb5\*\*\*\*\*  
  
E,532,1404  
\*DO,i,1404,3204,100  
E,i,i+100  
\*ENDDO  
E,3304,784

!Zb7\*\*\*\*\*  
E,542,1414  
\*DO,i,1414,3214,100  
E,i,i+100  
\*ENDDO  
E,3314,794

!Zb9\*\*\*\*\*  
E,552,1424  
\*DO,i,1424,3224,100  
E,i,i+100  
\*ENDDO  
E,3324,804

!Zb11\*\*\*\*\*  
E,562,1434

\*DO,i,1434,3234,100  
E,i,i+100  
\*ENDDO  
E,3334,814

!Zb12\*\*\*\*\*  
E,567,1439  
\*DO,i,1439,3239,100  
E,i,i+100  
\*ENDDO  
E,3339,819

!Zb14\*\*\*\*\*  
E,577,1449

\*DO,i,1449,3249,100  
E,i,i+100  
\*ENDDO  
E,3349,829

!zb16\*\*\*\*\*  
E,587,1459  
\*DO,i,1459,3259,100  
E,i,i+100  
\*ENDDO  
E,3359,839

!zb18\*\*\*\*\*  
E,597,1469  
\*DO,i,1469,3269,100  
E,i,i+100  
\*ENDDO  
E,3369,849

!zb20\*\*\*\*\*  
E,607,1479  
\*DO,i,1479,3279,100  
E,i,i+100  
\*ENDDO  
E,3379,859

!zt22\*\*\*\*\*  
E,486,643  
\*DO,i,643,733,5  
E,i,i+5  
\*ENDDO  
E,738,622

!Column Reinforcement

TYPE,2  
MAT,8

REAL,8

E,1157,253  
E,1217,313  
E,1160,256  
E,1220,316

E,1157,1217  
E,1217,1220  
E,1220,1160  
E,1160,1157

E,253,313  
E,313,316  
E,316,256  
E,256,253

!Shear Reinforcement

TYPE,2  
MAT,6  
REAL,6

E,2123,2223  
E,2223,2224  
E,2224,2524  
E,2524,2523  
E,2523,2623

E,2128,2228  
E,2228,2229  
E,2229,2529  
E,2529,2528  
E,2528,2628

E,2118,2218  
E,2218,2219  
E,2219,2519  
E,2519,2518  
E,2518,2618

E,2113,2213  
E,2213,2214  
E,2214,2514  
E,2514,2513  
E,2513,2613

E,2108,2208  
E,2208,2209  
E,2209,2509  
E,2509,2508  
E,2508,2608

E,2103,2203  
E,2203,2204  
E,2204,2504  
E,2504,2503  
E,2503,2603

I\*\*\*\*\*  
E,2153,2253  
E,2253,2244  
E,2244,2544  
E,2544,2553  
E,2553,2653

E,2158,2258  
E,2258,2249  
E,2249,2549  
E,2549,2558  
E,2558,2658

E,2163,2263  
E,2263,2254  
E,2254,2554  
E,2554,2563  
E,2563,2663

E,2168,2268  
E,2268,2259  
E,2259,2559  
E,2559,2568  
E,2568,2668

E,2173,2273  
E,2273,2264  
E,2264,2564  
E,2564,2573  
E,2573,2673

E,2178,2278  
E,2278,2269  
E,2269,2569  
E,2569,2578  
E,2578,2678

I\*\*\*\*\*Z

E,1628,1633  
E,1633,1729  
E,1729,1744  
E,1744,1648  
E,1648,1653

E,1728,1733

E,1733,1829  
E,1829,1844  
E,1844,1748  
E,1748,1753

E,1828,1833  
E,1833,1929  
E,1929,1944  
E,1944,1848  
E,1848,1853

E,1928,1933  
E,1933,2029  
E,2029,2044  
E,2044,1948  
E,1948,1953

E,2028,2033  
E,2033,2129  
E,2129,2144  
E,2144,2048  
E,2048,2053

E,2128,2133  
E,2133,2229  
E,2229,2244  
E,2244,2148  
E,2148,2153  
!\*\*\*\*\*

E,2628,2633  
E,2633,2529  
E,2529,2544  
E,2544,2648  
E,2648,2653

E,2728,2733  
E,2733,2629  
E,2629,2644  
E,2644,2748  
E,2748,2753

E,2828,2833  
E,2833,2729  
E,2729,2744  
E,2744,2848  
E,2848,2853

E,2928,2933  
E,2933,2829  
E,2829,2844  
E,2844,2948

E,2948,2953

E,3028,3033

E,3033,2929

E,2929,2944

E,2944,3048

E,3048,3053

E,3128,3133

E,3133,3029

E,3029,3044

E,3044,3148

E,3148,3153

!Loads\*\*\*\*\*

F,1157,FY,-10000,,1160,1

F,1177,FY,-10000,,1180,1

F,1197,FY,-10000,,1200,1

F,1217,FY,-10000,,1220,1

!Application of boundary conditions and solution using GUI

!/BATCH

!/COM,ANSYS RELEASE 5.4 UP19970828 23:25:43 103/15/2004

!/input,menust,tmp,,,,,,,,,,,,,1

!/GRA,POWER

!/GST,ON

!\*use,PSIH.txt

!/SOLU

IFINISH

!/SOLU

INLGEOM,0

INROPT,FULL, ,OFF

ILUMPM,0

IEQSLV,SPAR,1e-005,3,

ISSTIF PSTRES

!\*

IFLST,2,44,1,ORDE,6

IFITEM,2,1

IFITEM,2,-2

IFITEM,2,23

IFITEM,2,-44

IFITEM,2,65

IFITEM,2,-84

ID,P51X, ,0, , , ,UY

!/VIEW, 1 ,1

!/ANG, 1

!/REP,FAST

IFLST,2,44,1,ORDE,4

IFITEM,2,1

IFITEM,2,-23

!FITEM,2,44  
 !FITEM,2,-64  
 !D,P51X, ,0, , , ,UY  
 !/VIEW, 1 ,1,1,1  
 !/ANG, 1  
 !/REP,FAST  
 !!\*  
 !OUTRES,ALL,ALL,  
 !\*  
 !TIME,160  
 !AUTOTS,1  
 !NSUBST,160,160000,40,1  
 !KBC,0  
 !\*  
 !\*  
 !CNVTOL,U, ,0.05,2, ,  
 !\*  
 !LNSRCH,1  
 !\*  
 !PRED,ON,,ON  
 !NCNV,2,0,0,0,0,  
 !/STAT,SOLU  
 !SAVE  
 !SOLVE  
 !/POST1  
 !FINISH  
 !/POST1  
 !SET,FIRST  
 !AVPRIN,0,0,  
 !\*  
 !PLNSOL,U,Y,0,1  
 !SAVE  
 !FINISH

